

The Role of CD4+ T Cells in the Pathogenesis of Progressive Multifocal Leukoencephalopathy

Dissertation

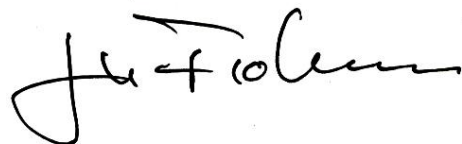
Sara Yousef

Hamburg 2012

Dissertation zur Erlangung des Dokortitels der Naturwissenschaften am Fachbereich
Biologie der Fakultät für Mathematik, Informatik und Naturwissenschaften an der
Universität Hamburg

Genehmigt vom Fachbereich Biologie
der Fakultät für Mathematik, Informatik und Naturwissenschaften
an der Universität Hamburg
auf Antrag von Professor Dr. R. MARTIN
Weiterer Gutachter der Dissertation:
Professor Dr. T. BURMESTER
Tag der Disputation: 03. Februar 2012

Hamburg, den 20. Januar 2012

A handwritten signature in black ink, appearing to read 'J. Fromm', written in a cursive style.

Professor Dr. J. Fromm
Vorsitzender des Promotionsausschusses
Biologie



**Universitätsklinikum
Hamburg-Eppendorf**

**Zentrum für Molekulare Neuro-
biologie**

Falkenried 94
20251 Hamburg

Research Group:
Neuronal Translational Control

Dr. Kent Duncan
Telefon: +49(0)40 7410-56274
Telefax: +49(0)40 7410-53436

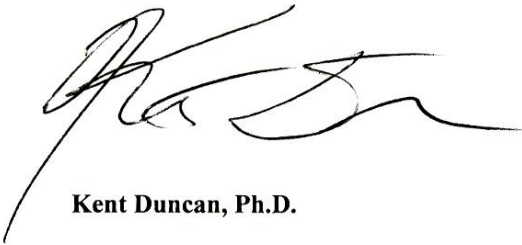
Kent.Duncan@zmnh.uni-hamburg.de
www.zmnh.uni-hamburg.de

Universitätsklinikum Hamburg-Eppendorf Martinistraße 52 20246 Hamburg
Zentrum für Molekulare Neurobiologie - Forschergruppen

To whom it may concern:

Sara Yousef (born 11.11.1983 in Hamburg) is submitting her doctoral dissertation in English. The title of her thesis is: 'The Role of CD4+ T Cells in the Pathogenesis of Progressive Multifocal Leukoencephalopathy'.

I hereby certify that the English language used in this thesis is correct.



Kent Duncan, Ph.D.

Universität Hamburg
Universitätsklinikum Hamburg-Eppendorf
Zentrum für Molekulare Neurobiologie
AG Duncan
Falkenried 94 · D-20251 Hamburg

Hamburg, 05.12.2011



Zertifikat Nr. QS-6568HH

Universitätsklinikum Hamburg-Eppendorf
Körperschaft des öffentlichen Rechts
Gerichtsstand: Hamburg
UST-ID-Nr.: DE218618948

Vorstandsmitglieder:
Prof. Dr. Guido Sauter (Vertr. des Vorsitzenden)
Dr. Alexander Kirstein
Prof. Dr. Dr. Uwe Koch-Gromus
Joachim Pröbß

Bankverbindung:
HSH Nordbank
Kto.-Nr.: 104 364 000
BLZ: 210 500 00
IBAN-Nr.: DE9721050000104364000

Die vorliegende Arbeit wurde von März 2009 bis Dezember 2011 am Institut für Neuroimmunologie und klinische MS-Forschung (INIMS) im Zentrum für molekulare Neurobiologie Hamburg (ZMNH) des Universitätsklinikums Hamburg-Eppendorf (UKE) unter der Leitung von Prof. Dr. Roland Martin und Dr. Mireia Sospedra durchgeführt.

1. Gutachter: Prof. Dr. Roland Martin
2. Gutachter: Prof. Dr. Thorsten Burmester

Content

1	Introduction	1
1.1	Basic immunobiology of CD4+ T cells	1
1.1.1	Anti-viral immune defense	1
1.1.2	T helper cell subsets	2
1.1.3	The T cell receptor	5
1.1.4	The trimolecular complex – TCR-peptide-MHC interaction	6
1.2	Progressive multifocal leukoencephalopathy	7
1.2.1	JC virus	7
1.2.2	Epidemiology of PML	9
1.2.3	Pathogenesis of PML	9
1.2.4	The host immune response against JC virus	10
1.2.5	PML and monoclonal antibody therapy	10
1.2.6	PML-Immune reconstitution inflammatory syndrome	12
1.2.7	Treatment options against PML	13
1.3	Objectives of the study	14
2	Patients, Material and Methods	15
2.1	Patients	15
2.2	Material	15
2.2.1	Frequently used reagents	15
2.2.2	Buffers, solutions and media	17
2.2.3	Cell lines	17
2.2.4	Peptides & Proteins	17
2.2.5	Antibodies	19
2.2.6	RNA isolation, cDNA synthesis and PCR	21
2.2.7	Primer	21
2.2.8	ELISA	23
2.2.9	Consumables	23
2.2.10	Equipment	24
2.2.11	Software	24
2.3	Methods	25
2.3.1	Brain, blood and CSF sample preparation and cell expansion	25
2.3.2	Neuropathology	25
2.3.3	Generation of T cell clones	25
2.3.4	T cell expansion for high cell numbers	26
2.3.5	Generation of EBV-transformed B cell lines	27
2.3.6	Proliferation Assays	27
2.3.7	Immune fluorescence staining	28
2.3.8	Cytokine assessment	29
2.3.9	Detection of JC viral load	29
2.3.10	ELISA for the detection of anti-VP1 IgG	30
2.3.11	Flow Cytometry Analysis	30
2.3.12	HLA-A*02:01/JCV36 JCV100 tetramer staining	31
2.3.13	TRBV receptor analysis by flow cytometry	31
2.3.14	RNA isolation and generation of cDNA	31

2.3.15	Quantitative real time PCR analysis	32
2.3.16	TRAV and TRBV chain PCR.....	32
2.3.17	Direct sequencing of TRAV and TRBV PCR amplified products.....	33
2.3.18	CDR3 spectratyping	33
2.3.19	Statistical analysis.....	33
3	Results	34
3.1	Analysis of the functional phenotype, fine specificity, and TCR-peptide-MHC interaction of brain-infiltrating CD4+ T cells during PML-IRIS	34
3.1.1	A case of natalizumab-associated PML-IRIS.....	34
3.1.2	Phenotypical characterization of brain-infiltrating CD4+ T cells.....	37
3.1.3	Phenotypical characterization of brain-infiltrating CD4+ T cells at the single cell level.....	38
3.1.4	Identification of immunodominant epitopes within VP1 protein.....	41
3.1.5	TCCs recognizing immunodominant epitopes are overrepresented in the brain.....	43
3.1.6	MHC-class II restriction analysis of VP1-specific TCC	46
3.1.7	TRBV20-1/TRAV13-1 T cells preferentially recognize VP1 ₃₄	48
3.2	Induction of a JCV-specific immune response after vaccination with VP1 in a PML patient with idiopathic CD4 lymphocytopenia	51
3.2.1	Treatment scheme of the individual healing attempt	51
3.2.2	Development of the JCV viral load and immune response	51
3.2.3	The treatment induces VP1-specific CD4+ memory T cells.....	53
4	Discussion	55
4.1	Characterization of the CD4+ T cell-mediated immune response against JC virus during PML-IRIS	55
4.1.1	Bi-functional Th1-2 T cells play a major role during PML IRIS.....	55
4.1.2	Several CD4+ immunodominant epitopes are located within VP1	57
4.1.3	JCV-specific T cells accumulate in the brain and not CSF.....	58
4.1.4	A high proportion of brain-infiltrating CD4+ T cells are restricted by multiple HLA-class II elements.....	59
4.1.5	TCR-pMHC interaction of TRBV20/TRAV13 TCC.....	61
4.2	Treatment of PML and idiopathic CD4+ lymphocytopenia	64
4.2.1	VP1 vaccination elicits CD4+ cellular and humoral immunity.....	64
5	Summary	66
6	Zusammenfassung	68
7	Literature	70
8	Appendix	84
	Abbreviations	84
	List of publications.....	85

1 Introduction

Progressive multifocal leukoencephalopathy (PML) is a severe demyelinating disease of the central nervous system (CNS) (1) which is caused by the polyomavirus JC (JCV) (2). The majority of people worldwide are latently infected with the virus (3) without leading to any symptoms in immunocompetent individuals (4). In a minority of people, solely immunocompromised individuals, this infection leads to PML. The immune mechanisms regulating the virus are poorly understood, especially the function of CD4+ T cells is not clear. Therefore the goal of this work was to describe the role of CD4+ T cells during PML and PML immune reconstitution inflammatory syndrome (IRIS) in more detail.

1.1 Basic immunobiology of CD4+ T cells

1.1.1 Anti-viral immune defense

The immune system's role is to defend the organism from detrimental influences of the outer world and pathological changes of the body's own cells and tissues. Viruses are the most rapidly changing and diverse threats the immune system has to cope with. Since viruses are obligate intracellular parasites and completely dependent on their cellular host, they have developed several strategies to evade the host's immune system. Nevertheless, there exist several potent mechanisms that protect the host from pathologic viral infections. The innate immune system, the body's first line defense mechanism, is able to recognize typical viral structures such as double-stranded RNA via pattern recognition receptors (5). This leads to the secretion of type I interferons (IFN) (6) and other pro-inflammatory cytokines that can initiate the second phase of the immune response, the activation of the adaptive immunity (7).

The major players of the cellular arm of adaptive immunity are CD8+ and CD4+ T cells. In the context of viral infections CD8+ T cells are commonly seen as the main "killers" of virus-infected cells due to several reasons: CD8+ T cells recognize their specific antigen with the **T cell receptor (TCR)** presented by **major histocompatibility complex class I (MHC-class I)** molecules that are expressed on all nucleated cells (8). MHC-class I molecules preferentially are loaded with peptides derived from intracellular proteins. This means CD8+ T cells are able to scan nucleated cells and differentiate whether these cells present self or foreign peptides. T cells normally are selected not to interact with high avidity to MHC molecules loaded with self-peptides to avoid auto-immunity. Thus, upon recognition of its cognate peptide by a specific CD8+ T cell presented by a cell that produces mutated or viral proteins, the CD8+ T cell starts to secrete cytotoxic substances such as perforin and

granzymes that leads subsequently to direct lysis of the virus-infected or mutated tumor cell. This major effector function of CD8+ T cells gives them their additional name of **cytotoxic T cells (CTLs)**. However, without help of CD4+ T cells the immune response of CD8+ cells alone would not be sufficient to combat viral infection and to mount an immune response after re-challenge of the virus (9-11). Due to their supporting function CD4+ T cells are also known as **T helper cells (Th)**. Furthermore CD4+ T cells are particularly important for controlling chronic virus infections. So it was shown in mice infected with lymphocytic choriomeningitis virus (LCMV) that a lack of CD4+ T cells leads to impaired function of CTLs and the inability to control viral replication (12). To give other examples, CD4+ T cells are necessary to sustain γ -herpesvirus-specific CTLs (13), and the decline of CD4+ T cells in HIV patients is accompanied by a loss of CTL function and AIDS progression (14). Similarly to CD8+ T cells T helper cells recognize their specific antigen in the context of MHC molecules. However, in the case of **CD4+ Th cells with MHC-class II molecules** that are expressed on **professional antigen presenting cells (APCs)** such as dendritic cells, macrophages and B cells. MHC-class II complexes usually are loaded with peptides derived from extracellular proteins that were taken up by APCs, processed in specialized processing compartments, loaded onto nascent MHC-class II molecules and then transported to the cell surface. Due to this divergent ways of antigen presentation CD4+ and CD8+ T cells recognize different sets of antigens. By secreting certain cytokines T helper cells mediate their effector functions. The different types of T helper cells and their typical cytokine signatures are in detail introduced below. The secretion of the growth factor Interleukin-2 (IL-2) can directly influence the proliferation capacity of CD8+ T cells and promote perforin expression (15). Interferon- γ (IFN- γ), that is secreted by both CTL and T helper cells, has direct anti-viral activity by inducing the production of anti-viral proteins in infected cells and indirect anti-viral activity by attracting macrophages (16, 17).

The **humoral** arm of the adaptive immune system, the **antibody-mediated response of B cells**, is also in many respects dependent on help by CD4+ T cells, which support antibody formation and B cells with IL-4, IFN- γ and CD40 ligand after presentation antigen to the T cell. Neutralizing virus-specific antibodies are particularly relevant for infections with viruses that lead to lysis of virus-infected cells and then are spread as free virus in distinction from viruses, which spread mainly by budding from the surface of an infected to a neighboring uninfected cell (18-20). These antibodies can initiate complement-mediated destruction, opsonization by engagement of Fc receptors on natural killer cells, macrophages and neutrophils as well as antibody-dependent cellular cytotoxicity (ADCC).

1.1.2 T helper cell subsets

In light of the vast number of different pathogens and conditions T helper cells are confronted with, the ability to react in an appropriate way is of great importance. The encounter of the naïve CD4+ T

cell with its cognate antigen presented by a MHC-class II molecule and a second signal from co-stimulatory molecules on the APC leads to activation and differentiation to a certain T helper subset. In which way the naïve T cell differentiates is strongly influenced by the cytokine milieu at the time of activation, and this again is dependent on the type of pathogen that is combated. In the classical point of view the naïve T cell stably differentiates into a certain T helper subset with a characteristic **cytokine signature** that is maintained throughout its lifetime and optimally adjusted for the kind of pathogen the T cell is specific for. 1986 Mosmann and coworkers described for the first time the existence of these T helper subsets (21).

Through the production of IL-12 and IFN- γ by macrophages during infections with intracellular pathogens CD4⁺ naïve T cells are primed to develop into **type 1 helper cells (Th1)** (22) that are characterized by the expression of the transcription factor **T-bet** (23). STAT4 (signal transducer and activator of transcription 4) (24) is responsible for the upregulation of T-bet that in turn leads to the production of the Th1 hallmark cytokine **IFN- γ** (21). Th1 cells are regarded as helper of cellular immunity due to their supporting influence on CD8⁺ T cells, macrophages, and the cytotoxic effector function of NK cells. Th1-dominated immune responses are prominent during infections with intracellular pathogens, but are also associated with several autoimmune conditions (25).

Conversely, **type 2 helper cells (Th2)** are regarded as helper of humoral immunity and in general associated with infections of extracellular pathogens, but also found in allergic diseases (26). Naïve T cells are committed to the Th2 lineage after priming with IL-4 (27) an inducer of STAT6 that in turn activates **GATA-3** (28, 29). Th2 cells are characterized by their cytokines **IL-4, IL-5** and **IL-13** (21).

The fates of Th1 and Th2 cells are considered as mutually exclusive and show a high stability in long-term cultures. The Th1-polarizing cytokines IFN- γ and IL-12 suppress the development of naïve CD4⁺ cells into Th2 cells (30), whereas the Th2-polarizing cytokine IL-4 acts in the same way on the development of Th1 cells (31). Similarly, the transcription factors T-bet and GATA-3 can interfere with the activity of one another (23).

For a long time Th1 and Th2 cells were the only known Th subsets until their family was extended by the discovery of new members characterized by stable expression of distinct transcription factors. Some of the more important subsets are mentioned here (Figure 1).

The existence of regulatory CD4⁺ T cells was long discussed, but their existence as distinct T cell subsets were not commonly accepted before the late 1990ties (32, 33). These CD4⁺ CD25⁺ T cells express the transcriptional regulator FoxP3 (forkhead box P3) (34) and can be differentiated into natural thymus-derived regulatory T cells (nTregs) and inducible IL-10-secreting regulatory T cells (iTregs). As their name implies Tregs mainly contribute to the regulation of inflammatory processes, which could be shown in FoxP3 knockout mice developing widespread autoimmunity, whereas overexpression of FoxP3 results in general immunosuppression (35, 36).

Another important T helper subtype was described almost 20 years after the discovery of Th1/Th2 cells and is characterized by the stable production of the transcription factor ROR γ t that in turn activates the expression of IL-17, which led to naming this Th subset Th17 cells (37). These cells are potent activators of neutrophils and mediate their migration to the site of inflammation. Th17 cells are often found at sites of fungal- and some bacterial infections, but also seem to play a role in several autoimmune diseases (38).

Follicular helper cells (Tfh) promote B cells in several ways e.g. by supporting immunoglobulin class switch, the formation of germinal centers, and the production of antibodies (39). Tfh cells express the transcriptional regulator Bcl-6 and are able to produce Th1 and Th2 cytokines and IL-21 (40).

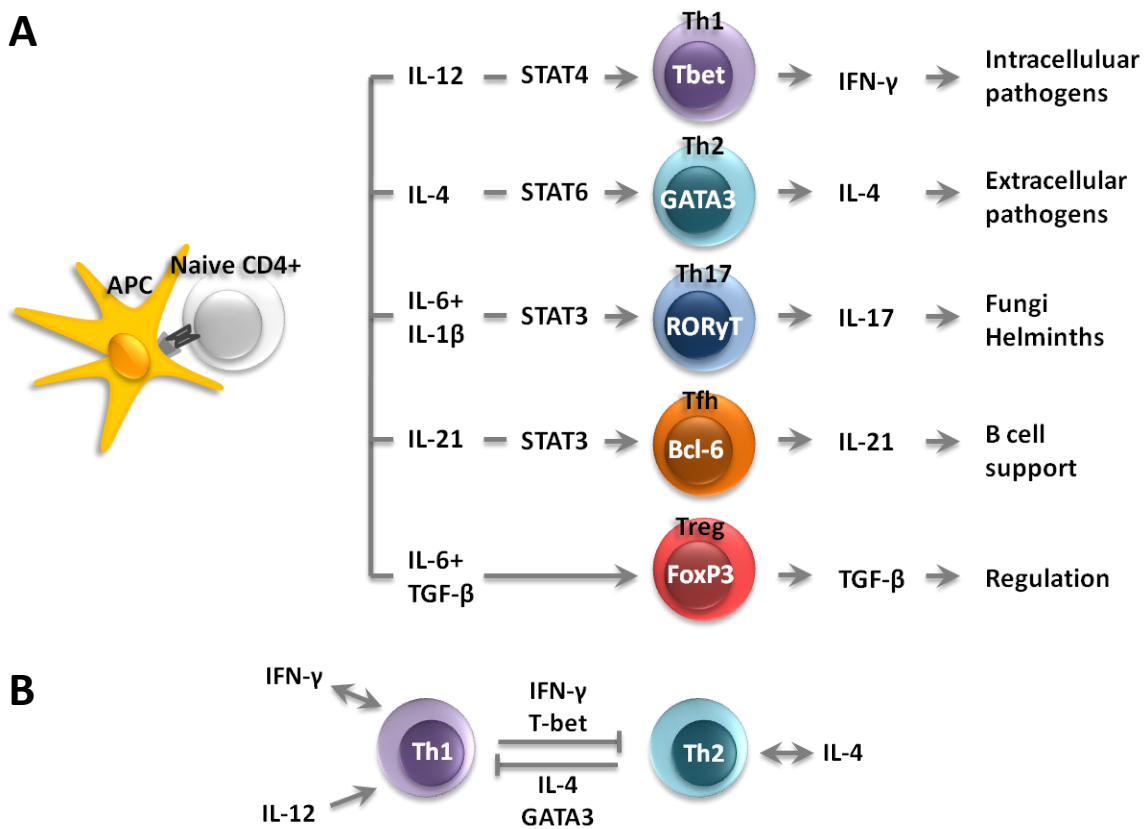


Figure 1 Differentiation of T helper subsets. A) A naive T cell is primed by the cytokine environment after encounter with its cognate antigen in presented by an MHC-class II molecule. B) Cytokines and transcription factors of Th1 and Th2 cells negatively regulate the development of each other.

The paradigm of T helper subsets with strictly fixed and terminal differentiation has already been challenged by early observations that the progeny of individual Th clones could secrete a diverse pattern of cytokines (41) and by mixed/intermediate phenotypes of antigen-specific T cell clones (42). Recent data indicates that Th lineage commitment is much more flexible and plastic than suggested by the Th1/Th2 paradigm (43, 44). In light of the newly emerging subsets and discovery of intermediate cell types some of these principles are reconsidered now (45, 46).

1.1.3 The T cell receptor

Different from antibodies, which usually interact with conformational determinants of antigens either in solution or on the surfaces of cells/tissues/microorganisms, T cells recognize via their **T cell receptor** (TCR) short antigenic peptides, which are derived from the abovementioned processing mechanisms and bound to self-MHC on the surface of an antigen-presenting- or virus-infected cell (8). Every T cell carries between 10.000 and 80.000 identical TCRs on its surface (47). As depicted in Figure 2 the TCR is a glycosylated heterodimer consisting of a **TCR α** and a **TCR β chain** connected via a disulfide bond. Around 30% of TCR $\alpha\beta$ T cells are able to produce a second productively rearranged α -chain (48), and less than 1% can bear a second β -chain (49, 50). A minority of T cells (around 10% of the total T cell population) carry a T cell receptor that is composed of a TCR γ and TCR δ chain (51). These so called $\gamma\delta$ T cells, belonging to the group of unconventional T cells, are predominant in intraepithelial tissue of lung and gut and differ in their antigen recognition from $\alpha\beta$ T cells since they do not require antigen processing and presentation by MHC molecules and respond to non-peptide antigens (52).

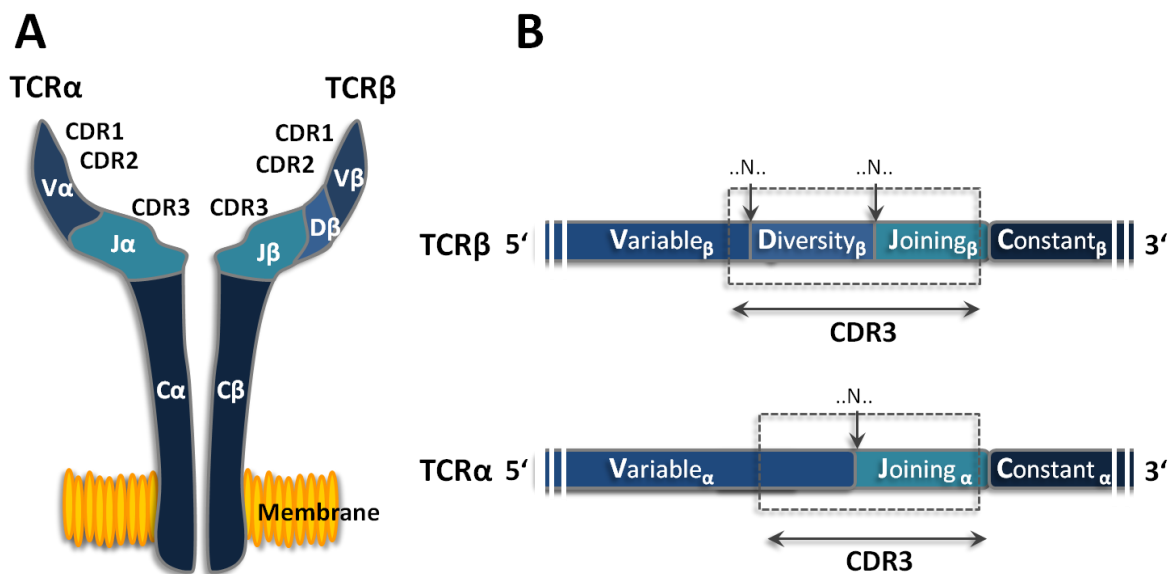


Figure 2 A) Structure of the T cell receptor showing the different segments of TCR α and TCR β chain. B) Location of the CDR3 region within the TCR α and TCR β chain. N indicates nucleotide insertions at the site of junction.

Each TCR chain can be subdivided into a short cytoplasmic region, a hydrophobic transmembrane domain, a constant and a variable region. The N-terminal variable region of both chains is responsible for antigen and MHC contact. The highest diversity of the amino acid composition can be found in the complementarity determining regions (CDR) located in the variable part of the T cell receptor. These CDRs are also known as hypervariable regions. They can be divided into CDR1, CDR2, and **CDR3**. CDR1 and CDR2 regions are part of the TCR V alpha- and V beta chains, while the CDR3 region is made up by TCR joining (J) and diversity (D) segments as well as nucleotide additions. The highest

diversity is found in the CDR3 region due to junctional rearrangements, which is mediated by **somatic recombination**.

The process of somatic recombination takes place during thymic development and due to random combination of different modules a unique T cell receptor is created. These modules are gene segments for the already mentioned constant (C) and variable (V) region and are extended by joining (J), and in the case of the TCR β chain diversity (D) gene segments are added (53). Due to this reason somatic recombination also is known as V(D)J recombination. Somatic recombination of a large number of germline-encoded TCR segments leads to the enormous number of theoretical TCR combinations (in the range of 10^{14}). In humans one C α gene segment (two C β gene segments, resp.) can be combined with one out of 42 different V α gene segments (48 V β segments, resp.) and these again are linked to one out of 61 J α segments (13 D β J β combinations, resp.) which eventually leads to a functional V α -J α -C α or V β -D β -J β -C β chain, respectively (47). Somatic recombination is driven by V(D)J recombinases such as recombination-activating gene proteins (RAG) that are expressed during thymocyte development. Diversity is further increased by the addition and deletion of nucleotides at the V(D)J joining sites (53). After expression of a functional TCR on the surface RAG genes become silenced. Eventually the random combination of one TCR α with one TCR β chain creates a unique T cell receptor.

1.1.4 The trimolecular complex – TCR-peptide-MHC interaction

Antigen-specific activation of T cells requires MHC molecules presenting the cognate peptide (8). The transient interaction of the three molecules is known as the **trimolecular complex**. In addition to these three components further molecules play a role for T cell activation and T cell/APC interaction, such as the co-receptors CD8 and CD4, mediating the specific binding to MHC-class I and MHC-class II, respectively and other co-stimulatory and adhesion molecules from both the T cell and the APC (54).

In the human system MHC molecules are also known as **human leukocyte antigens (HLA)**. Therefore both terms are henceforth used synonymically. T cells are selected to interact with self-MHC molecules carrying a non-self peptide, i.e. a peptide derived from a foreign pathogen or mutated cell. The endogenously processed antigens are loaded into the **peptide binding pocket** of the MHC molecule and are then brought to the cell surface. Due to the distinct structure of the peptide binding pocket of MHC-class II molecules, which is open at both ends, the presented peptides usually have a length of 15-25 amino acids (55) with a core region of 9-10 amino acids and peptide protrusions at either end. The MHC-class II α and β chain are encoded within the HLA-DP, -DR and DQ loci. HLA molecules are expressed co-dominantly, this means that the haplotypes inherited from both parents are present at the cell surface simultaneously. Together with the fact that MHC molecules

belong to the most polymorphic genes in the genome (of each locus exist a vast number of different alleles), it leads to an almost unique composition of HLA molecules in every individual. Due to the characteristic binding preferences each MHC molecule binds and presents a distinct peptide repertoire to T cells. Most likely this peptide selectivity plays an important role for the association of certain HLA haplotypes with several autoimmune diseases such as multiple sclerosis (56).

The T cell receptor interacts with both components – the MHC molecule and the peptide. The hypervariable regions of the TCR are responsible for most contacts. Crystallized TCR-peptide-MHC molecules revealed that the CDR3 region frequently interacts with the peptide in the binding pocket, whereas the less variable CDR1 and CDR2 regions make contact to the MHC molecule and the ends of the peptide (57-59). However, considerable variation has been found in different structures of trimolecular complexes (60-62).

The specificity of the T cell receptor for a certain peptide/MHC complex is less stringent than originally anticipated (63). The use of synthetic combinatorial peptide libraries (PS-SCL), an approach for the assessment of T cell specificity, and amino acid substitution experiments revealed that most T cells are able to recognize a spectrum of structurally related, but in their amino acid composition considerably differing sets of peptides (64-69). Hemmer and coworkers were even able to demonstrate that a peptide differing in all amino acid positions from the native antigen still is able to stimulate the specific T cell (70). In addition to **cross-reactivity** of individual T cell clones, recent data indicates that flexibility in TCR-MHC/peptide interactions extends to the MHC and that single or multiple peptides can be recognized with more than one MHC element (**cross-restriction**), which has been shown by several research groups (71-75).

1.2 Progressive multifocal leukoencephalopathy

1.2.1 JC virus

JC virus is the causative agent of PML and was named after the initials of the PML patient John Cunningham, from whose brain tissue it was first possible to isolate and describe the virus in 1971 (76). The primary infection with JC virus occurs during childhood through inhalation but also uptake through the gastrointestinal tract is discussed (77, 78). The virus establishes a lifelong persistent infection without causing any symptoms in immunocompetent individuals. The tonsils are one possible site of primary infection. JC virus DNA can be detected within tonsil tissue and tonsillar-associated B lymphocytes (79, 80). It is likely that JCV is distributed in the organism through infected B cells and is eventually carried to its sites of latency – the bone marrow and kidney epithelium (81, 82). JCV has a very restricted cellular tropism. The virus uses N-linked glycoproteins containing

terminal α -2,6-linked sialic acids for docking at the cell surface but this cannot be the determinant for cell tropism because these receptors are expressed by a wide variety of cells (83). Cell entry is mediated by binding to a secondary receptor the serotonergic 5HT_{2A} receptor (84). Then internalization is rapidly mediated by clathrin-dependent endocytosis. Both receptors are expressed on oligodendrocytes, astrocytes, B lymphocytes and kidney epithelium - all of these cell types are known for their JCV abundance (85-88). JC virus not only has a very narrow cell tropism, it is also highly host-specific by infecting only human beings. Due to the lack of animal models the study of JC virus biology is difficult.

JC is a member of the **polyomavirus** family, which now encompasses 9 different members that are pathogenic for humans (76, 89-95), including the ubiquitous BK virus. These non-enveloped viruses share some features like a double stranded supercoiled DNA genome and an icosahedral capsid structure. Indeed the sequence similarity between BKV and JCV is so high that cross-recognition by specific CD4+ and CD8+ cells can be observed (96). BK virus is as common in the human population as JCV without causing symptoms in healthy individuals but being responsible for BKV related nephropathy and rejection of renal transplant in 2.5% of cases (82).

JCV and the other members of polyomavirus family have relatively small genomes. The genome of JCV consists of 5.1 kb and the coding region makes up more than 90%. This relatively preserved area encodes the early genes large and small T that are responsible for regulatory processes and the late genes encoding the **capsid forming proteins VP1**, VP2, VP3, and the associated Agno protein (4). Most mutations can be found within the non-coding region of the genome - the hypervariable regulatory region (RR) of JCV that is responsible for the cell tropism and determination of the latent or lytic state of the virus (97). Due to rearrangements within the regulatory region one can differentiate between JCV variants. In the urine of healthy individuals usually the archetypic form of the RR can be found which is characterized by a 98 bp sequence with a 23 and a 66 bp insert that lacks several transcription factor binding sites essential for viral replication (98-100). Conversely, JCV DNA isolated from cerebrospinal fluid (CSF) of PML patients often shows a characteristic tandem repeat of the 98 bp sequence of the archetypic variant (97) and a limited number of mutations at distinct positions of the structural protein VP1 (101). This so called neurotropic Mad-1 strain contains several transcription factor binding sites and TATA-boxes that are responsible for enhanced viral activity and reactivation from the latent to the active lytic state of JCV (102). The factors that lead to reactivation of JC virus remain elusive, but immunosuppression is the most likely trigger of this process. Reactivated JC virus reaches the brain most likely through activated B cells that are able to cross the blood brain barrier. Infected B cells could be located in brain tissue of PML patients (103).

1.2.2 Epidemiology of PML

Progressive multifocal leukoencephalopathy (PML) is a severe demyelinating disease of the central nervous system that is caused by the polyomavirus JC (JCV). It is estimated that more than 60% of the human population worldwide are latently infected with JCV (104), but despite its high prevalence PML is a very rare disease with an incidence of 4.4 cases in 100.000 individuals (105). It occurs mainly in a state of severe cellular immunodeficiency, whereas immunocompetent persons do not develop PML. JCV can cause PML in individuals with inherited immunodeficiencies such as idiopathic CD4 lymphocytopenia, a syndrome characterized by low CD4 T cell counts (106), or in states of acquired immunocompromise based on infection such as HIV. Most frequently PML is observed in AIDS patients. In the beginning of the HIV era up to 5% of AIDS patients developed PML (107). Meanwhile this number is in decline since the introduction of highly active retroviral therapy (HAART) (108-110). Another risk group consists of patients that underwent immunosuppressive treatment in context of organ transplantation or also individuals with autoimmune diseases who are treated with monoclonal antibodies. This includes multiple sclerosis patients receiving the anti-VLA-4 antibody natalizumab.

1.2.3 Pathogenesis of PML

PML was first described by Astrom et al. in 1958 (1). This disease is characterized by lytic infection of oligodendrocytes and abortive infection of astrocytes in the CNS in the absence of a notable immune response (111, 112). The destruction of the myelin-forming oligodendrocytes leads to demyelination of neurons and subsequently can lead to loss of axonal function. Magnetic resonance imaging of the brain from PML patients typically shows multiple lesions without contrast enhancement (contrast enhancement=indicator for opening of blood brain barrier) usually located in the subcortical hemispheric white matter. The **symptoms** of the patients correlate with the affected areas of the brain and can be of motoric, sensory, or cognitive nature. Often observed are speech deficits, limb weakness, cognitive dysfunctions, coordination difficulties, ataxia (lack of control over muscle movement) or hemianopsia (one sided impairment of vision or blindness).

PML is **diagnosed** by detection of viral DNA in the cerebrospinal fluid. Conversely, detection of viral DNA in the urine is not useful for the diagnosis because 30-75% of healthy infected individuals excrete JCV particles (104). A more invasive diagnostic tool is the in situ hybridization of JC viral DNA or proteins in brain biopsy material. Histological examinations of these biopsies can reveal demyelinated areas, reactive gliosis and multinucleated, giant shaped astrocytes.

The **prognosis** of PML is in general poor. If the host is not able to develop a sufficient immune response against the virus the disease is inevitably fatal.

1.2.4 The host immune response against JC virus

In healthy individuals the immune response against JCV is highly efficient in controlling the virus so that the infected persons do not develop any symptoms. Yet, it is not clear how the different components of the immune system contribute to its elimination.

Early investigation focused on the **humoral immune** response against JCV. Methods for the detection of JCV-specific antibodies already exist since the 1970s. Anti-JCV IgG antibodies have a high seroprevalence in the human population, the data range from 60 to 80% depending on the research group (3, 113-116). Nevertheless, there are contradicting results about the relevance of the humoral response for the better outcome of PML patients. In a study with 62 PML patients the production of intrathecal JCV-IgG antibodies could not be correlated with a prolonged survival (117). In contrast, Khanna et al. were able to show that high JCV-specific antibody titers at the onset of disease are associated with long-term survival of PML patients and the rise of JCV-IgG levels correlate to increasing CD4+ counts after initiation of HAART therapy in AIDS patients (118).

The **CD8+ T cell response** has been studied in some detail. Du Pasquier and coworkers were able to identify immunodominant CD8+ epitopes located within the VP1 and large T protein that are restricted by the most common HLA-class I molecule of the Caucasian population A*02:01 (119, 120). Additionally it has been shown that JCV-specific CTLs were abundant in the majority of PML survivors whereas these cells had a lower frequency in PML progressors (121, 122).

Less is known about the role of **CD4+ T cells** in the defense against JC virus. It has been shown that higher CD4+ counts in PML AIDS patients are associated with prolonged survival (14), and restoration of JCV-CD4+ T cell responses is correlated with clearance of JCV DNA in the CSF of PML patients with better outcome (123). Furthermore, PML survivors tend to have more JCV-specific CD4+ T cells in the blood than progressors (124). The association of CD4+ deficiencies with the increased susceptibility of developing PML, as it is observed in AIDS and CD4 lymphocytopenia patients, indicates that CD4+ T cells play an important role in control of JC virus.

1.2.5 PML and monoclonal antibody therapy

Until recently PML was seen as a disease mainly affecting profoundly immunocompromised AIDS- or tumor patients. Relatively recently, a new risk group came into the focus of attention: patients treated with monoclonal antibodies due to an underlying autoimmune disease. Cases have been reported so far after treatment with **rituximab**, a monoclonal antibody directed against the B cell marker CD20 that is mainly used for the treatment of rheumatoid arthritis; **efalizumab**, targeting CD11a expressed on lymphocytes, used for the treatment of psoriasis patients, and **natalizumab**, an

anti-VLA4 antibody that is used for the treatment of multiple sclerosis and patients with Crohn's disease.

For a better understanding of the following work the next part will point out multiple sclerosis and its treatment with natalizumab.

Natalizumab and multiple sclerosis

Multiple sclerosis (MS) is a neuroinflammatory disorder affecting mainly young adults. In the long term it leads to motor disability and cognitive impairment of the affected persons (125). This autoimmune disease is largely driven by autoreactive CD4+ T cells that are able to cross the blood brain barrier (126, 127). Within the central nervous system these autoreactive T cells encounter their specific antigens that are part of the myelin sheath (128). Following the release of proinflammatory cytokines and chemokines, other immune cells are recruited from the peripheral blood such as monocytes, B cells and CD8+ T cells and activation of resident cells including microglia and astrocytes. Subsequently, the myelin sheath may be destroyed, which then leads to axonal loss. In most cases such an episode of inflammation (relapse) is followed by a phase of remission. The disease course of more than 90% of MS patients follows this pattern and is therefore termed relapsing-remitting MS (RRMS). The remaining 10% are classified as primary-progressing MS (PPMS) which is characterized by a continuously deterioration of the patients' condition. However, the majority of RRMS patients later also develop a secondary-progressing form of MS (SPMS). The different stages of RRMS are reflected on the cellular level by the abovementioned initial inflammatory episodes that can proceed after years to a neurodegenerative phase due to chronic activation of microglia and a toxic ion milieu after redistribution of ion channels as adaption in the demyelinated axons (129). Patients benefit mainly from early treatment during the inflammatory stage of their disease and with drugs/treatments that are immunomodulatory or -suppressive.

Among the currently approved drugs for MS, **natalizumab** (Tysabri® from Biogen-IDEC and Elan) represents probably the most effective treatment of RRMS with the ability to reduce the risk of sustained progression of disability and the rate of clinical relapses (130). In a phase III clinical trial natalizumab also showed efficacy in the treatment of patients with Crohn's disease, an auto-inflammatory disease of the gut.

Natalizumab is a humanized monoclonal antibody targeting the $\alpha 4$ subunit of the VLA-4 integrin that is expressed on the surface of all activated leukocytes. VLA-4 specifically interacts with the vascular cell adhesion molecule-1 (VCAM-1) that is located on endothelial cells of the blood brain barrier and is preferentially induced by inflammatory cytokines. VCAM-1 then mediates the crossing of activated leukocytes into the inflamed tissue of the central nervous system (131). Due to blockage of the VLA-4

integrin by natalizumab the infiltration of leukocytes such as activated T cells and dendritic cells into the CNS is markedly reduced (132, 133). This leads to a reduction of the number of auto-reactive T cells reaching the CNS and consequently a blocking of MS relapses. On the other hand the lack of migration of immune cells into the CNS compromises immune surveillance of the brain, which is most likely a contributing factor for the increased risk of developing PML in natalizumab-treated patients. Furthermore, it has been considered that the inhibition of VLA-4/VCAM-1 interactions, which serve as a retention signal for hematopoietic precursor cells in the bone marrow, leads to release of JCV from one of its natural niches (134), increased viral replication and occurrence of JCV variants with tropism for CNS cells (135).

2004 the food and drug administration (FDA) approved the use of natalizumab but already 2005, after the appearance of three cases of PML, two of them with fatal outcome, it was withdrawn from the market. 2006 natalizumab was reintroduced with the restriction just to be applied as mono therapeutic agent. Until April 2011 more than 83.000 MS patients have been treated with natalizumab. Out of these patients 124 have developed PML (136) this corresponds to a total incidence of 1,44 in 100.000 patients. The risk of developing PML increases with the number of infusions a patient received.

1.2.6 PML-Immune reconstitution inflammatory syndrome

Immunocompromise is a prerequisite for the development of PML, and consequently is considered an opportunistic infection. PML is therefore characterized by an absence of an immune response against JCV in the CNS so that the virus is able to replicate within myelin-forming cells of the brain and cause destruction. Upon reconstitution of the immune system, in AIDS patients by initiating HAART therapy or by cessation of natalizumab treatment in the case of MS patients, the immune system mounts a JCV-specific response, which in turn leads to rapid infiltration of immune cells into the brain and elimination of JC virus-infected cells. This phenomenon is described as PML-immune reconstitution inflammatory syndrome (PML-IRIS). Typically MRI scans of PML-IRIS lesions show contrast enhancement as a sign for opening of the blood brain barrier and inflammation, which is normally absent in PML lesions (137). For the patient this can have the beneficial effect that JCV is cleared from the brain and in the best case cure from PML. However, the inflammatory response in the CNS may be so acute that the clinical state of the patients worsens during PML-IRIS. PML-IRIS may in fact lead to massive infiltration of the brain with immune cells and life-threatening brain swelling and herniation. It is critical to find the right balance between the immune reaction against JCV and avoiding damage of the brain. The administration of corticosteroids at a late stage of PML-IRIS is recommended (138). PML and PML-IRIS show very poignantly the fragile equilibrium of the

interactions of host and viral intruder and emphasizes the importance of the understanding of the immune response against JCV.

1.2.7 Treatment options against PML

Besides the restoration of the host immune system there is no effective treatment against JC virus infection during PML at the moment. Some drugs showed promising results in small cohorts but failed to show efficacy in large phase III trials. Among these were cidofovir, an anti-viral drug used for cytomegalovirus infection (139); cytarabine, that belongs to the group of nucleoside analogs (140); mirtazapine, a serotonin receptor antagonist (141) and mefloquine, that is used in the treatment of malaria (4, 142). Considering the increasing number of PML cases after treatment with monoclonal antibodies in autoimmune diseases, the need for an effective treatment option against PML becomes of growing importance.

Individual healing attempt of a PML patient with underlying CD4 lymphocytopenia

In the case of a patient with CD4 lymphocytopenia his immune system was not able to develop sufficient protection against JC virus, which led subsequently to PML. CD4 lymphocytopenia (ICL) is a rare congenital defect that is characterized by low CD4+ counts (<300 cells/mm³) (143) or <20% of total lymphocytes at two different time points without having any evidence of an HIV infection (144). In most cases ICL is asymptomatic but it can lead to accumulation of opportunistic infections. Several cases of PML have been reported in context of ICL (145-147). Due to the lack of therapy options we developed a treatment strategy with the goal to reinstall sufficient immune protection against JC virus and halt PML progression. The therapeutic regimen comprised vaccination with the major capsid-forming protein VP1 together with an adjuvant containing a Toll-like receptor (TLR) 7 agonist. TLRs are expressed on APCs such as dendritic cells (148). Ligand binding induces maturation of the APCs so that they start to express HLA-class II and secrete inflammatory cytokines. Binding of ligands on TLR7 induces anti-viral immunity by the production of IL-12 and IFN- α that mediate Th1 development (149). Since imiquimod (Aldara, 3M) containing a TLR7 agonist is approved for the dermal use in humans, this was the adjuvant of choice. Since the rise of CD4+ counts in AIDS patients after initiation of HAART therapy is correlated with a better survival in the case of PML (14) the ICL patient received recombinant IL-7 (CYT107, Cytheris) that was shown to increase CD4+ and CD8+ counts (150). CYT107 is currently tested in phase II and III trials in patients with pathologic low CD4+ counts.

1.3 Objectives of the study

As mentioned above, only little is known about the specific immune response against JC virus and even less is known about the immune response during PML-IRIS. We recently had the opportunity to examine a brain biopsy sample of a patient during PML-IRIS, which had been obtained for diagnostic purposes after testing for JCV viral DNA in the CSF had been repeatedly negative and hence clarification of the diagnosis was sought by in situ hybridization and immunohistochemistry. The patient had developed PML after treatment of his RRMS with natalizumab. With the brain biopsy we were able to perform an in depth characterization of the infiltrating T cells in the inflamed tissue and addressed the following questions:

- 1. Analysis of the phenotype of brain-infiltrating CD4+ T cells**
- 2. Generation of JCV-specific CD4+ T cell clones for an in depth analysis of**
 - a. the phenotype at the single cell level
 - b. the comparison of T cell composition in brain, CSF, and peripheral blood
 - c. the fine-specificity and avidity
 - d. MHC-class II restriction

The second part of the study focuses on the individual healing attempt of the PML patient with underlying CD4 lymphocytopenia. My part was to analyze the development and type of immune response of the patient induced by the vaccination. The following work will emphasize on:

- 3. The development of the immune response against JCV-VP1 after vaccination**
 - a. Identification of the major cell types driving the immune response

2 Patients, Material and Methods

2.1 Patients

Table 1 PML patients

Number	Sex	Age	PML-IRIS	Trigger of PML
PML 1*	Male	43 years old	Yes	RRMS, Natalizumab treatment
PML 2	Male	48 years old	Yes	AIDS
PML 3	Male	63 years old	No	Idiopathic CD4 lymphocytopenia
PML 4	Male	20 years old	No	Hyper-IgE syndrome

* HLA-class II types PML patient 1: DRB1*11:03, -*15:01; DRB3*02:02; DRB5*01:01; DQA1*01:02, -*05:XX (X indicating not typed to the exact subtype); DQB1*03:01, -*06:02.

Table 2 Non PML controls

Number	Sex	Age	Diagnosis
Control 1	Male	53 years old	Neurosyphilis.
Control 2	Female	32 years old	Relapsing remitting MS
Control 3	Female	37 years old	Clinical isolated syndrome
Control 4	Female	76 years old	Ataxia
Control 5	Female	20 years old	Clinical isolated syndrome

2.2 Material

2.2.1 Frequently used reagents

Table 3 Cell isolation and cell culture

Reagent	Company	Catalog number
³ H-thymidine	Hartmann Analytic	#MT6038E
Brefeldin A	eBioscience	#00-4506
Collagenase A	Roche	#10103578001
DNase I	Roche	#11284932001
Dulbecco's Phosphate Buffered Saline (PBS), 1x	Gibco	H15-002
Fetal calf serum	Biochrom	#S0115
Ficoll LSM 1077	PAA	#J15-004
Fluoromount G	Southern Biotech	#0100-01
Genitacin G-418 Sulphate	PAA	#P11-021
Gentamicin	Lonza	#17-5192
Hoechst33258	Sigma-Aldrich	# B1155

Reagent	Company	Catalog number
Human serum	PAA	#C05-021
Interleukin-2	Kindly provided by Federica Sallusto Institute for Research in Biomedicine, Bellinzona	
Interleukin-2, recombinant	Roche, Tecin	
Ionomycin calcium salt	Sigma-Aldrich	#I0634
L-Glutamine, 200 mM	Gibco	#25030
Penicilin/Streptomycin	Gibco	#15140
Percoll	GE Healthcare	#17-0891-01
Phorbol myristyl acetate (PMA)	Sigma-Aldrich	#P1585
Phytohemagglutinin PHA-P	Sigma	#L 9017
Poly-L-Lysine, 0,01%	Sigma	#P4707
RPMI 1640	PAA	#E15-885
T Cell Activation and Expansion Kit	Miltenyi Biotec	#130-091-441
Trypan blue solution, 0.4%	Sigma Aldrich	#T8154
X-Vivo™ 15	Lonza	#BE04418F

Table 4 Flow cytometry

Reagent	Company	Catalog number
CellTrace™ CFSE Cell Proliferation Kit	Invitrogen	#C34554
FACS Clean	BD Biosciences	#340345
FACS Flow, 20l	BD Biosciences	#342003
FACS Lysing Solution	BD Biosciences	#349202
FACS Rinse	BD Biosciences	#340246
IC Fixation Buffer	eBioscience	#00-8222
LIVE/DEAD® Fixable Dead Cell Stain Kits	Invitrogen	#MP 34955
Permeabilization Buffer, 10X	eBioscience	#00-8333

Table 5 Other reagents

Reagent	Company	Catalog number
Agarose	Invitrogen	#15510-027
Betaplate Scint	Perkin-Elmer	#1205-440
Bovine serum albumin (BSA)	PAA	#K45-001
Ethidium bromide	Roth	#2218.1
Isopropanol	Roth	#6752.4
Milkpowder	Roth	#T145.2
Na ₂ CO ₃	Roth	#8563.1
NaCl ₂	AppliChem	#A1149,5000
NaHCO ₃	Merck	#1.06329.1000
Tris	AppliChem	#A1086
Tween20	Sigma	#P1379-500ML

2.2.2 Buffers, solutions and media

- **T cell medium complete:** 5% Human serum, 1% Penicilin/Streptomycin, 2 mM L-Glutamine, 50 µg/ml Gentamicin, In RPMI 1614 GlutaMax™ GIBCO® Invitrogen
- **B cell medium*:** 10% Fetal calf serum, 1% Penicilin/Streptomycin, In RPMI 1614 GlutaMax™ GIBCO® Invitrogen
* in case of BLS cells fresh Genitacin 1 mg/ml
- **General freezing medium:** 25 % fetal calf serum, 10% DMSO, in RPMI 1614
- **Freezing medium TCC:** 10 % DMSO, in fetal calf serum
- **FACS Buffer:** 0.1% BSA, 0.02% NaN₃, in 1x PBS
- **ELISA Wash Buffer:** 0.05% Tween20, in 1x PBS
- **1X TAE Buffer:** 40mM Tris, 20mM acetic acid, 1mM EDTA, in H₂O
- **Coating buffer:** 15 mM Na₂CO₃, 35 mM NaHCO₃, 3 mM NaN₃, in H₂O
- **ELISA blocking buffer:** 5% non-fat powdered milk, 25 mM Tris, 150 mM NaCl, in H₂O

2.2.3 Cell lines

- Epstein-Barr virus (EBV)-transformed tamarin (*Saguinus oedipus*) cells (B95-8) (151) for production of EBV particles.
- For assessment of HLA-class II restriction bare lymphocytes syndrome (BLS) cells (152) were used transfected with either DR2A (DRB5*01:01), DR2B (DRB1*15:01) or DQW6 (DQB1*06:02) kindly provided by Dr. G. Nepom and Dr. W. Kwok, Benaroya Research Institute, Seattle, WA, USA.

2.2.4 Peptides & Proteins

For the identification of immunodominant epitopes of VP1 JC virus-specific T cell clones, 63 (13–16-mer) peptides covering the entire VP1 capsid protein, were applied (Table 6). Peptides were synthesized and provided by Peptides and Elephants GmbH. These 63 peptides overlap by five amino acids and include 35 common single amino acid mutations. To account for amino acid variations that occur among the different JC virus genotypes and strains, amino acid sequences of JC virus VP1 protein from all 479 JC virus genomic sequences available in GenBank (by March 2008), were aligned and those polymorphisms which were prevalent in 41% of all retrieved sequences were defined as common mutations.

Table 6 Peptide library spanning the whole VP1 protein of JC virus. Peptide variants are indicated with Roman numerals. Peptide direction C → N terminus.

#	Name	Sequence	Length	#	Name	Sequence	Length
14	VP1 ₁₋₁₄ I	MAPTKRKGERKDPV	14	17	VP1 ₈₋₂₂ II	GERHDPVQVPKLLIR	15
15	VP1 ₁₋₁₄ II	MAPTKRKGERHDPV	14	18	VP1 ₁₇₋₃₁	PKLLIRGGVEVLEVK	15
16	VP1 ₈₋₂₂ I	GERKDPVQVPKLLIR	15	19	VP1 ₂₆₋₄₀	EVLEVKTGVDSITEV	15

#	Name	Sequence	Length	#	Name	Sequence	Length
20	VP1 ₃₄₋₄₈	VDSITEVECFLTPEM	15	49	VP1 ₁₇₁₋₁₈₆	FPKNATVQSQVMNTEH	16
21	VP1 ₄₄₋₅₈ I	LTPEMGDPDEHLRGF	15	50	VP1 ₁₈₂₋₁₉₆	MNTEHKAYLDKNKAY	15
22	VP1 ₄₄₋₅₈ II	LTPEMGDPNEHLRGF	15	51	VP1 ₁₉₃₋₂₀₈	KNKAYPVECWVDPDTR	16
23	VP1 ₅₄₋₆₈	HLRGFSKISISDTF	15	52	VP1 ₂₀₃₋₂₁₇	PDPTRNENTRYFGTL	15
24	VP1 ₆₄₋₇₈ I	ISDTFESDSPNRDML	15	53	VP1 ₂₁₀₋₂₂₄	NTRYFGTLTGGENVP	15
25	VP1 ₆₄₋₇₈ II	ISDTFESDSPNFDML	15	54	VP1 ₂₂₀₋₂₃₄ I	GENVPPVLHITNTAT	15
26	VP1 ₆₄₋₇₈ III	ISDTFESDSPNKDML	15	55	VP1 ₂₂₀₋₂₃₄ II	GENVPSVLHITNTAT	15
27	VP1 ₇₄₋₈₈ I	NRDMLPCYSVARIPL	15	56	VP1 ₂₂₀₋₂₃₄ III	GENVPPVLHITKTAT	15
28	VP1 ₇₄₋₈₈ II	NFDMLPCYSVARIPL	15	57	VP1 ₂₂₉₋₂₄₃ I	ITNTATTVLLDEFV	15
29	VP1 ₇₄₋₈₈ III	NKDMLPCYSVARIPL	15	58	VP1 ₂₂₉₋₂₄₃ II	ITKTATTVLLDEFV	15
30	VP1 ₈₁₋₉₅	YSVARIPLPNLNEDL	15	59	VP1 ₂₃₉₋₂₅₃ I	DEFGVGPLCKGDNLY	15
31	VP1 ₉₁₋₁₀₅	LNEDLTCGNILMWEA	15	60	VP1 ₂₃₉₋₂₅₃ II	DEFGVRRPLCKGDNLY	15
32	VP1 ₁₀₁₋₁₁₅	LMWEAVTLKTEVIGV	15	61	VP1 ₂₄₉₋₂₆₃	GDNLVLSAVDVCGMF	15
33	VP1 ₁₀₈₋₁₂₂ I	LKTEVIGVTSLMNVH	15	62	VP1 ₂₅₉₋₂₇₃ I	VCGMFTNRSGSQQWR	15
34	VP1 ₁₀₈₋₁₂₂ II	LKTEVIGVTTLMNVH	15	63	VP1 ₂₅₉₋₂₇₃ II	VCGMFTKRSGSQQWR	15
35	VP1 ₁₀₈₋₁₂₂ III	LKTEVIGVTALMNVH	15	64	VP1 ₂₅₉₋₂₇₃ III	VCGMFTNRSGFQQWR	15
36	VP1 ₁₁₈₋₁₂₉ I	LMNVHSNGQATH	12	65	VP1 ₂₅₉₋₂₇₃ IV	VCGMFTNRAGSQQWR	15
37	VP1 ₁₁₈₋₁₂₉ II	LMNVHSNGQAAH	12	66	VP1 ₂₅₉₋₂₇₃ V	VCGMFTNGSGSQQWR	15
38	VP1 ₁₁₈₋₁₂₉ III	LMNVHSNGQASH	12	67	VP1 ₂₆₉₋₂₈₃	SQQWRGLSRYFKVQL	15
39	VP1 ₁₂₃₋₁₃₇ I	SNGQATHDNGAGKPV	15	68	VP1 ₂₇₀₋₂₈₃	FQQWRGLSRYFKVQL	15
40	VP1 ₁₂₃₋₁₃₇ II	SNGQAAHDNGAGKPV	15	69	VP1 ₂₇₉₋₂₉₄	FKVQLRRRVKNPYPI	16
41	VP1 ₁₂₃₋₁₃₇ III	SNGQASHDNGAGKPV	15	70	VP1 ₂₉₀₋₃₀₄	NPYPISFLLDLINR	15
42	VP1 ₁₃₃₋₁₄₇	AGKPVQGTFSHFFSV	15	71	VP1 ₃₀₀₋₃₁₄	DLINRRTPRVDGQPM	15
43	VP1 ₁₄₃₋₁₅₇	HFFSVGGAELELQGV	15	72	VP1 ₃₁₀₋₃₂₁	RVDDGQPMYGMDAQV	15
44	VP1 ₁₅₁₋₁₆₅ I	ALELQGVLFNYRTKY	15	73	VP1 ₃₁₉₋₃₃₁	MAQVEEVVFEFEGTE	14
45	VP1 ₁₅₁₋₁₆₅ II	ALELQGVLFNYRTTY	15	74	VP1 ₃₂₇₋₃₄₁ I	FEGTEELPGDPMMR	15
46	VP1 ₁₆₁₋₁₇₅ I	YRTKYPDGTIFPKNA	15	75	VP1 ₃₂₇₋₃₄₁ II	FEGTEQLPGDPMMR	15
47	VP1 ₁₆₁₋₁₇₅ II	YRTTYPDGTIFPKNA	15	76	VP1 ₃₃₅₋₃₄₉	GDPDMMRYVDKYGQL	15
48	VP1 ₁₆₁₋₁₇₅ III	YRTTYPHGTIFPKNA	15	77	VP1 ₃₄₁₋₃₅₄	RYVDKYQLQTKML	14

Table 7 Peptide VP1₃₄₋₄₈, alanine-scans and peptide VP1₃₄₋₄₈ variants with decreasing length

Name	Sequence	Length	Name	Sequence	Length
VP1 20	VDSITEVECFLTPEM	15	20 Ala.14	VDSITEVECFLTPEM	15
20 Ala.1	ADSITEVECFLTPEM	15	20 Ala.15	VDSITEVECFLTPEA	15
20 Ala.2	VASITEVECFLTPEM	15	VP1 20-1	VDSITEVECFLTPE	14
20 Ala.3	VDAITEVECFLTPEM	15	VP1 20-2	VDSITEVECFLTP	13
20 Ala.4	VDSATEVECFLTPEM	15	VP1 20-3	VDSITEVECFLT	12
20 Ala.5	VDSIAEVECFLTPEM	15	VP1 20-4	VDSITEVECFL	11
20 Ala.6	VDSITAVECFLTPEM	15	VP1 20-5	VDSITEVECF	10
20 Ala.7	VDSITEAECFLTPEM	15	VP1 20-6	VDSITEVEC	9
20 Ala.8	VDSITEVACFLTPEM	15	VP1 1-20	DSITEVECFLTPEM	14
20 Ala.9	VDSITEVEAFLTPEM	15	VP1 2-20	SITEVECFLTPEM	13
20 Ala.10	VDSITEVECALTPEM	15	VP1 3-20	ITEVECFLTPEM	12
20 Ala.11	VDSITEVECFATPEM	15	VP1 4-20	TEVECFLTPEM	11
20 Ala.12	VDSITEVECFAPEM	15	VP1 5-20	EVECFLTPEM	10
20 Ala.13	VDSITEVECFATAEM	15	VP1 6-20	VECFLTPEM	9

Table 8 Other peptides and proteins

Name	Type	Source
VP1/Virus like particles (VLP1)	JCV protein	Life science Inkubator
Tetanus toxoid (TTx)	Protein	Novartis, Behring
BKV VP1 ₄₂₋₅₆	Peptide (VDAITEVECFLNPEM)	Peptides and elephants
JCV VP1 ₃₆₋₄₈	Peptide (SITEVECFL)	Peptides and elephants
JCV VP1 ₁₀₀	Peptide (ILMWEAVTL)	Peptides and elephants

2.2.5 Antibodies

Table 9 T cell receptor beta chain antibodies from Muraro 2000 (153)

Name	Clone	IMGT gene name	Conjugate	Company
Vbeta 1	BL37.2	TRBV9	PE	Immunotech
Vbeta 11	C21	TRBV25-1	FITC	Immunotech
Vbeta 12	VER2.32.1	TRBV10-3	PE	Beckman Coulter
Vbeta 13.1	IMMU 222	TRBV6-5 – 6-9	PE	Beckman
CoulterVbeta 13.6	IMMU 222/JU74.3	TRBV6-6	FITC	Beckman Coulter
Vbeta 14	CAS1.1.3	TRBV27	PE	Immunotech
Vbeta 16	TAMAYA1.2	TRBV14	FITC	Immunotech
Vbeta 18	BA62.6	TRBV18	PE	Beckman Coulter
Vbeta 2	MPB2D5	TRBV20-1	PE	Beckman Coulter
Vbeta 20	ELL1.4	TRBV30	PE	Beckman Coulter
Vbeta 21.3	IG125	TRBV11-2	FITC	Immunotech
Vbeta 22	IMMU 546	TRBV2	FITC	Beckman Coulter
Vbeta 23	AF23	TRBV13	PE	Beckman Coulter
Vbeta 3	CH92	TRBV28	FITC	Immunotech
Vbeta 5.1	IMMU157	TRBV5-1	FITC	Immunotech
Vbeta 5.2	36213	TRBV5-6	FITC	Immunotech
Vbeta 5.3	3D11	TRBV5-5	PE	Immunotech
Vbeta 6.7	OT145	TRBV7-2	FITC	Pierce Endogen
Vbeta 7	ZOE	TRBV4-1-4-3	PE	Immunotech
Vbeta 8	56C5.2	TRBV12-3	FITC	Beckman Coulter
Vbeta 9	FIN9	TRBV3-1	PE	Beckman Coulter

Table 10 Antibodies for flow cytometry and immunofluorescence

Specificity	Conjugate	Clone	Company	Catalog number
CCR4 (CD194)	AlexaFluor®647	TG6/CCR4	Biologend	#335401
CCR5 (CD195)	FITC	HEK/1/85a	Biologend	#313705
CD25	BV421	BC96	Biologend	#302629
CD27	APC-Cy7	M-T271	BD Pharmingen	#560222
CD3	PE-Cy7	UCHT1	eBioscience	#25-0038
CD3	PE	UCHT1	Dako	#R0810

Specificity	Conjugate	Clone	Company	Catalog number
CD4	APC	RPA-T4	eBioscience	#17-0049
CD4	PE	L3T4	eBioscience	#12-0049
CD45RO	APC	UCHL1	Biologend	#304210
CD45RO	FITC	UCHL1	Biologend	#304204
CD8	Pacific Blue	DK25	Dako	#PB 984
CXCR3 (CD183)	Pacific Blue	TG1/CXCR3	Biologend	#334907
HLA-II DR	APC	L243 (G46-6)	BD Pharmingen	#347403
HLA-II DQ	PE	HLADQ1	Biologend	#318106
IFN- γ	-	polyclonal IgG	AbD Serotec	#AHP775
IFN- γ	FITC	4S.B3	BD Pharmingen	#554551
IL-17	AlexaFluor®647	eBio64DEC17	eBioscience	#51-7179
IL-4	-	MP4-25D2	Biologend	#500801
IL-4	PE	8D4-8	Biologend	#500703
IL-4	PE-Cy7	8D4-8	eBioscience	#25-7049

Table 11 Isotype control antibodies for flow cytometry and immunofluorescence

Isotype	Conjugate	Clone	Company	Catalog number
Mouse IgG1	PE-Cy7	-	eBioscience	#25-4714
Mouse IgG1	AlexaFluor®647	-	eBioscience	#51-4714
Mouse IgG1	FITC	MOPC-21	BD Pharmingen	#554679
Mouse IgG1	PB	MOPC-21	Biologend	#400131
Mouse IgG1	PE	MOPC-21	BD Pharmingen	#550617
Mouse IgG2a	APC	X39	BD Pharmingen	#340473
Mouse IgG2b	AlexaFluor®647	MPC-11	Biologend	#400330
Rabbit IgG	-	Polyclonal	Dianova	#011-000-003
Rat IgG1	-	RTK2071	Biologend	#400401
Rat IgG1	PE	-	eBioscience	#12-4301
Rat IgG2a	FITC	RTK2758	Biologend	#400505
Rat IgG2a	PE	R35-95	BD Pharmingen	#554689
Rat IgM	FITC	-	eBioscience	#11-4341

Table 12 Secondary antibodies for immunofluorescence

Antigen	Label	Host	Company	Catalog number
Rat Ig	Dy549	Donkey	Jackson	712-506-150
Rabbit Ig	Dy488	Donkey	Jackson	711-486-152

2.2.6 RNA isolation, cDNA synthesis and PCR

Reagent	Company	Catalog number
DEPC	Sigma-Aldrich	#D5758
dNTP Mix, 2 mM each	Fermentas	#R0242
Exonuclease I (Exo I)	Fermentas	#EN0581
FastAP™ Thermosensitive Alkaline Phosphatase	Fermentas	#EF0651
Maxima Hot Start Taq DNA Polymerase	Fermentas	#EP0602
Pfu DNA Polymerase	Fermentas	#EP0571
QIAshredder	Qiagen	#79654
RevertAid™ H Minus First Strand cDNA Synthesis Kit	Fermentas	#K1631, #K1632
RNeasy Mini Kit	Qiagen	#74104
TaqMan® Gene Expression Master Mix	Applied Biosystems	#P/N:4369016
TaqMan® Ribosomal RNA Control Reagents	Applied Biosystems	#4308329

2.2.7 Primer

Table 13 T cell receptor variable beta chain gene primer (forward) obtained from biomers

Primer name	IMGT gene name	Primer Sequence (5'→3')	Reference
1	TRBV9	CGCACAACAGTTCCTGACT	Currier 1996
2	TRBV20-1	TCAACCATGCAAGCCTGA	Currier 1996
4	TRBV29-1	GAGGCCACATATGAGAGTGG	Currier 1996
5A	TRBV5-1	TCAGTGAGACACAGAGAAAC	Currier 1996
5B	TRBV5-3 - 5-8	TGTGTCTGGTACCAACAGG	Currier 1996
6	TRBV7-1 - 7-9	CTCAGGTGTGATCCAATTC	Currier 1996
7	TRBV4-1 - 4-2	CTCAGGTGTGATCCAATTC	Currier 1996
8	TRBV12-3 - 12-5	TCTGGTACAGACAGACCATG	Currier 1996
9	TRBV3-1	CCTAAATCTCCAGACAAAGC	Currier 1996
11	TRBV25-1	TCAACAGTCTCCAGAATAAGGACG	Currier 1996
12	TRBV10-1 - 10-3	CATGGGCTGAGGCTGATC	Currier 1996
13A	TRBV6-6 - 6-9	CGACAAGACCCAGGCATGGG	Currier 1996
13B	TRBV6-4	AGACAAGATCTAGGACTGGG	Currier 1996
14	TRBV27	GTCTCTCGAAAAGAGAAGAG	Currier 1996
15	TRBV24-1	GTGTCTCTCGACAGGCACAG	Currier 1996
16	TRBV14	AGTCTAAACAGGATGAGTCCG	Currier 1996
17*	TRBV19	CAGAAAGGAGATATAGCTGAAGGGTAC	Utz 1996
18	TRBV18	GAGTCAGGAATGCCAAAGGA	Currier 1996
20	TRBV30	CAGCTCTGAGGTGCCCCAGA	Currier 1996
21	TRBV11-1 - 11-3	TCACAGTTGCCTAAGGATCG	Currier 1996
22	TRBV2	GCAGAAAGTCGAGTTTCTGG	Currier 1996

Primer name	IMGT gene name	Primer Sequence (5'→3')	Reference
23	TRBV13	GCAGGGTCCAGGTCAGGACCCCA	Currier 1996
24	TRBV15	ACAATGAAGCAGACACCCCT	Currier 1996
25	TRBV16	TAAGTGCCTCCCAAATTCAC	Currier 1996
GnvB_23*	TRBV23-1	CGCTTCTCCCGATTCTGGAGTCC	Genevee 1992
TRBV20 complete	TRBV20	GGTGCTGCTCTCTCAACATCCGAGC	

Table 14 T cell receptor variable alpha chain gene primer (forward) obtained from biomers

Primer name	IMGT gene name	Primer Sequence (5'→3')	Reference
1A	TRAV8-2 - 8-6	TCTGGTATGTGCAATACCCCAACC	Han 1999
1B	TRAV8-1 -8-3	CTGAGGAAACCTCTGTGCA	Han 1999
2	TRAV12-1 - 12-2	GATGGAAGGTTACAGCACAGCTC	Han 1999
3	TRAV17	CACAGTGAAGATTAAGAGTCACGC	Han 1999
4A	TRAV26-2	AACAGAATGGCCTCTCTGGC	Han 1999
4B	TRAV26-1	GGATTGCGCTGAAGGAAGAG	Han 1999
5	TRAV6	TGAAGGTCACCTTTGATACCACCC	Han 1999
6	TRAV14/DV4	AATCCGCCAACCTGTCTATCTCCG	Han 1999
7	TRAV1-1 - 1-2	AACTGCACGTACCAGACATC	Han 1999
8	TRAV13-1 - 13-2	ACCCTGAGTGTCCAGGAGGG	Han 1999
9	TRAV16	CACTGCTGACCTTAACAAAGGCG	Han 1999
10	TRAV27	TCCTGGTGACAGTAGTTACG	Han 1999
11	TRAV2	AGGCTCAAAGCCTTCTCAGCAGGG	Han 1999
12	TRAV19	TCCACCAGTTCCTTCAACTCACC	Genevee 1992
13	TRAV22	TTCATCAAACCTTGGGGACAGC	Han 1999
14	TRAV38-1 - 38-2/DV8	CCCAGCAGGCAGATGATTCTCGTT	Han 1999
15	TRAV5	GGATAAACATCTGTCTCTGCG	Han 1999
16	TRAV3	AAGGGAATCCTCTGACTGTG	Han 1999
17	TRAV23/DV6	GATAGCCATACGTCCAGATG	Han 1999
18	TRAV24	TGCCACTCTTAATACCAAGGAGGG	Han 1999
19	TRAV41	ACACTGGCTGCAACAGCATC	Han 1999
20	TRAV4	TTACAAACGAAGTGGCCTCC	Han 1999
21	TRAV29/DV5	ACCCTGCTGAAGGTCCTACATTCC	Han 1999
22	TRAV9-1 - 9-2	CTTGGAGAAAGGCTCAGTTC	Han 1999
23	TRAV21	TGCCTCGCTGGATAAATCATCAGG	Han 1999
24	TRAV10	TCCCAGCTCAGCGATTCAGCCTCC	Han 1999
25	TRAV35	GTCCTGTCTCTTGATAGCC	Han 1999
26	TRAV34	AGCCCAGCCATGCAGGCATCTACC	Han 1999
27	TRAV39	TTGATACCAAAGCCCGTCTC	Han 1999
28	TRAV36/DV7	GAACATCACAGCCACCCAGACCGG	Han 1999
29	TRAV30	GCAAAGCTCCCTGTACCTTACGG	Han 1999
30	TRAV20	TTTCTGCACAGCACAGCCC	Han 1999
31	TRAV40	AGCAAAACTTCGGAGGCGG	Han 1999
32	TRAV25	AAGGAGAGGACTTCACCACG	Han 1999
TRAV9 complete	TRAV9	GGAAATTCAGTGACCCAGATGGAAGGGC	

Table 15 T cell receptor constant alpha and beta chain genes primer (reverse) obtained from biomers

Primer name	IMGT gene name	Primer Sequence (5'→3')
TRAC1*FAM	TRAC	GCAGACAGACTTGTCCTGG
TRAC3	TRAC	GTTGCTCTTGAAGTCCATAGACC
TRBC1*FAM	TRBC1+2	TTGGGTGTGGGAGATCTCTGC
TRBC3	TRBC1+2	GACAGCGGAAGTGGTTGCGGGGGT

Table 16 Quantitative real time PCR TaqMan® Gene Expression Assays from Applied Biosystems

ID	Gene	Conjugate
Hs00203436_m1	TBX21/T-bet	FAM
Hs00231122_m1	GATA3	FAM

2.2.8 ELISA

Name	Company	Catalog number
Anti-human IgG Biotin	eBioscience	#13-4998
Avidin-HRP	eBioscience	#18-4100
IFN-γ ELISA Kit	Biosource Invitrogen	#090401
IL-4 ELISA Kit	Biosource Invitrogen	#CHC1283
Substrate Reagent Pack (A+B)	R&D Systems	#895000 #895001
TMB Single Solution	Invitrogen	#00-2023

2.2.9 Consumables

Name	Company
Cell culture flasks	Sarstedt
Cell culture plates	Greiner, Sarstedt
Cell strainer (40, 70 and 100 μm)	BD
Cover slips (15 – 50mm)	Menzel
Eppendorf tubes	Eppendorf
ELISA EIA/RIA plates	Costar, 9018
FACS tubes, 5 ml	Sarstedt 55.1579
Falcon tubes, 15 and 50 ml	BD
Filtermat A (GF/C)	Perkin-Elmer 1450-421
Filtermat bag	Perkin-Elmer 1450-432
Liquid reservoir for multichannel pipettes	Roth
Multiplay-PCR plate, 96 well, half margin	Sarstedt
Pipette tips	Sarstedt
Pipettes (2, 5, 10 and 25 ml)	Greiner, Sarstedt
Syringes and needles	BD and Braun
Syringe filter, 0.22μm	Roth

2.2.10 Equipment

Name	Company
ABI Prism 7900	Applied Biosystems
Axiovert 40	Zeiss
Beta counter, 1450 Microbeta	Perkin-Elmer
Centrifuges	Eppendorf and Heraeus
Electrophoresis Unit, SE260 mighty small II	Hoefer (#SE260-10A-.75)
Filtermat Cassettes	Perkin-Elmer
FlexCycler	AnalytikJena
Freezers	Liebherr and Sanyo
Freezing Container, Nalgene Cryo 1°C	Roth
Fridges	Liebherr
Gamma irradiator, Cs-137;49.2 TBq, Biobeam 2000	Eckert & Ziegler
Harvester 96 MACH III M	Tomtec
Heat Sealer 1295-012	Wallac
Incubator, (Hera Cell 240)	Thermo Scientific
LSRII FACS analyser	BD Bioscience
Microscope Axiovert 40	Zeiss
Nitrogen tank	Tec-lab
Nanodrop Nd-1000	Peqlab
Pipets	Gilson, Eppendorf
Sterile bankSafe 2020	Thermo Scientific
Thermomixer	Eppendorf
UV Transilluminator	Peqlab
Wallac Victor 1420 multilabel plate reader	Perkin-Elmer

2.2.11 Software

Name	Company
AxioVision 4.6	Zeiss
FACSDiVa analysis software	BD Biosciences
FlowJo FACS analysis software	TreeStar Inc.
IMGT/V-Quest V 3.2.20 (26 July 2011)	www.IMGT.org
PRISM Graphpad V5.02	Graphpad Software Inc.
Peak Scanner software V1.0	Applied Biosystems
SDS V2.4	Applied Biosystems

2.3 Methods

2.3.1 Brain, blood and CSF sample preparation and cell expansion

Biological samples were obtained after informed written consent. Peripheral blood mononuclear cells (PBMCs) were separated from EDTA-blood by Ficoll (#J15-004, PAA) density gradient. Cerebrospinal fluid (CSF)-derived mononuclear cells were directly obtained by centrifugation of diagnostic spinal tabs. To isolate brain-derived mononuclear cells, brain tissue was cut into small pieces and disrupted by incubation in a solution containing 1 mg/ml collagenase A (#10103578001, Roche) and 0.1 mg/ml DNase I (#11284932001, Roche) at 37°C in a water bath for 45 min. The resulting cell suspension was washed three times, and cells separated using a Percoll density gradient (#17-0891-01, GE Healthcare). Cells were resuspended in a 30% Percoll solution and carefully underlayered with a 78% Percoll solution. After centrifugation brain-derived mononuclear cells were gathered from the interface of the gradient.

Peripheral blood-, CSF- and brain-derived mononuclear cells were expanded by seeding 2000 cells/well plus 2×10^5 irradiated (45 Gy) allogeneic feeder cells per well in a 96-well U-bottom microtiter plate in presence of 1 µg/ml phytohemagglutinin-P (PHA, #L9017, Sigma) and 20 IU/ml rIL-2 (Tecin, Roche). IL-2 was added every 3-4 days until day 14.

2.3.2 Neuropathology

Small tissue fragments of a total volume of ~0.1 ml were obtained by open biopsy. Following fixation in buffered formalin for 2 h, tissue was embedded in paraffin. Microtome sections of 4 µm were stained with haematoxylin and eosin, van Gieson's trichrome, periodic acid-Schiff, Turnbull's stain for siderin and Luxol. Immunohistochemical staining was performed on an automated Ventana HX immunohistochemistry system, benchmark (Ventana-Roche Medical Systems) following the manufacturer's instructions using the following antibodies: anti-CD45/LCA (Dako; M701), anti-CD3 (Dako; M1580), anti-CD45RO (Dako; M0742), anti-CD20 (Dako; M0755), anti-CD79a (Dako; M7050), anti-CD68 (Immunotech/Beckmann-Coulter), anti-HLA-DR (Dako; M775), anti-NF (Zymed/Invitrogen; 80742971), anti-GFAP (Dako; Z334) and anti-p53 (Dako; M7001).

2.3.3 Generation of T cell clones

The generation of JCV-specific T cell clones (TCC) is schematically depicted in Figure 3. Brain-derived PHA pre-expanded T cells (2.5×10^4 /well) were incubated in T cell medium (see Buffers, solutions and media 2.2.2) with 2 µg/ml VP1 protein using autologous PBMCs as feeder (1×10^5 /well, 45 Gy

irradiated) as antigen presenting cells. After 7 days plates were splitted in mother and daughter plates. One plate was used for a ^3H -thymidine incorporation assay to identify proliferating VP1-specific colonies. Positive wells were then identified in the corresponding plate and rIL-2 (20 IU/ml) (Roche, Tecin) was added. On day 12 cells were restimulated with VP1 and autologous feeders for another VP1-specific expansion round and the addition of IL-2 was repeated every 3-4 days until day 12 (enrichment step). These pre-expanded T cells were then seeded per limiting dilution (1 cell/well and 0.3 cells/well, respectively) and restimulated with PHA (1 $\mu\text{g}/\text{ml}$) and allogeneic feeders (2×10^5 cells/well, 45 Gy irradiated) for 14 days to generate clonal cell lines. Growing colonies were analysed for their clonality and VP1-specificity.

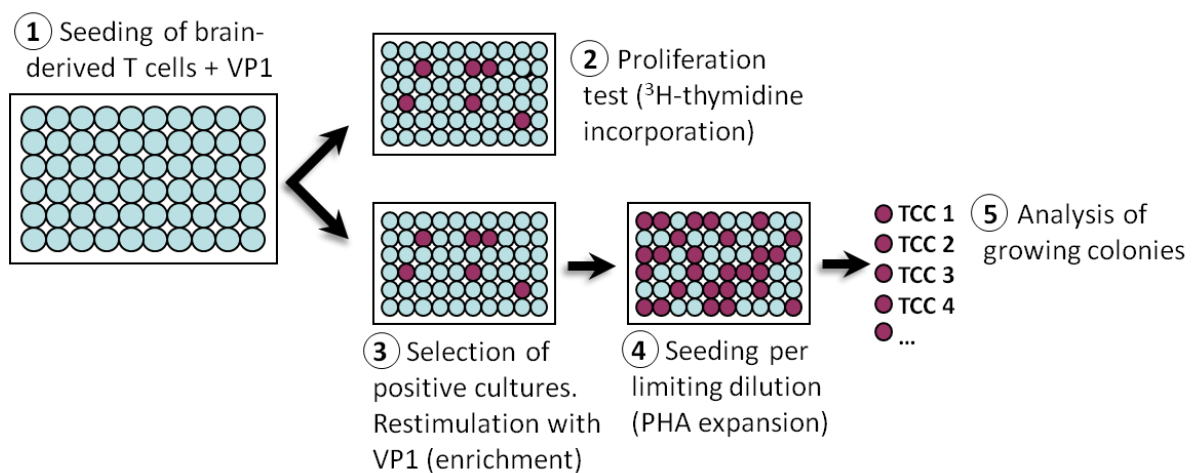


Figure 3 Generation of VP1-specific T cell clones. Step 1 specificity test for VP1. Step 2 proliferation test. Step 3 selection and restimulation of wells containing VP1-specific T cells (enrichment phase). Step 4 seeding T cells per limiting dilution (1 and 0.3 cells/well, respectively). Step 5 analyses of growing colonies for clonality, VP1-specificity, etc.

2.3.4 T cell expansion for high cell numbers

The strategy for expansion of TCC to obtain as much cells as possible basically refers to the protocol of Geiger and coworkers (154). In brief, TCC were seeded in 96-well plates at a density of 2000 cells/well plus 2×10^5 allogeneous feeders. PHA (1 $\mu\text{g}/\text{ml}$) and IL-2 (500 U/ μl , kindly provided by Federica Sallusto, Institute for Research in Biomedicine, Bellinzona, CH) were added at the day of seeding. At day 7 and 10 cells were transferred into 48-well and 24-well plates, respectively. IL-2 was renewed at day 3, 7, and 10. After 14 days cells were cryo-preserved or restimulated.

2.3.5 Generation of EBV-transformed B cell lines

Generation of EBV-containing culture supernatants

B95.8 cells were seeded in a 48-well plate at a density of 1×10^6 cells/ml in RPMI containing 10% FCS and 1% Pen/Strep. Upon color change of medium, cells were subsequently transferred into larger plates and flasks. When sufficiently expanded (>60 ml medium) B95.8 cells were incubated without medium change for accumulation of EBV (Ebstein-Barr virus) particles that are shed into the supernatant. After 10 days supernatant was harvested and centrifuged with 400 g for 15 minutes and afterwards filtrated (0.45 μ m) to remove cellular debris. Aliquots were stored at -80°C .

Generation of immortalized B cell lines

In order to obtain immortalized autologous B cell lines, which can be used as antigen presenting cells, PBMCs were infected with EBV. Therefore, $\sim 1 \times 10^6$ PBMCs were incubated in 2.5 ml B cell medium together with 2.5 ml EBV containing supernatant for 2 h at 37°C in a waterbath. Subsequently, cells were transferred into a 25 cm^2 flask and filled up with B cell medium to obtain a total volume of 10 ml. OKT3 (1 $\mu\text{g}/\text{ml}$, #BE001-2, BioXell) was added to kill T cells by a strong stimulus without additional co-stimulatory signal. Immortalized B cells were transferred into larger flasks when cell clusters were visible and medium color changed to yellow. Efficiency of transformation was validated by flow cytometry.

2.3.6 Proliferation Assays

All proliferation tests were performed in 96-well U-bottom microtiter plates using x-VIVO15 medium (#BE04418F, Lonza) for incubation of the cells. If not indicated otherwise proliferation was measured by ^3H -thymidine (#MT6038E, Hartmann Analytic) incorporation. ^3H -thymidine was added 15h prior harvesting of the cells. Stimulatory indices (SI) were calculated by dividing the mean CPM (counts per minute) of the wells plus antigen by the mean CPM of the wells without antigen.

The **primary proliferative response** of PBMCs to VP1 (kindly provided by Viktorya Demina, Life Science Inkubator, Bonn, Germany) and Tetanus toxoid (TTx, Novartis, Marburg, Germany) was tested by seeding 2×10^5 cells in a 96-well U-bottom microtiter plate. VP1 was used at a concentration of 2 $\mu\text{g}/\text{ml}$ and TTx at 5 $\mu\text{g}/\text{ml}$. After 7 days incubation, proliferation was measured.

The **fine-specificity** of VP1-specific T cell clones was tested between day 11 and 14 after PHA-expansion. Therefore, all peptides derived from the VP1 protein (Table 6) were tested in duplicates using 10 μM . Clone cells were seeded at a density of 2.5×10^4 cells/well plus 5×10^4 cells/well of an autologous, EBV-transformed B cell line (irradiated with 200 Gy). Proliferation was measured 72h after stimulation with antigen by ^3H -thymidine incorporation. **Alanine-scans** and **truncation experiments** of peptide VP1₃₄₋₄₈ were conducted similar. Peptides listed in Table 7 were used.

Antigen-sensitivity of TCC (2.5×10^4 cells/well) was measured by using declining concentration of congenital antigen. In 1:2 serial dilution steps starting with 10 μ M, ending with the lowest concentration of 0.01 μ M. Peptides were tested in duplicates. Autologous EBV-transformed B cell lines (5×10^4 cells/well, irradiated with 200 Gy) were used as antigen-presenting cells. Proliferation was measured 72h after antigen stimulation by 3 H-thymidine incorporation.

For assessing the **HLA-class II restriction**, bare lymphocyte syndrome (BLS) cells were used as antigen-presenting cells (5×10^4 cells/well, irradiated with 300 Gy). BLS cells were either untransfected or transfected with a vector containing single HLA-II molecules such as DQW6 (DQB1*060:2), DR2A (DRB5*01:01) and DR2B (DRB1*15:01) as described previously (152). Other alleles (DRB1*11:03) were tested with HLA-matched PBMCs (donor haplotype: DRB1*08:01, DRB1*11:03, DRB3*02:02, DQA1*04:01, DQA1*05:xx, DQB1*03:01, DQB1*04:02) at a concentration of 1×10^5 cells/well, irradiated with 35 Gy. The cognate peptide of each T cell clone was used as antigen at a concentration of 10 μ M. Clone cells were seeded with 2.5×10^4 cells/well. Proliferation was measured 72h after antigen stimulation by 3 H-thymidine incorporation.

To measure **proliferative responses** to VP1 and TTx by **flow cytometry** the CellTrace™ CFSE Cell Proliferation Kit (#C34554, Invitrogen) was used. Therefore, 1×10^5 PBMCs/well were seeded together with VP1 (2 μ g/ml) and TTx (5 μ g/ml). Cell were restimulated with antigen after six days and treated with CFSE following the manufacturer's instruction. In brief cells were incubated in 10 ml 1 μ M CFSE for 10 minutes incubation in a water bath 37°C. CFSE-labeling was stopped by adding 1 ml FCS (#S0115, Biochrome). Then cells were seeded again in a 96-well U-bottom plate together with appropriate antigen. After five days cells were stained with anti-CD4 (Biolegend), anti-CD3 (eBioscience), anti-CD25 (Biolegend), and anti CD45RO (Biolegend) and subsequently analysed by flow cytometry.

2.3.7 Immune fluorescence staining

Cover slips were placed into 24-well plates and coated with a 1:10 dilution of Poly-L-Lysine (#P4707, Sigma) for 1h at 37°C. All incubation steps were followed by washing the cover slips at least three times with PBS. PBMCs or brain-derived T cells were seeded in 300 μ l X-VIVO™15 medium (#BE04418F, Lonza) and stimulated with PMA (50 ng/ml, #P1585, Sigma) and ionomycin (1 μ g/ml, #I0634, Sigma) for 5 h at 37°C. Cytokine secretion was blocked by the addition of Brefeldin A (10 μ g/ml, #00-4506, eBioscience). Cells were fixed by adding 500 μ l IC fixation buffer (#00-8222, eBioscience) and they were kept overnight at 4°C in PBS containing 0.1% BSA (#K45-001, PAA). Next, cells were permeabilized with a 1:10 dilution of Permeabilization Buffer (#00-8333, eBioscience) for 30 min at room temperature and stained with 0.3 μ g/ml anti-IFN- γ antibody (#AHP775, AbD Serotec),

16 µg/ml anti-IL-4 antibody (#500801, Biolegend) and 1:50 dilution of Hoechst33258 (#B1155, Sigma) that stains nuclei. Isotype controls were used at the same concentration as primary antibodies (#400401, Biolegend and #011-000-003, Dianova). After incubation for 2 h at room temperature, the cover slip was placed on a drop of FluomountG (#0100-01, Southern Biotec) with the cell layer upside down. Immunofluorescence was analysed with an Axiovert 40 (Zeiss) and captured with AxioVision software 4.6 (Zeiss).

2.3.8 Cytokine assessment

The production of cytokines by TCC and PHA-expanded bulk T cell populations was analysed by supernatant ELISA (enzyme linked immunosorbent assay) and intracellular cytokine staining (ICS). Supernatants were collected 72h after PHA-restimulation. IFN-γ and IL-4 were detected by use of ELISA kits from Biosource (IL-4 #CHC1283, IFN-γ #090401, Invitrogen) following the manufacturers instruction.

Cytokine detection by intracellular cytokine staining was performed between day 12 and 14 after PHA-restimulation of brain-derived T cells. Cells were stimulated with PMA (50 ng/ml, #P1585, Sigma) and ionomycin (1mg/ml, #I0634, Sigma) in the presence of Brefeldin A (10 µg/ml, #00-4506, eBioscience) for 5 h. After incubation steps cells were washed with FACS buffer. Cells were stained with LIVE/DEAD Fixable Dead Cell Stain Kit (#MP 34955, Invitrogen). For fixation cells were then incubated 20 min at room temperature with IC fixation buffer (#00-8222, eBioscience), followed by 30 min of permeabilization with PermBuffer (#00-8333, eBioscience). Staining was conducted in FACS buffer for 30 minutes with the following antibodies: anti-CD3 (PE, #R0810, Dako), anti-CD8 (PB, #PB 984, Dako), anti-IFN-γ (FITC, #554551, BD), anti-IL-4 (PE-Cy7, #25-7049 eBioscience), anti-IL-17A (Alexa Fluor647, #51-7179, eBioscience) and the appropriate isotype controls.

For determination of cytokine production after antigen stimulation PBMCs were preincubated in 96-well plates in X-Vivo15 (Lonza) medium at a density of 1×10^5 /well in triplicates. Cells were either stimulated with VP1 (1.5 µg/ml), TTx (5 µg/ml), or without antigen. Six days after seeding cells were restimulated with appropriate antigen in the evening and after 1h 10 µg/ml Brefeldin A (eBioscience) was added. Cells were incubated overnight (15h), then fixation, permeabilization, and staining followed as described above.

2.3.9 Detection of JC viral load

Results of the assessment of viral load in CSF, serum and urine of patient 1 were provided by Dr Eugene O. Major, Laboratory of Molecular Medicine and Neuroscience, NINDS, NIH, Bethesda, USA. JCV loads were quantified by PCR-based molecular assays as described previously (155, 156) and in

the laboratory of Prof. H. H. Hirsch (Transplantation Virology, Institute for Medical Microbiology, Department of Biomedicine, University of Basel, Switzerland). JCV loads were quantified by PCR-based molecular assays as described previously (157).

The detection of JC viral load of CSF of patient 3 was performed in the laboratory of Rosina Girones (University of Barcelona, Department for Microbiology, Spain) using qT-RT PCR methods as previously described (158).

2.3.10 ELISA for the detection of anti-VP1 IgG

ELISA plates were coated with 2 µg/ml VP1 protein in 100 µl coating buffer (15 mM Na₂CO₃, 35 mM NaHCO₃, 3 mM NaN₃) over night at 4°C. After every incubation step, plates were washed 3-5 times with ELISA washing buffer (0.05% Tween20 in PBS). Blocking was accomplished with 200 µl/well ELISA blocking buffer (5% non-fat powdered milk in 25 mM Tris and 150 mM NaCl) for 1 h at 37°C. Serum and CSF samples were diluted in blocking buffer (1:200 – 1:10.000). 100 µl/well diluted samples were added and plate incubated for 2 h at 37°C. Then 100 µl of a 1:1000 dilution of anti-human IgG biotin antibody (#13-4998, eBioscience) in blocking buffer was applied and incubated for 2 h at 37°C. Avidin-HRP (#18-4100, eBioscience) was added at a dilution of 1:1000 in 100 µl/well. Incubation time was 1 h at 37°C. This was followed by development of plates by mixing substrate solution A with substrate solution B (#895000/1, R&D Systems) at a 1:1 ratio and pipetting 100 µl/well. The enzymatic reaction was stopped after 15 minutes by addition of 1.8 N H₂SO₄. Analysis was performed directly after development in a Wallac Victor 1420 Multilable Plate Reader (Perkin Elmer) at a wavelength of OD450.

2.3.11 Flow Cytometry Analysis

Whole blood stainings were performed by adding 50 µl of a 3x concentrated antibody cocktail to 100 µl blood. The mixture was incubated for 30 minutes at room temperature, followed by 10 minutes of red blood cell lysis with FACS Lysing Solution (#349202, BD). After washing, the samples were analysed by flow cytometry in a LSR II (BD). The following antibodies were used:

CD25 (Biolegend, #302629), CD27 (BD, #560222), CD3 (eBioscience, #25-0038), CD4 (eBioscience, #17-0049, #12-0049), CD45RO (Biolegend, #304210, #304204), CD8 (Dako, #PB 984) and appropriate isotype controls.

Surface stainings of PBMC and TCC were achieved similarly. 0.5-1x10⁶ Cells were stained in 100 µl FACS buffer and fixed with 1% PFA. The following antibodies were used: CCR4 (Biolegend, #335401), CCR5 (Biolegend, #313705) CXCR3 (Biolegend, #334907), HLA-II DR (BD Pharmingen, #347403), HLA-II

DQ (Biolegend, #318106) and appropriate isotype controls (#400131, #400330, #400505 Biolegend, #340473, #550617 BD Pharmingen).

2.3.12 HLA-A*02:01/JCV36 JCV100 tetramer staining

HLA-A*02:01 tetrameric complexes were synthesized by Louise Jones in the laboratory of Graham Ogg (Weatherall Institute of Molecular Medicine, University of Oxford) as previously described (159). Briefly, HLA-A*02:01, β 2 microglobulin and epitope peptide were refolded and isolated using size exclusion chromatography. Tetramers were loaded with two immunodominant, HLA-A*02 restricted CD8+ T cell peptides (119, 120) (Table 8). Site-specific biotinylation was achieved through addition of the BirA target sequence to the last C terminal extracellular domain of the HLA-A*0201 molecule. Tetrameric complexes were generated using Extravidin-PE (Sigma).

PHA- expanded brain biopsy cells were used 14 days after restimulation and activated with anti-CD2/CD3/CD28 MACs beads (#130-091-441, Miltenyi Biotec) for 5 days. Cells were washed and resuspended to a concentration of 5×10^6 cells/ml. 100 μ l were stained with 3 μ l of PE-coupled tetrameric HLA-A*02:01/JCV VP₁₃₆ or HLA-A*02:01/JCV VP₁₀₀. After 30 min incubation at 37°C, the cells were washed and stained with anti-CD3 (PB, #R0810, eBioscience) and anti-CD8 (FITC, #F0765, Dako) for additional 30 min on ice. Cells were then washed and fixed with 0.5% paraformaldehyde before analysis by flow cytometry.

2.3.13 TRBV receptor analysis by flow cytometry

TCR V β chain analysis by flow cytometry was performed for rapid assessment of clonality of TCC and to monitor expansions of brain-derived T cells in bulk populations after several stimulation rounds. Therefore cells were used 12-14 days after last PHA-restimulation and stained for 20 minutes on ice with 22 different TRBV (T cell receptor variable beta chain) antibodies (153) (Immunotech and Beckman Coulter, Table 9) together with anti-CD4 (APC, #17-0049, eBioscience) and anti-CD8 (PB, #PB984, Dako). Analysis was performed on a LSR II (BD).

2.3.14 RNA isolation and generation of cDNA

14 days after restimulation $1-2 \times 10^6$ TCC cells were centrifuged at 450 g. The cell pellet was resuspended in 350 μ l RLT buffer (RNeasy Mini Kit, #74104, Qiagen) and frozen at -80°C until further processing of the sample. In case of RNA isolation for quantitative real time PCR (qRT-PCR) TCCs were stimulated with PMA (50 ng/ml, Sigma) and ionomycin (1 μ g/ml, Sigma) overnight prior to resuspension in RLT buffer. Isolation of RNA was conducted following the manufacturers instruction

(RNeasy Mini Kit, #74104, Qiagen) without addition of β -mercaptoethanol. For homogenization of the lysate QIAshredder columns (#79654, Qiagen) were used. RNA concentration was assessed on a Nano Drop (ND1000 v3.5.2, Thermo Fisher). Processed RNA was stored at -80°C . Reverse transcription from RNA to cDNA was performed using Revert Aid™ H Minus First Strand cDNA Synthesis Kit (#K1631/2, Fermentas) following the manufacturer's protocol. 1 μg RNA was transcribed to cDNA. Either oligo dT primer or random hexamer primers were used in case of cDNA synthesis for qRT-PCR. cDNA was stored at -20°C .

2.3.15 Quantitative real time PCR analysis

For the detection of mRNA levels of the transcription factors GATA3 and Tbet TaqMan® Gene Expression Assays (Tbet, Hs00203436_m1 and Gata3, Hs00231122_m1, Applied Biosystems) were applied. The transcription level of ribosomal 18srRNA (#4308329, Applied Biosystems) was used as endogenous control. One qT-RT PCR sample consisted of 2 μl 1:5 diluted cDNA, 0.5 μl TaqMan Gene Expression Assay mix, 5 μl TaqMan Gene Expression Master Mix (#P/N:4369016) plus and 2.5 μl RNase-free H_2O . qT-RT PCR was run on a ABI Prism 7900 (Applied Biosystems). Relative gene expression was calculated by the $\Delta\Delta\text{Ct}$ method defining brain-derived PHA-expanded cells as calibrator. Data were analysed with the program SDS V2.4 (Applied Biosystems).

2.3.16 TRAV and TRBV chain PCR

If not indicated otherwise, the T cell receptor variable alpha (TRAV) chain repertoire was assessed by use of a primer set published by Han et al. (160), while the T cell receptor variable beta (TRBV) chain primer set was based on a publication of Currier and co-workers (161) (Table 13 and Table 14). The nomenclature used in this work follows the rules of IMGT (ImMunoGeneTics, www.IMGT.org). PCR amplification was performed in 50 μl reaction volume containing 1x HotStart PCR Buffer, 200 μM dNTP (#R0242, Fermentas), 2.5 mM MgCl_2 , 1.25 μM C3 primer, 1.25 U Maxima Hot Start Taq DNA Polymerase (#EP0602, Fermentas), 1.25 μM forward primer and 1 μl of 1:10 diluted cDNA. The PCR protocol involved an initial denaturation of 4 min at 95°C and 35 cycles of 95°C 30 s, primer annealing 60°C 20 s and primer extension at 72°C for 60 s, terminated by a final extension at 72°C for 10 min. The PCR product was validated by electrophoresis in a 1.5% agarose gel (1.5 g agarose in 100 ml TAE buffer).

2.3.17 Direct sequencing of TRAV and TRBV PCR amplified products

Sample preparation for sequencing was performed with 5 µl of PCR product described in 2.3.16. The PCR product was incubated with 10 u exonuclease I (#EN0581, Fermentas) and 1 u FastAP thermosensitive alkaline phosphatase (#EF0651, Fermentas) in a reaction volume of 6.5 µl for 15 min at 37°C. The reaction was terminated by heating for 15°C at 85°C. After the addition of 5 pmol of C3 primer (see Table 13 and Table 14) direct sequencing of the PCR products was carried out with fluorescent dideoxy terminators, and analysis was performed on an ABI 3130 Genetic Analyzer and with Sequence Analysis v 5.4 software (Applied Biosystems) at the bioanalytics facility, ZMNH, Hamburg.

2.3.18 CDR3 spectratyping

For assessment of the CDR3 length, the product of the PCR described in 2.3.16 was subjected to a second PCR (run-off), which was composed of 1x Pfu Buffer containing MgSO₄, 200 µM dNTPs (#R0242, Fermentas), 0.1 µM C1-FAM labeled primer (see table 15), 0.5 U Pfu DNA polymerase (#EP0571) and 5 µl of first PCR product in a reaction volume of 20 µl. The run-off PCR consisted of 5 cycles repeating 2 min at 95°C, 2 min 60°C and 10 min 72°C. Subsequently the run-off products were cleaned with microclean (Biofidal) and, thereafter, 1 µl (0.1 - 3) of each reaction was mixed with 10 µl formamide containing GeneScan LIZ 600 Size Standard (Applied Biosystems) in a 96-well plate. After denaturation at 95°C for 5 min followed by incubation at 4°C for 5 min, the samples were analyzed using a 3130 Genetic Analyzer (Applied Biosystems). Spectratype analysis was performed with Peak Scanner software V1.0 from Applied Biosystems. The percent contribution of each TCC's TRBV or TRAV CDR3 peak in a CDR3 spectrum was calculated according to the formula $\%AUC V_n = (AUC V_n / \sum AUC \text{ all } V) \times 100$. Since for each TCC two different %AUC were obtained corresponding to TRBV and TRAV, in order to estimate conservatively, we considered always the lowest one and if several TCCs shared the same TRAV or TRBV CDR3 the %AUC was divided by the number of known TCCs contributing to the peak.

2.3.19 Statistical analysis

Statistical analysis was performed using Graph Pad Prism V5.02. After testing for Gaussian distribution (Kolmogorov-Smirnov test) either student's t test or Mann-Whitney U test was used for comparison of two groups of non-paired samples. For comparison of more than two unpaired sample groups ANOVA for non-parametrical (Kruskal-Wallis) data and post hoc test (Dunns Test) was performed.

3 Results

3.1 Analysis of the functional phenotype, fine specificity, and TCR-peptide-MHC interaction of brain-infiltrating CD4+ T cells during PML-IRIS

3.1.1 A case of natalizumab-associated PML-IRIS

A 43-year old relapsing-remitting MS patient (patient 1) showed first signs of PML after 40-month of natalizumab treatment Figure 4. The therapy was stopped immediately and several rounds of plasmapheresis were performed to wash out residual anti-VLA4 antibodies. Subsequently, the patient developed PML-IRIS accompanied by deterioration of his condition. Due to difficulties to prove the diagnosis PML by CSF JC virus DNA PCR Figure 4 and to rule out another inflammatory disease of the CNS, a diagnostic brain biopsy was performed. Neuropathological examination of the brain tissue revealed a paucity of CNS cells and massive immune cell infiltration, but a lack of typical signs of PML so that the diagnosis could not be confirmed (Figure 5). Eventually, PML was verified by a positive PCR slightly above the threshold (12 copies JCV DNA/ml CSF, E. O. Major, NINDS, NIH Bethesda, USA) (Figure 4) and later also by positive in situ hybridization and immunohistochemistry.

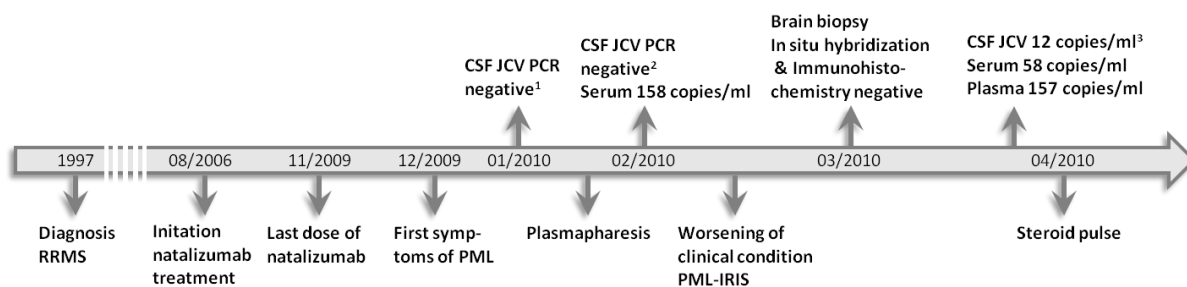


Figure 4 PML disease course of patient 1. ¹⁾ Results provided by the Virology Department University Medical Center Eppendorf, Hamburg. ²⁾ Results provided by Prof. H. Hirsch, University of Basel. ³⁾ Results provided by Dr. E.O. Major, NINDS, NIH, Bethesda.

Neuropathological examination failed to show the typical signs of PML, i.e. nuclear inclusions in hyperchromatic oligodendrocytes and bizarre astrocytes, but rather a paucity of CNS cells and massive perivascular and parenchymal lymphomononuclear infiltrates (Figure 5A), reactive gliosis with stellate astrocytes (Figure 5B) and predominance of diffuse and destructive parenchymal infiltrates of foamy macrophages (Figure 5C). The majority of cells stained positive for MHC-class II (HLA-DR), which is usually exclusively found on activated microglia and absent in normal brain tissue (Figure 5D). T cells (Figure 5E) and B cells (Figure 5G) were present in the infiltrate, and a high proportion of the latter stained positive for the plasma cell marker CD138 (Figure 5H). Part of the biopsy tissue was processed, and CNS-derived mononuclear cells were also characterized by flow

cytometry. Cells expressed the pan-hematopoietic cell marker CD45 (data not shown) and among them 42% expressed the pan-T cell marker CD3+ (Figure 5F). Of these, 24% were CD8+ and 70% CD4+ T cells (Figure 5F). Almost all T cells expressed the memory marker CD45RO (Figure 5F). Twenty nine per cent of CNS-infiltrating cells expressed the B cell marker CD19 (Figure 5I), and among these 86% were positive for CD27/CD38 (Figure 5I), i.e. they were memory B cells/plasma cells. A marker for microglia/monocytes/macrophages was not included in the fluorescence-activated cell sorting panel, but from the immunohistochemistry studies these cells probably constitute another important part of immune cell infiltrate.

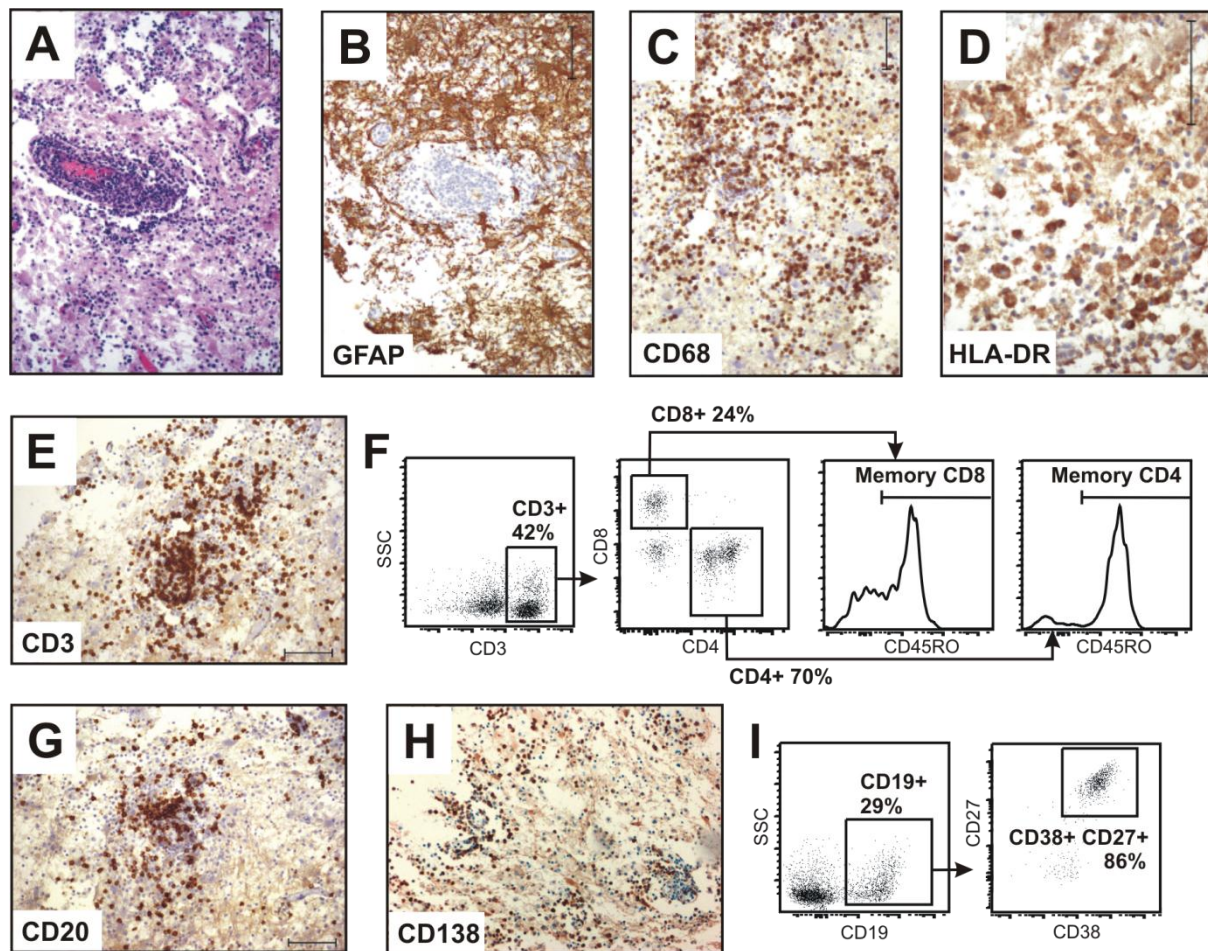


Figure 5 **A)** PML-IRIS with massive perivascular and parenchymal infiltration (haematoxylin). **B)** Reactive gliosis with numerous stellate astrocytes (anti-gliofibrillary acidic protein) and **C)** diffuse and destructive parenchymal infiltration of foamy macrophages (anti-CD68). **D)** The vast majority of infiltrating and resident cells express HLA-DR. **E)** Perivascular and parenchymal infiltrates are rich in T cells (anti-CD3). **F)** Brain-infiltrating cells (42%) of CD45+ are CD3+ T cells (boxed population on left), and of these 24% and 70%, respectively, CD8+ and CD4+ T cells, respectively (middle). In both T cell populations, almost all cells express the memory marker CD45RO (right). **G)** Perivascular and parenchymal infiltrates are also rich in B cells (anti-CD20) and **H)** can further be characterized as plasma cells (anti-CD138). **I)** Flow cytometric analysis shows that 29% of CD45+ cells are B cells (anti-CD19; left), and of these 86% are memory B cells/plasmablasts or plasma cells (right). The hallmarks of PML, bizarre giant astrocytes and oligodendrocytes with enlarged hyperchromatic nuclei, were absent. Scale bar = 100 μ m. Histological stainings were performed at the Department for Neuropathology, University Medical Center, Hamburg-Eppendorf.

Another part of the isolated brain-derived T cells were used for phenotypic analysis by flow cytometry. Therefore, T cells were expanded by stimulation with the antigen-unspecific, global stimulus PHA for several rounds to yield sufficient cell numbers for a detailed characterization.

Staining with TCR V beta chain antibodies revealed that the relative composition of CD4+ T cells remained stable over the different expansion rounds whereas a preferential expansion of some CD8+ populations occurred with the results that the overall composition of the CD8+ population changed with respect to TCR composition (Figure 6A). Additionally, the ratio between CD4+ and CD8+ T cells increased in favor of CD4+ cells (Figure 6B). Since the flow cytometry analysis of the freshly isolated material from the brain biopsy showed that CD4+ T were predominant over CD8+ T cells (Figure 5F), we decided to focus our further analysis on CD4+ T cells.

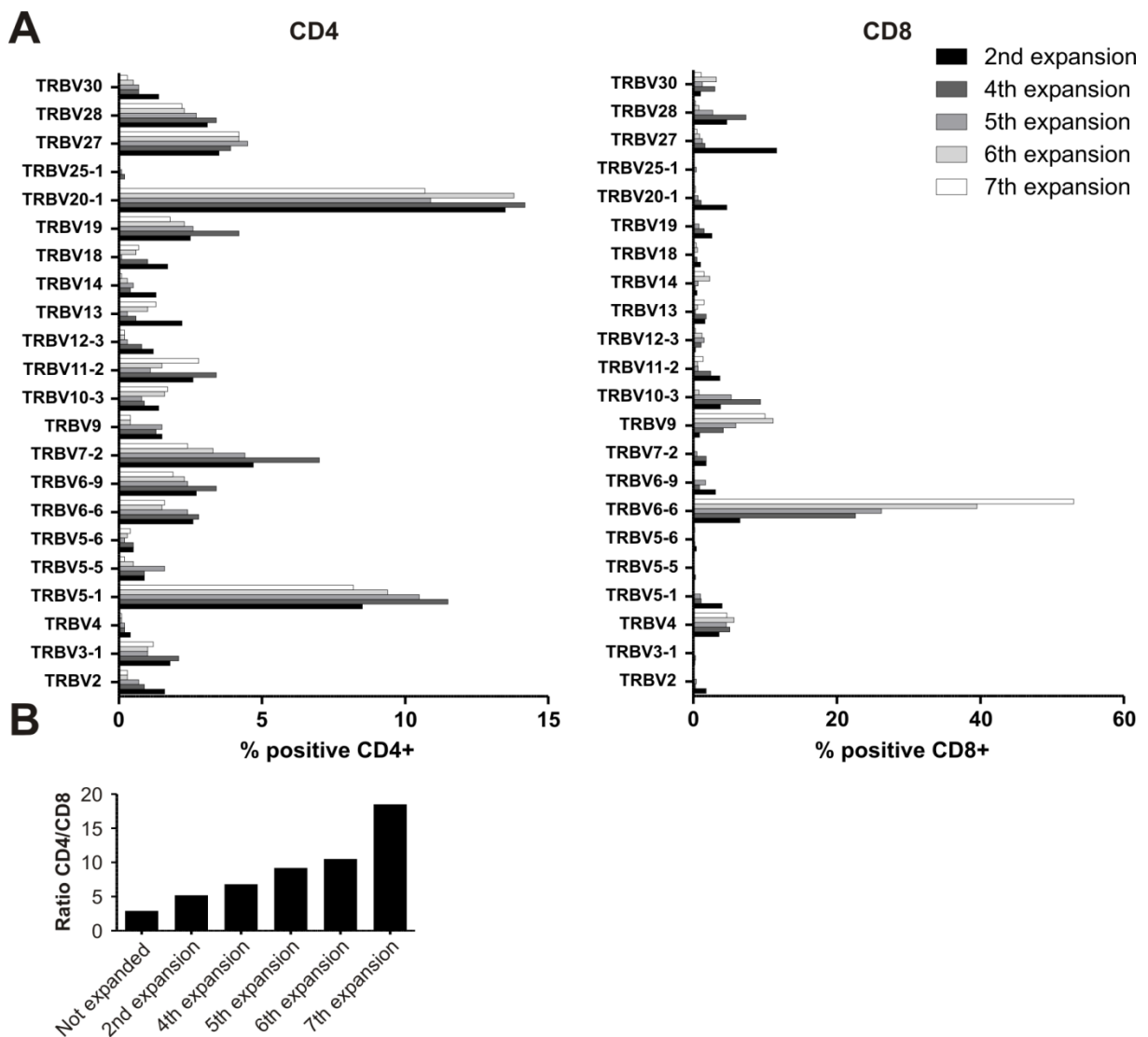


Figure 6 Monitoring of brain-derived CD8+ and CD4+ T cell expansion. A) Composition of TCR variable beta chain families in brain-derived CD4+ and CD8+ T cells from PML-IRIS patient 1 after various rounds of PHA-stimulation assessed by flow cytometry. B) The change of CD4+/CD8+ ratio after several rounds of expansion.

3.1.2 Phenotypical characterization of brain-infiltrating CD4+ T cells

Next, the T helper subsets dominating the brain infiltrates were investigated by assessing their cytokine profile. To this end, brain and CSF-derived expanded T cells after one round of stimulation, as well as expanded and non-expanded PBMCs were stained for intracellular expression of the cytokines IFN- γ (Th1), IL-4 (Th2), IL-17 (Th17) and then analyzed by flow cytometry (Figure 7B). The number of IL-17-expressing Th17 cells was negligible (data not shown). After one expansion round the majority of CD4+ T cells showed a Th1 phenotype, characterized by secretion of IFN- γ (PBMC 49%, brain 51%, CSF 68%). Further, a high number of IL-4/IFN- γ double-positive cells was found (PBMC 6%, brain 30%, CSF 22%). Since Th1 and Th2 cells are considered mutually exclusive differentiation states this finding was unexpected. Since the double-positive cells were memory cells and hence fully differentiated, we termed cells with the dual Th1 and Th2 characteristics bifunctional Th1-2 cells.

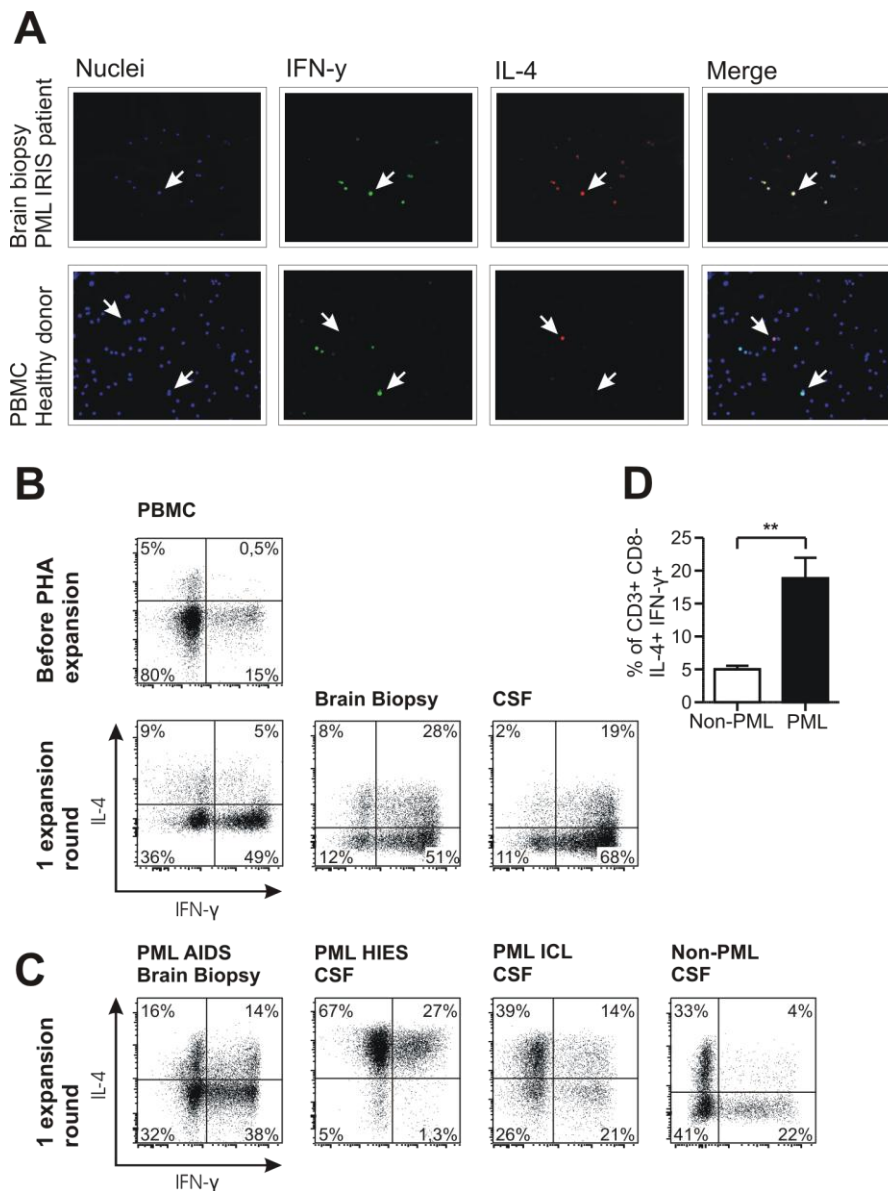


Figure 7 Phenotypical analysis of CD4+ T cells from PML patients. **A)** Intracellular immune fluorescence staining for the cytokines IL-4 and IFN- γ and Hoechst staining for cell nuclei. The upper row is showing non-manipulated brain-derived mononuclear cells from PML-IRIS patient 1. The bottom row depicts non-expanded PBMCs of a healthy donor. The white arrows indicate a Th1-2 cell (IFN- γ + and IL-4+) in the brain biopsy sample and a Th1 (IFN- γ +) and a Th2 (IL-4+) cell in the sample from the healthy donor, respectively. **B)** Flow cytometric intracellular cytokine staining for detection of IL-4 and IFN- γ producing CD4+ T cells (defined as CD3+, CD8-, gated on vital cells [LIVE/DEAD negative]) in brain and CSF-derived cells and PBMCs from PML-IRIS patient 1 after one round of PHA expansion. Additionally, the PBMCs are shown prior to expansion. Numbers represent the percentage of positive cells. **C)** Quantification of Th1, Th2 and Th1-2 cells by intracellular staining of IL-4 and IFN- γ after one round of PHA-stimulation from brain-derived CD4+ cells from PML-IRIS AIDS patient 2 (first panel), CSF-derived cells from PML patient 4 with hyper-IgE syndrome (HIES, panel 2), PML patient 3 with CD4 lymphocytopenia (ICL, third panel) in comparison one example of CSF-derived cells from non-PML control 1. **D)** The percentage of Th1-2 cells in CSF-derived mononuclear cells after one expansion round from non-PML patients (white bar, $n=5$) and PML patients (black bars, $n=4$, patients 1-4). Statistical significance is indicated by * ($p \leq 0.05$).

Non-expanded PBMCs showed a low frequency Th1-2 cells (0.5%). Due to the limited number of directly isolated lymphocytes from brain and CSF no intracellular flow cytometric analysis could be performed. To rule out a strong influence of the PHA expansion conditions on the proportion of Th1-2 cells an immunofluorescence staining was conducted with non-expanded brain-derived lymphocytes (Figure 7A) since much less cells are required to perform this method. In parallel PBMCs from healthy donors were stained. Brain-derived lymphocytes of the PML-IRIS patient showed a high frequency of IL-4/IFN- γ double positive cells whereas these cells were absent in the samples from healthy donors.

To assess if bi-functional Th1-2 cells are also observed in patients, who developed PML from other reasons than patient 1, CSF-infiltrating cells from a PML-IRIS patient with AIDS and CSF-derived lymphocytes from PML patients with underlying hyper-IgE syndrome and idiopathic CD4 lymphocytopenia were compared with CSF cells from non-PML patients (Figure 7C). Th1-2 cells were found in all PML patients, and their proportion varied between 14-27% and were significantly higher than in non-PML controls (Figure 7D).

3.1.3 Phenotypical characterization of brain-infiltrating CD4+ T cells at the single cell level

In order to investigate the Th1-2 cells that were found in high proportions in the intrathecal compartments of PML patients in more detail, T cell clones were generated from the brain-derived bulk expanded cells from PML-IRIS patient 1, allowing an in depth characterization at the single cell level. Out of 35 growing colonies 22 were specific for JCV VP1 protein and characterized in more detail (Table 17). The purity was determined by TRBV antibody staining. Sequencing of the CDR3 region of the variable beta and alpha chain revealed that out of the 22 growing colonies 15 were unique clones. These 15 clones were subsequently used for phenotypical analyses.

Table 17 Characteristics of brain-infiltrating CD4+ T cell clones. If available purity of TCCs was assessed by flow cytometry with monoclonal antibodies against specific V beta chains. TCC are grouped by the peptide specificity of the respective TCC.

Clone Number	Fre-quency	Pheno-type	Specificity	TRBV	Purity	CDR3 Beta	TRAV	CDR3 Alpha
1	1x	Th1	VP1 34-48	20-1*01	94%	CSPGPRGQETQYF	13-1*02	CAAKGAAGNKLTF
2	1x	Th1-2	VP1 34-48	20-1*01	85%	CSARGQGAQGYTF	13-1*02	CAASGTSTLTF
3	1x	Th1-2	VP1 34-48	20-1*01	95%	CSSPPGGNSPLHF	13-1*02	CAAKGGGNKLTF
4	1x	Th1	VP1 34-48	20-1*01	99%	CSAKYVNTEAFF	13-1*02	CAASRSTGGFKTIF
5	1x	Th1	VP1 34-48	20-1*01	99%	CSAGGRGLDGYTF	13-1*02	CAAKGAAGNKLTF
6	1x	Th1	VP1 54-68	18*01	99%	CASSLQSGPIYEQYF	3*01	CAVRDNGNDMRF
7	5x	Th1-2	VP1 74-88	5-1*01	99%	CASSGGETAYEQY	3*01	CAVRDSRGGATNKLIF
8	1x	Th1	VP1 91-105	7-9*0x	-	CASSSIVYEQYF	12-1*01	CVVKGGNNATLMF
9	1x	Th1	VP1 143-157	11-1*01	-	CASSLPGLKPEQYF	35*0x	CAGPEYGGSQGNLIF
10	1x	Th1-2	VP1 229-243	20-1*0x	99%	CSATRAPGTGTYEQYF	21*0x	CAVKEAAGNKLTF
11	1x	Th1-2	VP1 319-331	27*01	-	CASSFSXAGVNEQFF	9-2*0x	CALTSDGQKLLF
12	3x	Th1	VP1 319-331	5-8*01	-	CASSPRDSRGDEQFF	9-2*0x	CALVQGAQKLVF
13	2x	Th1-2	VP1 335-349	5-5*0x	99%	CASSLRQGGGEQYF	38-2	CAYRSPRGANSKLTF
14	1x	Th1	VP1 335-349	6-1*01	-	CASSERGLSSYSNQPQHF	13-2*01	CAEKYRGKLIF
15*	1x	Th1	VP1 ???	5-1*01	99%	CASSLGSRNTEAFF	34*01	GADAGGTSYKGLTF

* Fine specificity of TCC 15 could not be determined. Therefore, it does not appear in the restriction/affinity analyses.

Intracellular cytokine staining of the T cell clones revealed that all had a Th1 or Th1-2 phenotype (Figure 8A). Eleven (50%) VP1-specific TCC showed a Th1-2 phenotype and the other eleven a Th1 profile (50 %) (Figure 8B). The cytokine profiles assessed by flow cytometry could be validated by testing the culture supernatant for IL-4 and IFN- γ secretion (Figure 8C). Since the various T helper subsets are mainly characterized by the expression of certain signature transcription factors, i.e. Tbet (Th1) and GATA3 (Th2), a qT-RT-PCR analysis for these transcription factors was performed to address if Th1-2 bifunctional T cells addressed both transcription factors (Figure 8D). Indeed, Th1-2 simultaneously expressed Tbet and GATA3 that are commonly considered to exclude each other (23, 30, 31). Additionally, the assessment of Th1/Th2-typical chemokine receptors revealed that all Th1 and Th1-2 TCC expressed CCR5 and CXCR3 that are often found on Th1 cells (162-164). Further, significantly more Th1-2 expressed the Th2-typical chemokine receptor CCR4 (165, 166) (Figure 8F). The chemokine receptor profile of a typical Th1 and a Th1-2 TCC is shown in Figure 8E.

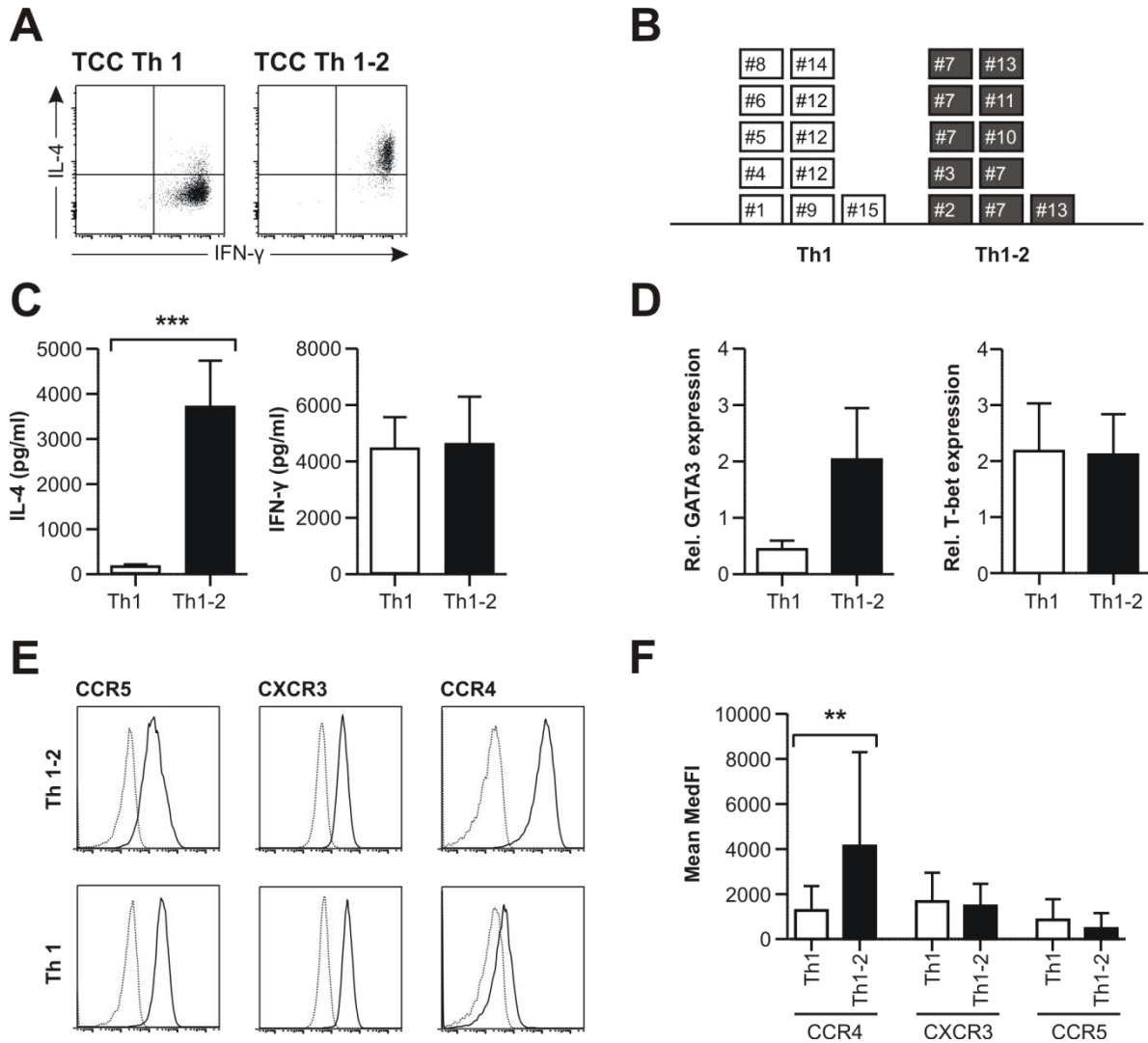


Figure 8 Phenotypical analysis of brain-derived CD4+ T cell clones **A**) Representative cytokine profile assessed by flow cytometry of a Th1 (left) and a Th1-2 (right) TCC characterized by their IL-4 and IFN- γ production. **B**) TCCs grouped by their fine-specificity. Each number represents a single TCC and each square stands for a growing colony. Th1 TCCs are displayed with white squares, Th1-2 TCCs with dark squares. **C**) ELISA detection of IFN- γ and IL-4 production in culture supernatants of Th1-2 T cell clones ($n=6$, black bars) and Th1 T cell clones ($n=9$, white bars) 72 h after stimulation with PHA. **D**) QT-RT PCR analysis for transcription factors GATA3 and T-bet of Th1-2 T cell clones ($n=6$, black bars) and Th1 T cell clones ($n=9$, white bars). Values are relative expression compared with brain-derived PHA-expanded cells (calibrator=1). **E**) Staining for the chemokine receptors CCR5, CXCR3 and CCR4 on a Th1-2 (upper row) and Th1 (bottom row). Histogram overlays of isotype control (grey) and antibody staining (black) are shown. **F**) Quantification of the median fluorescence intensity (MedFI) of Th1 (white bars, $n=9$) and Th1-2 (black bars, $n=6$) TCC for the chemokine receptors CCR4, CXCR3 and CCR5. Results show the mean \pm SEM. Statistical significance is indicated by * ($p<0.05$).

To exclude that the Th1-2 phenotype was caused by the PHA stimulus and/or expansion protocol, two Th1 and two Th1-2 TCCs were expanded simultaneously using either PHA or VP1 as stimulus. Figure 9A shows that the cytokine profiles assessed by flow cytometry of a representative Th1 and Th1-2 TCC did not differ after the use of VP1 or PHA as expansion stimulus. This was confirmed by culture supernatant ELISA (Figure 9B).

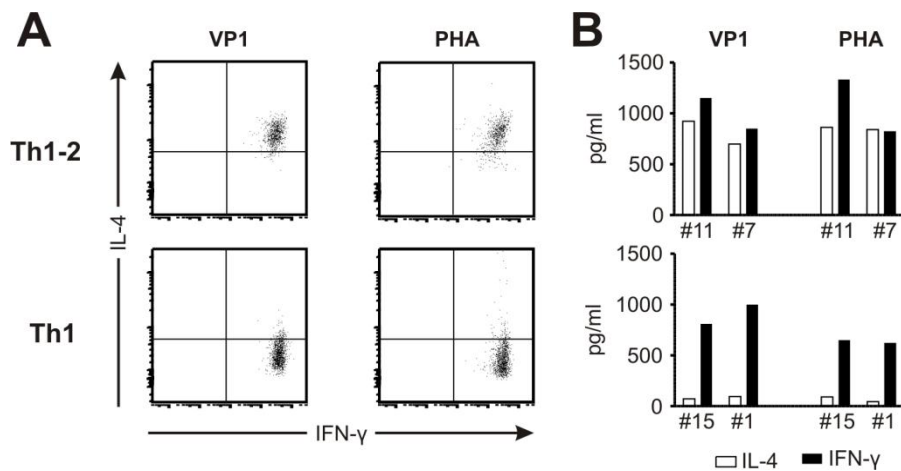


Figure 9 Th1-2 and Th1 cytokine secretion patterns are comparable after VP1 and PHA stimulation. **A**) Intracellular cytokine staining for IFN- γ and IL-4 in a Th1-2 (upper row) and a Th1 clone (bottom row), respectively, 12 days after stimulation with VP1 (left dot plots) and PHA (right dot plots). **B**) ELISA detection of IFN- γ (black bars) and IL-4 (white bars) production in culture supernatants of two representative Th1-2 (TCC 7 + 11) and two Th1 clones (TCC 1+15) 72h after stimulation with VP1 and PHA, respectively.

3.1.4 Identification of immunodominant epitopes within VP1 protein

Next, it was of interest against which JCV VP1 epitope the TCC responded. To address this point, epitope mappings with bulk expanded brain-derived CD4⁺ T cells from the PML-IRIS patient were tested first and revealed several immunodominant epitopes within the major capsid-forming protein VP1 (Figure 10C). To confirm these data at the clonal level, the fine-specificity of the isolated VP1 protein-specific T cell clones was assessed by using proliferative response against a set of 64 overlapping 15-mer peptides spanning the entire JCV VP1 protein. This allowed the determination of the fine specificity of each clone (Figure 10A). The following specificities were found: VP1₃₄ (recognized by TCC 1, 2, 3, 4, and 5), VP1₅₄ (TCC 6), all three variants of peptide VP1₇₄ (TCC 7), VP1₉₁ (TCC 8), VP1₁₄₃ (TCC 9), variant I of VP1₂₂₉ (TCC 10), VP1₃₁₉ (TCC 11 and 12), and VP1₃₃₅ (TCC 13 and 14). If the frequency, how often each single TCC were isolated from the bulk T cell population is taken into account (number of growing colonies), the epitopes VP1₃₄ (five growing colonies), VP1₇₄ (five growing colonies), VP1₃₁₉ (four growing colonies), and VP1₃₃₅ (three growing colonies) were identified as immunodominant (Figure 10B). This correlates very well with the data obtained from the epitope mapping with the bulk brain-derived T cell populations (Figure 10C).

Interestingly, different recognition patterns were observed for two of the main epitopes (VP1₃₄ and VP1₇₄, Figure 10B). While VP1₇₄ is targeted by a single strongly expanded clone (TCC 7 with five growing colonies), VP1₃₄ is recognized by five different clones sharing a TCR consisting of TRBV20 and TRAV13 (Figure 10B, Table 17).

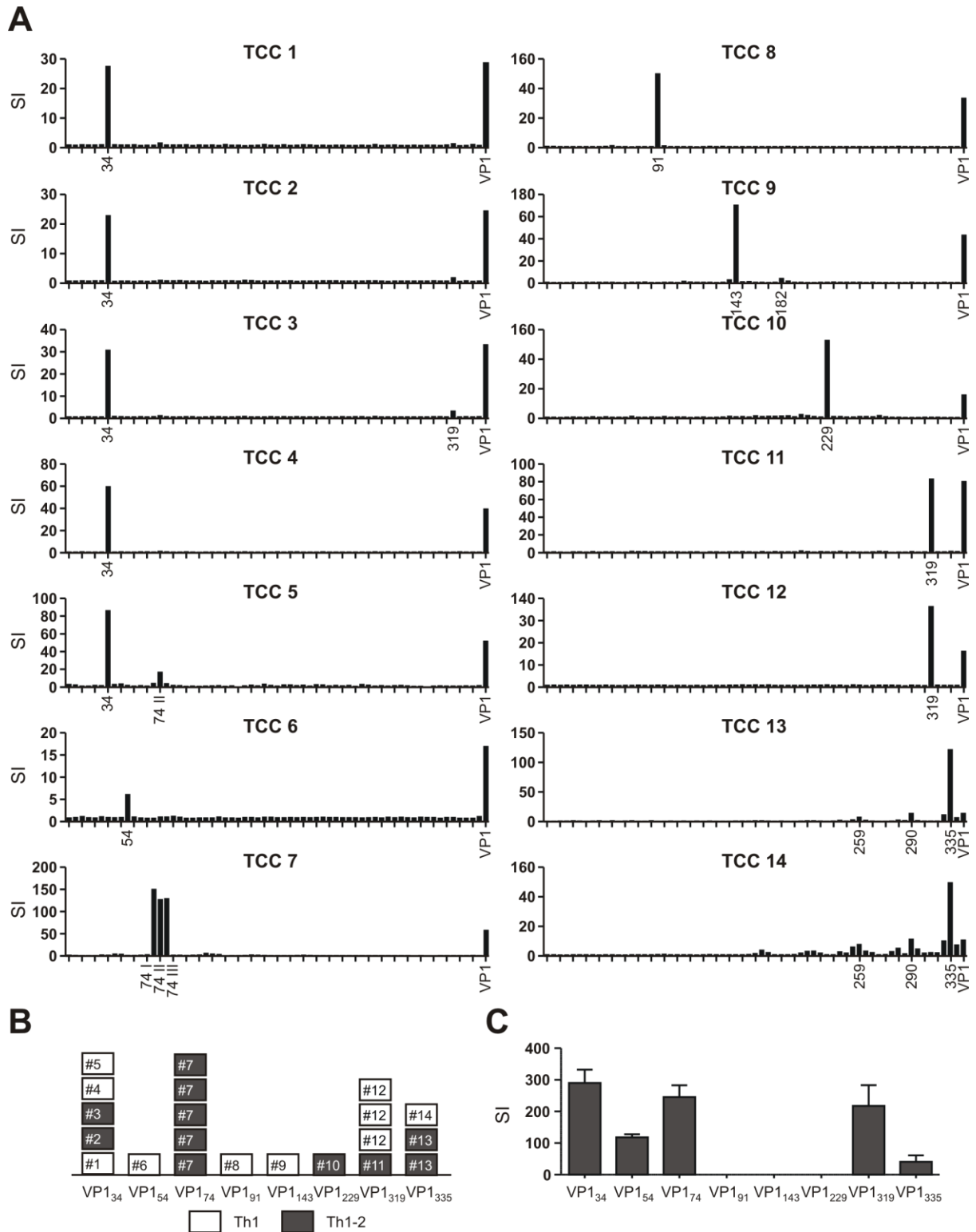


Figure 10 Fine specificity and frequency of brain-derived CD4+ T cell clones. **A**) ³H-thymidine incorporation proliferation assay analyzing the response to individual overlapping 15-mer peptides spanning the entire VP1 sequence of JCV. Last column of each TCC shows as positive control whole VP1 protein. Proliferation response is indicated as stimulation index (SI). **B**) Frequency of Th1 (white squares) and Th1-2 (black squares) TCCs ordered by their specific epitope. **C**) Proliferation response of brain-derived T cells against immunodominant VP1 epitopes. The results show the mean stimulation index ±SD.

Some T cell clones showed weak recognition of more than one peptide. Cross-recognition occurred in TCC 3, 5, 13, and 14 (Figure 10A). No correlation between the phenotype and fine specificity of the clones was observed (Figure 10B).

When considering the JCV specificity of CD8+ T cells it had previously been shown by tetramer staining that peptides VP1₃₆ and VP1₁₀₀ are immunodominant in HLA-A*02:01 positive individuals (119, 167). To address at least in part also the fine specificity of the CD8+ infiltrate in patient 1, G. Ogg (Weatherall Institute of Molecular Medicine, Oxford) provided us with HLA-A2*02:01 tetramers loaded with the above peptides, and with these binding of 0.8% and 0.6% of brain-derived PHA-expanded CD8+ T cells from the PML IRIS patient, could be shown (Figure 11). Interestingly, the epitope VP1₃₄₋₄₈ that was identified as immunodominant for CD4+ T cells, contains the CD8+ immunodominant epitope VP1₃₆, highlighting the interplay between JC virus-specific CD4+ and CD8+ T cells.

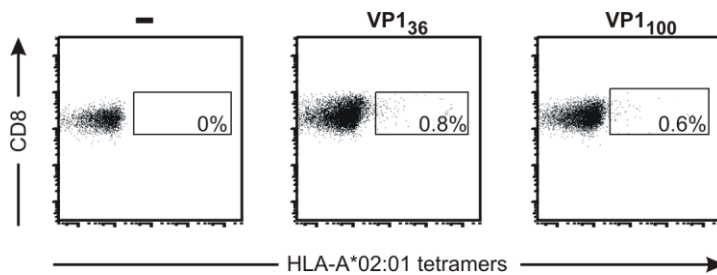


Figure 11 FACS analysis of brain-derived CD8+ T cells binding HLA-A*02:01-VP1₃₆ (middle) and HLA-A*02:01-VP1₁₀₀ (right) tetramers.

3.1.5 TCCs recognizing immunodominant epitopes are overrepresented in the brain

In order to compare the representation of the JCV-specific T cell clones in the brain, CSF, and PBMCs of this patient, CDR3 spectratyping was performed. This method allows the assessment of the individual length of the CDR3 region of the T cell receptor. The total length of the variable chain is determined by the highly diverse CDR3 region, which is specific for a T cell. A mixed peripheral T cell population of healthy individuals is characterized by a Gaussian distribution of peaks, each peak representing T cells of a particular V alpha or V beta family with the same CDR3 length. Due to an underlying disease or in immune privileged organs such as the brain, the peak profile can highly differ from a Gaussian distribution because of clonal expansion of certain T cell populations and an overall reduced T cell variability. Additionally, this method can provide information about the abundance of a certain T cell clone in the different compartments by assessing the contribution of the clone peak to the total of peaks in the tissue of interest.

CDR3 spectratyping of the TRBV (Figure 12A) and TRAV families (Figure 12B) showed a higher T cell diversity in the peripheral blood than in CSF or brain-derived T lymphocyte populations. Some PBMC spectratypes (TRBV18, 11, 27 and TRAV38) showed a dominant peak indicating clonal expansion of certain T cell populations. The peak profiles of the immune privileged compartments CSF and brain were much less diverse showing frequently just one peak or few oligoclonal peaks. Interestingly, the CDR3 spectratypes of CSF and brain were very divergent. A peak that was dominant in one compartment could be completely absent in the other (e.g. TRBV11 and TRAV13). For each TCC a corresponding peak in the mixed brain lymphocyte population and PBMCs could be identified whereas this was not always the case in the CSF, pointing towards different T cell compositions in the brain and CSF compartment. Figure 13 summarizes the proportion of each clone in the brain calculated by the relative AUC of the corresponding peak in the mixed brain-derived lymphocyte population. The CDR3 spectratypes confirm the results of the identified immunodominant epitopes with the bulk population (Figure 10C) concerning the frequency of clones recognizing these epitopes (VP₁₃₄, VP₁₇₄, VP₁₃₁₉, and VP₁₃₃₅).

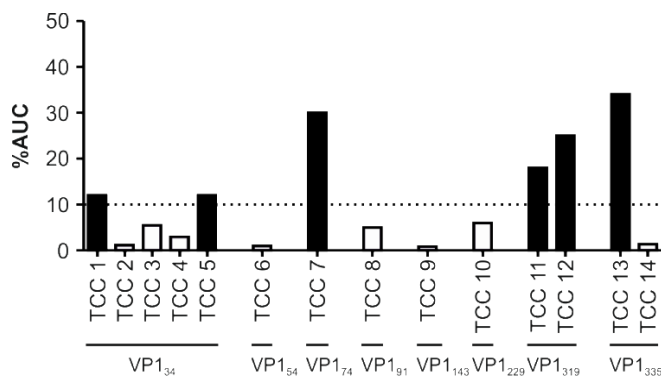
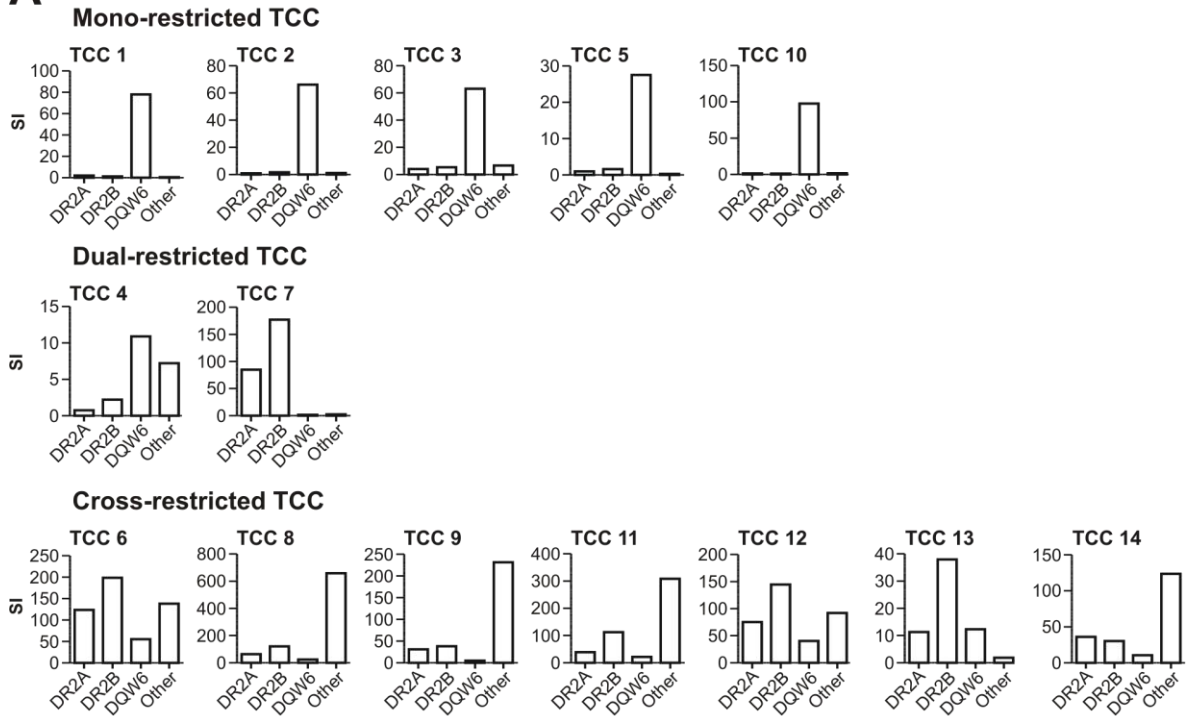


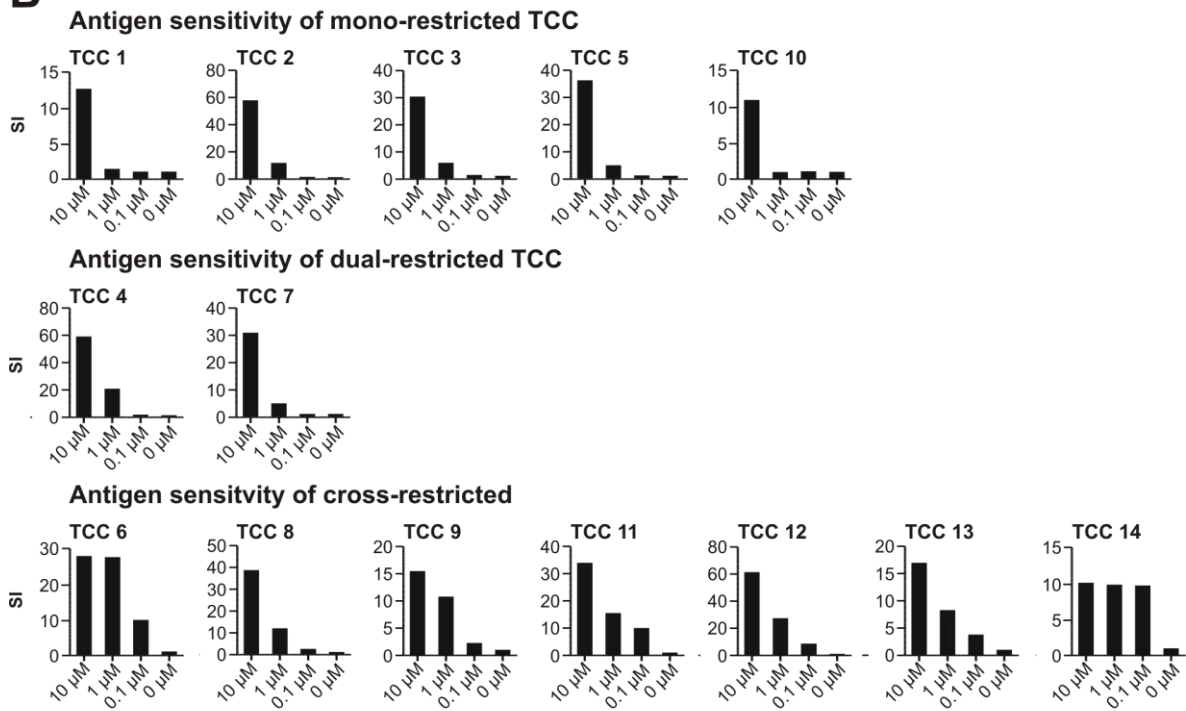
Figure 13 Proportion of different TCC in the brain. Bars represent area under the curve (AUC) in percent calculated by the CDR3 spectratypes of mixed lymphocyte population of brain and TCC. Always the peak with lower frequency was taken into account. If more than one clone contributed to the corresponding peak in the mixed lymphocyte population in the brain AUC was divided by the number of clones. Dotted line indicates 10% AUC. Black bars show TCCs with %AUC > 10.

3.1.6 MHC-class II restriction analysis of VP1-specific TCC

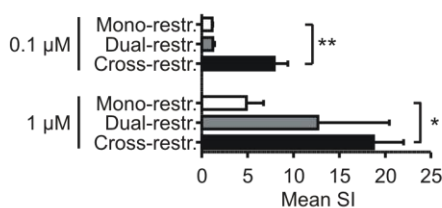
A



B



C



D

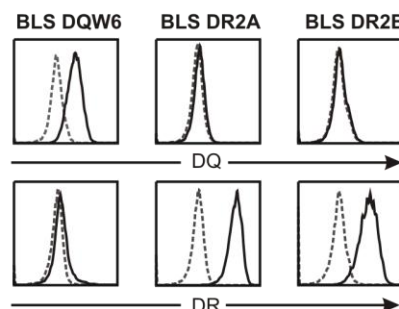


Figure 14 Restriction and antigen sensitivity analysis of JC virus-specific CD4+ T cell clones. **A)** TCCs were tested with cognate antigen presented by HLA-matched PBMCs (Other = DRB1*11:03) or BLS cell lines carrying a certain HLA class II molecule (DR2A = DRB5*01:01, DR2B = DRB1*15:01, or DQw6 = DQB1*06:02). A positive response is defined by SI>5. Upper panel shows mono-restricted TCCs, the middle shows TCC restricted by two HLA class II elements, and the lower panel shows TCCs restricted by more than three HLA class II molecules. **B)** For assessment of antigen sensitivity the proliferative response was tested with declining amounts of cognate antigen presented by autologous B cell lines expressing all HLA class II molecules of the donor. TCCs are ordered by their restriction. **C)** Mean stimulatory index of mono, dual, or cross-restricted TCC at a peptide concentration of 0.1 μ M (up) and 1 μ M (bottom), respectively. Statistical significance is indicated by * ($p \leq 0.05$). **D)** Flow cytometric analyses of HLA-DQ and -DR expression on BLS DQw6, BLS DR2A, and BLS DR2B cells. Histograms show isotype control (dotted line) and antibody staining (black line). Black bars represent the median fluorescence intensity (MedFI) of HLA-DQ and HLA-DR expression.

To investigate the HLA-class II restriction of JCV-specific CD4+ TCC isolated from the brain during PML IRIS, HLA-matched PBMCs (DRB1*11:03) or BLS cell lines transfected with the appropriate HLA class II molecules of the patient (DR2A = DRB5*01:01, DR2B = DRB1*15:01, DQw6 = DQB1*06:02) were used as antigen presenting cells. Unexpectedly, several clones were identified that were able to recognize their cognate antigen in the context of more than one restriction element (Figure 14A). Seven out of 14 clones were able to use three or more HLA-class II molecules and are henceforth called cross-restricted (TCC 6, 8, 9, 11, 12, 13, 14). Two T cell clones were restricted by two HLA-class II molecules (dual-restricted, TCC 4 and 7), and five TCC used only one HLA-class II element (mono-restricted, TCC 1, 2, 3, 5, and 10). Remarkably, all mono-restricted clones recognized their specific peptide in the context of DQB1*06:02 (DQw6). Their T cell receptor consisted of a TRBV20 chain (Table 17), which points towards critical contribution of this variable beta chain for binding this HLA molecule. Additionally, TCC 4, which is categorized as dual-restricted, also has the strongest antigen recognition in context of DQB1*06:02 and expresses TRBV20. To ensure that the results were not influenced by contamination with other HLA molecules on the BLS cells, stainings with appropriate antibodies were performed and cells analyzed by flow cytometry (Figure 14D).

Then, the antigen sensitivity of the T cell clones was assessed by using autologous immortalized B cell lines as antigen presenting cells, which express all HLA-class II molecules of the patient (Figure 14B). Some clones were highly sensitive, e.g. TCC 14 that was able to respond even at very low concentrations of 0.1 μ M, and other clones such as TCC 10 were much less sensitive and needed a 100fold higher concentration of its cognate antigen to proliferate. If one combines the results of the HLA-class II restriction with the antigen sensitivity it becomes clear that T cell clones that are able to use several restriction elements for recognition of their cognate peptide need significantly less amount of antigen than dual- or mono-restricted clones (Figure 14C).

3.1.7 TRBV20-1/TRAV13-1 T cells preferentially recognize VP1₃₄

One group of clones displayed characteristics that led us to focus on these clones. The five unique clones TCC 1, 2, 3, 4, and 5 identified by their different alpha and beta CDR3 regions all have a TCR consisting of a TRBV20-1*01 and TRAV13-1*02 chain (Table 17 and Figure 15). They share the specificity for the VP1 epitope 34-48 (Table 17 and Figure 10A), they all are DQB1*06:02-restricted (Figure 14A) (TCC 4 additionally has slight recognition in DRB1*11:03), and have similar antigen sensitivity (Figure 14B). In Figure 15 the amino acid composition of the variable chains of all clones are compared. The sequences are almost identical with the exception of the CDR3 regions and the associated J segments (Table 18 and Figure 15).

TRBV20-1		CDR1 (27-38)		CDR2 (56-65)		
1	10	20	30	40	50	60
TCC 1SQHPSWVICKSGTSVKIECRSL	DFQ.....ATT	MFWYRQFPKQSLMLMAT	SNEG...SKA		
TCC 2SQHPSWVICKSGTSVKIECRSL	DFQ.....ATT	MFWYRQFPKQSLMLMAT	SNEG...SKA		
TCC 3	..VVSQHPSWVICKSGTSVKIECRSL	DFQ.....ATT	MFWYRQFPKQSLMLMAT	SNEG...SKA		
TCC 4SQHPSWVICKSGTSVKIECRSL	DFQ.....ATT	MFWYRQFPKQSLMLMAT	SNEG...SKA		
TCC 5	..VVSQHPSWVICKSGTSVKIECRSL	DFQ.....ATT	MFWYRQFPKQSLMLMAT	SNEG...SKA		

		CDR3 (105-118)		Constant region	
70	80	90	100	110	120
TCC 1	TYEQGVEKDKFLINHA.SLTLSTLTVTSAHPEDSSFYIC	SE <u>GP</u> RG..QETQYF	GPGTRLLVL	EDLKNVFPP...	
TCC 2	TYEQGVEKDKFLINHA.SLTLSTLTVTSAHPEDSSFYIC	SARGQG..AQGYTF	GSSTRLLTVV	EDLNKVFPP...	
TCC 3	TYEQGVEKDKFLINHA.SLTLSTLTVTSAHPEDSSFYIC	SSPPGG..NSPLHF	GNGTRLTVT	EDLNKVFPP...	
TCC 4	TYEQGVEKDKFLINHA.SLTLSTLTVTSAHPEDSSFYIC	SAKYV...NTEAFF	GQGTRLTVV	EDLNKVFPP...	
TCC 5	TYEQGVEKDKFLINHA.SLTLSTLTVTSAHPEDSSFYIC	SAGGRG..LDGYTF	GSSTRLLTVV	EDLKNVFPP...	

TRAV13-1		CDR1 (27-38)		CDR2 (56-65)			
1	10	20	30	40	50	60	70
TCC 1AVIKCTYS	DSA.....SNY	FPXXKQELGKRPQLI <u>V</u> D	IRSN...VGE	KKD.....		
TCC 2SVQEGDSAVIKCTYS	DSA.....SNY	FPWYKQELGKRPQLI <u>I</u> D	IRSN...VGE	KKD.....		
TCC 3AVIKCTYS	DSX.....SNY	FPWYKQELGKRPQLI <u>V</u> D	IRSN...VGE	KKD.....		
TCC 4SVQEGDSAVIKCTYS	DSA.....SNY	FPWYKQELGKRPQLI <u>V</u> D	IRSN...VGE	KKD.....		
TCC 5QEGDSAVIKCTYS	DSA.....SNY	FPWYKQELGKRPQLI <u>V</u> D	IRSN...VGE	KKD.....		

		CDR3 (105-118)		Constant region	
80	90	100	110	120	
TCC 1	QRIAVTLNKTAHFSLHITETQPEDSAVYFC	AAK <u>G</u> AA..GNKLT	GGGTRVLVKP	NIQNPDPAVYQLRDSK...	
TCC 2	QRIAVTLNKTAHFSLHITETQPEDSAVYFC	AAS <u>G</u> T...STLTF	GKGTMLLVSP	DIQNPDPAVYQLRDSK...	
TCC 3	QRIAVTLNKTAHFSLHITETQPEDSAVYFC	AAK <u>G</u> G...GNKLT	GTGTQLKVEL	NIQNPDPAVYQLRDSK...	
TCC 4	QRIAVTLNKTAHFSLHITETQPEDSAVYFC	AASR <u>S</u> T.GGFKTIF	GAGTRLFVKA	NIQNPDPAVYQLRDSK...	
TCC 5	QRIAVTLNKTAHFSLHITETQPEDSAVYFC	AAK <u>G</u> AA..GNKLT	GGGTRVLVKP	NIQNPDPAVYQLRDSK...	

Figure 15 Amino acid sequences of variable alpha and beta chain of TCC 1-5 using the IMGT nomenclature and numbering. Non-germ line encoded sequences are highlighted in grey.

Table 18 V, J, and D segment usage of TCC1-5

Clone	TRBV	TRBD	TRBJ	TRAV	TRAJ
1	20-1*01	2*01	2-5*01	13-1*02	17*01
2	20-1*01	1*01	1-2*01	13-1*02	11*01
3	20-1*01	1*01	1-6*02	13-1*02	10*01
4	20-1*01	-	1-1*01	13-1*02	9*01
5	20-1*01	1*01	1-2*01	13-1*02	17*01

Additionally, at position 54 there is one amino acid exchange downstream of the CDR2 region of TRAV13-1 differing from the germ line encoded sequence. There we find a valine (V, nucleotide codon GTA) instead of the germ line encoded isoleucine (I, nucleotide codon ATA) due to a point mutation of one nucleotide. TCC 1 and TCC 5 have identical CDR3 α amino acid sequences but use different non-germline encoded nucleotide codons (Figure 16). In general the CDR3 β region amino acid composition is more heterogeneous than the CDR3 α sequences of the clones 1-5, indicating that some conserved residues within CDR α might be important for antigen/MHC recognition.

TCC 1



TCC 5

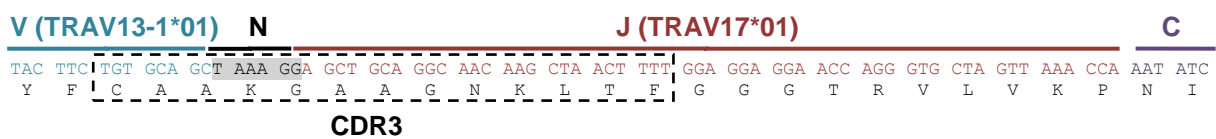


Figure 16 CDR3 region of TCC1 and TCC 5. Highlighted in grey are non-germ line encoded nucleotide insertions (N).

To get a better understanding of the amino acids within peptide VP₁₃₄₋₄₈ that are relevant for TCR binding or possibly also for binding of the peptide to the HLA-DQw6 molecule, peptides with single alanine substitutions were used in ³H-thymidine proliferation assays. The neutral and small amino acid alanine is considered best for this purpose, because it lacks a side chain and is not charged. By progressively substituting single amino acid residues of a peptide by alanine, the contribution of each amino acid to the TCR and MHC interaction can be assessed.

The alanine scan showed that substitutions of C-terminal residues were well tolerated (Figure 17A). A negatively charged glutamic acid (E) in position 41 (E41) of peptide VP₁₃₄ is most critical for the recognition by all five TCC (Figure 17A). Notably, this amino acid also is a possible MHC anchor for DQB1*06:02 (calculated with <http://epitope.zmnh.uni-hamburg.de>, developed by the ZMNH IT service: Jan-Christoph Meier, Laura Glau, Dr. Hans-Martin Zietzen, and INIMS lab: Malte Mohme, Prof. Dr. Roland Martin). Another critical amino acid is phenylalanine (F) in position 43 (F43) whose substitution leads to complete abrogation of recognition by TCC 2 and 4. The recognition patterns of TCC 1 and TCC 5 showed striking similarities, indicating an important contribution of the CDR3 alpha

chain residues for the peptide contacts. Stimulation experiments with truncated peptides (Figure 17B) for the determination of the minimal epitope revealed the core sequence VP1₃₅₋₄₄ DSITEVECF. Although, some clones behaved different. TCC 2, 3, and 5 still showed weak recognition after removal of aspartatic acid (D35) of the minimal epitope and the removal of proline (P46) abrogated recognition by TCC 1, 3, and 5 and was restored if threonine (T45) was removed.

Remarkably, TCC 1, 2, and 5 were able to cross recognize the homologous VP1₃₄₋₄₈ peptide for the polyoma virus BKV that differs in just two amino acid positions from JCV VP1 peptide 34-48 (Figure 17C).

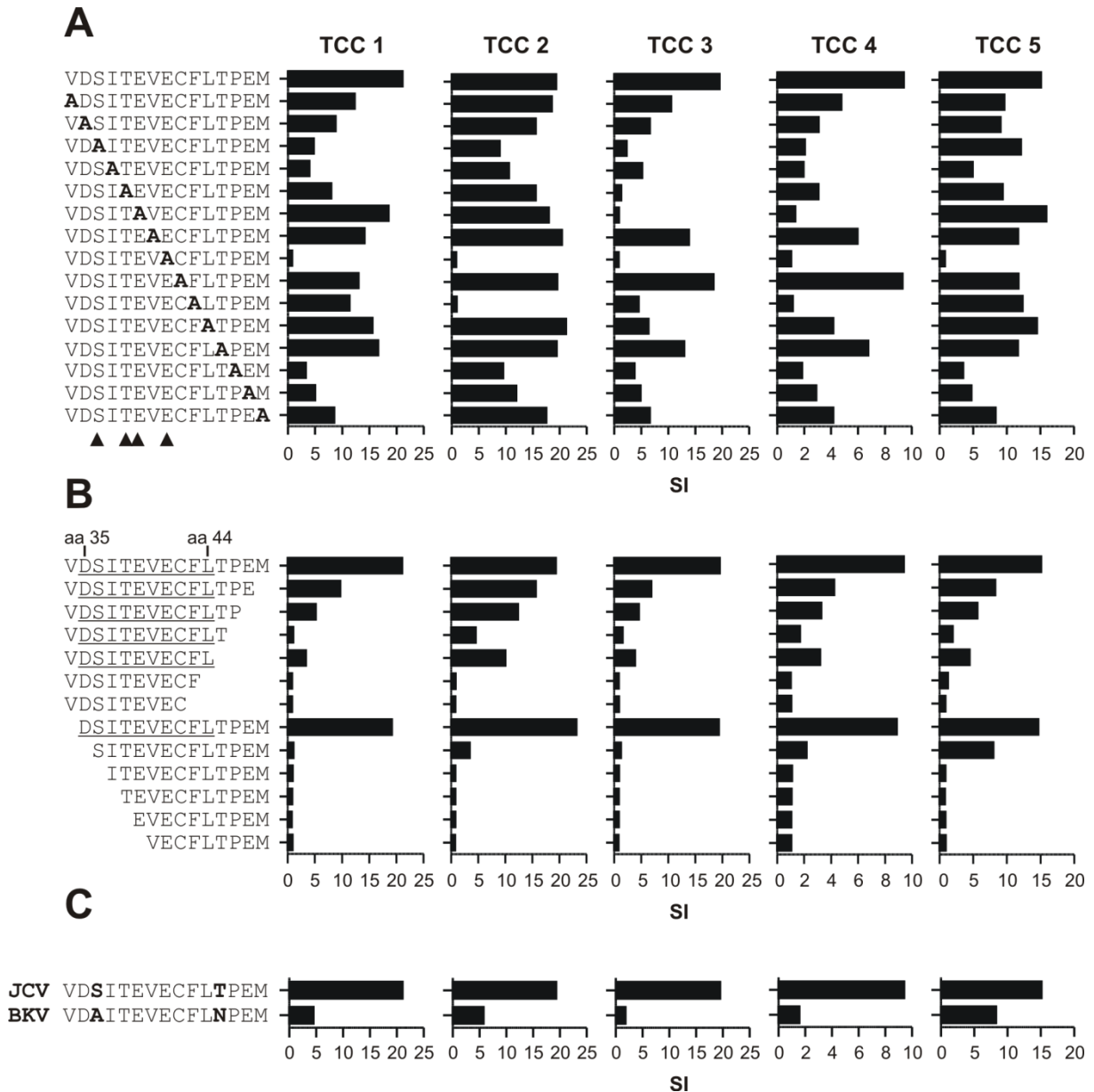


Figure 17 Comparison of TCR motifs of TCC 1-5. A) L-alanine-substitution of subsequent amino acids of the cognate peptide VP1₃₄₋₄₈ from TCC 1-5. The wild-type peptide is located at the upmost position of the Y-axis. Ala-substitutions are indicated by bold letters. MHC anchor residues are indicated by arrows. The proliferative response of TCC 1-5 are displayed from left to right. **B)** Assessment of the minimal epitope with truncated variants of the wild type peptide VP1₃₄₋₄₈. The amino acid sequence of the minimal epitope is underlined. **C)** Test for cross-reactivity to BKV VP1₄₂₋₅₆ homologous peptide (bottom row) to JCV VP1₃₄₋₄₈ (upper row). Bars represent the mean stimulatory indices (SI). C-termini of peptides are on the left, N-termini on the right side.

3.2 Induction of a JCV-specific immune response after vaccination with VP1 in a PML patient with idiopathic CD4 lymphocytopenia

3.2.1 Treatment scheme of the individual healing attempt

A 63-year old male (patient 3) was diagnosed with PML on the basis of CD4 lymphocytopenia (absolute CD4 counts ≤ 300 cells/ μl , CD4/CD8 ratio of 0.5, laboratory of University Medical Center, Hamburg-Eppendorf, UKE, Hamburg) after positive in-situ hybridization of JCV DNA in brain tissue (UKE). Due to the lack of conventional therapies against JC virus infection a new treatment strategy was applied one year after onset of first PML symptoms. The individual healing attempt was performed by the Institute for Neuroimmunology and Clinical MS Research after obtaining written informed consent from the patient. Since the patient had no detectable immune response against the immunodominant major capsid protein VP1 (Figure 19A) the idea was to vaccinate the patient with VP1 to boost the immune response against JC virus. For that purpose, 1 mg whole VP1 protein (kindly provided by Victorya Demina, Life Science Inkubator) in 1 ml Ringer lactate solution was injected subcutaneously, accompanied with the local (skin) application of Aldara[®] cream (imiquimod, MEDA Pharm) containing a TLR (toll like receptor) 7 agonist. The procedure was repeated at different time points (Figure 18). Additionally, the patient received subcutaneously injected IL-7 (CYT107, Cytheris) 48h prior to the first VP1 vaccination and at various different time points during the treatment program (Figure 18). IL-7 was given with the intent to provide newly stimulated cells with a relative growth advantage.

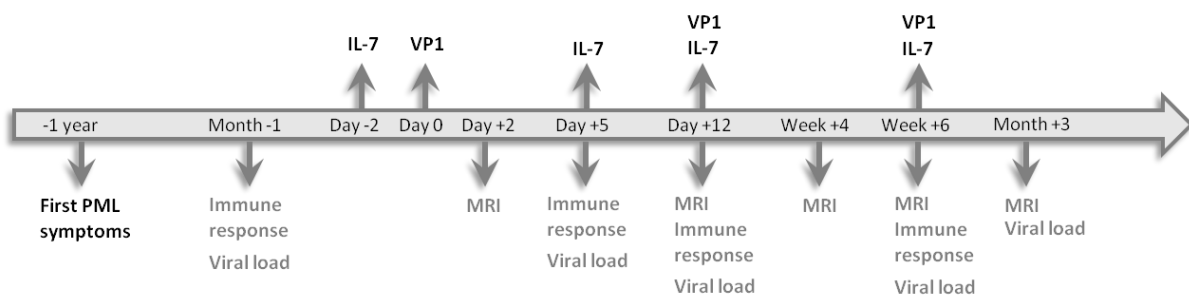


Figure 18 Treatment scheme of individual healing attempt. Application of pharmaceutical compounds are indicated above the big arrow. Monitoring of VP1-specific immune response, assessment of viral load and measurement of inflammatory activity in the brain by magnet resonance imaging (MRI) are indicated in grey.

3.2.2 Development of the JCV viral load and immune response

As indicated in Figure 18 at several different time points before and after the treatment the proliferative T cell response against VP1, the JCV viral load in serum, as well as leukocyte counts in the CSF were monitored. Figure 19A shows the development of the T cell response, measured by a

primary proliferation assay, against the viral load. Before initiation of the treatment (week -16, week -4, and day -2) and shortly after the first VP1 injection (day +5) the VP1-specific T cell response was absent with mean stimulatory indices below 2 (responses \geq SI 2 are considered positive). Already 12 days after the vaccination a considerable increase of the immune response was detectable (mean SI 2.7) and reached a plateau after the second vaccination with a mean SI of 4.4 and 3.8, respectively (week +4 and +6). The third vaccination six weeks after treatment start was able to boost the immune response considerably with a detectable mean SI of 6.8. Conversely, the JC viral load in the serum declined to a not-detectable level. Before treatment (16 and 12 weeks, respectively) the viral load was > 1200 copies/ml and dropped steadily afterwards. In Figure 19B the viral load is set in context with the increase of leukocytes in CSF after initiation of treatment. Before vaccination the absolute counts of leukocytes in CSF was below 500/ml and increased steadily afterwards to a maximum number of >2000 /ml. The number of infiltrating leukocytes in the CSF, as part of the immunoprivileged central nervous system, is usually low, but can increase considerably upon inflammatory conditions.

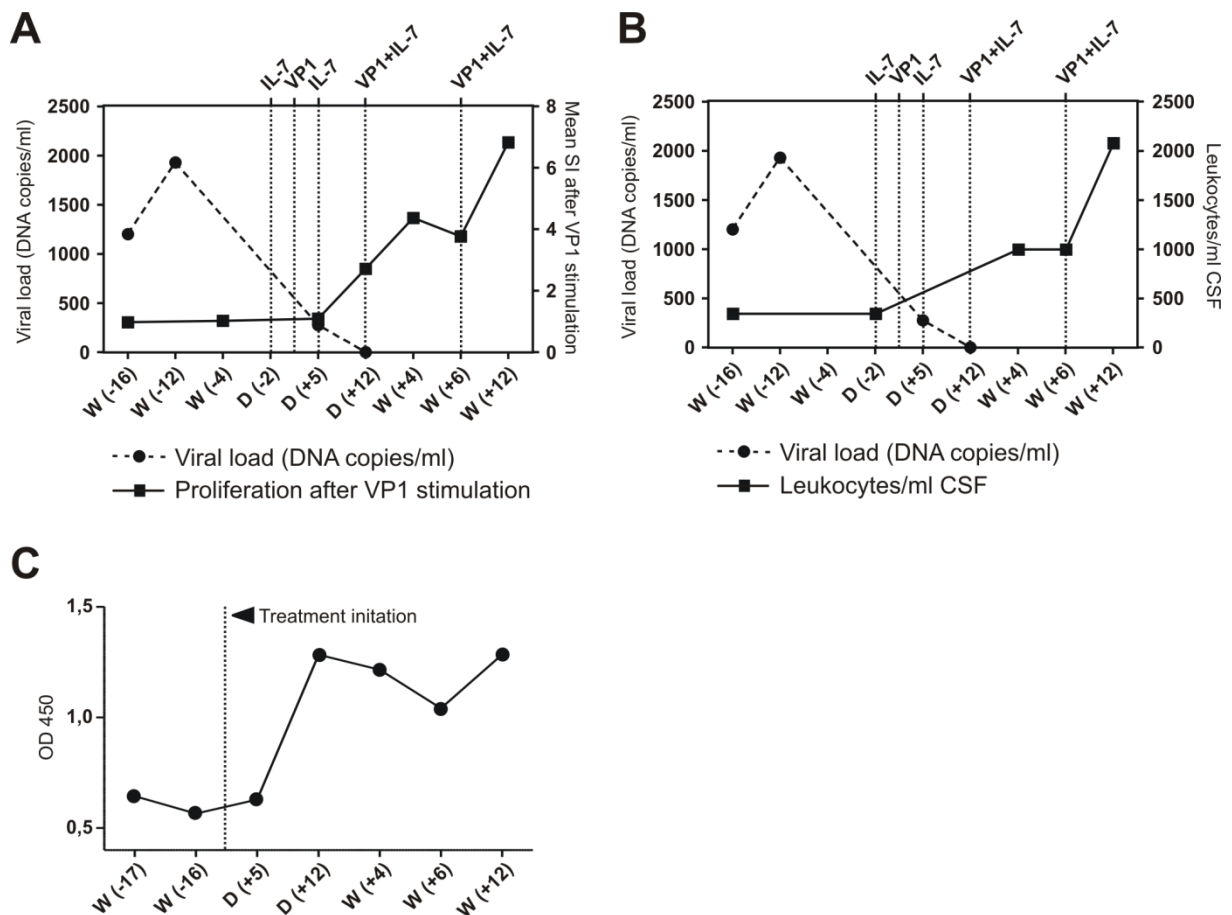


Figure 19 Development of the immune response against VP1. **A**) Analysis of the JC viral load (dashed line) in the serum and the proliferative response against VP1 (solid line) measured by ^3H -thymidine incorporation during the treatment. **B**) Number of leukocytes in the CSF against the JC viral load in the serum. Time points of IL-7 or VP1 administration are indicated by dotted lines. **C**) ELISA measurement in the serum for VP1-specific IgGs to different time points of treatment. Serum was used at a dilution of 1:5000. Initiation of therapy is indicated with a spotted line. W=week, D=day.

A similar trend was observed for the development of the B cell response, measured by VP1-specific IgG antibodies in the serum of the patient (Figure 19C). After treatment initiation the signal of VP1-specific IgGs almost doubled and remained on a stable level until the last time point of measurement.

Consistent with the assumption that the above vaccination led to boosting the JCV-specific immune response and to elimination of the virus from the brain, the clinical course of the patient stabilized. Figure 20A-C show MRI scans 12 month before, 2 month before, and 2 month after treatment, respectively. Between MRI scan A and B were 10 month and these scans show the accumulation of large lesions which correlated with the severity of the patients symptoms. After the treatment the patient did not develop any new lesions. No signs of a PML IRIS were detectable on the scans shown in Figure 20.

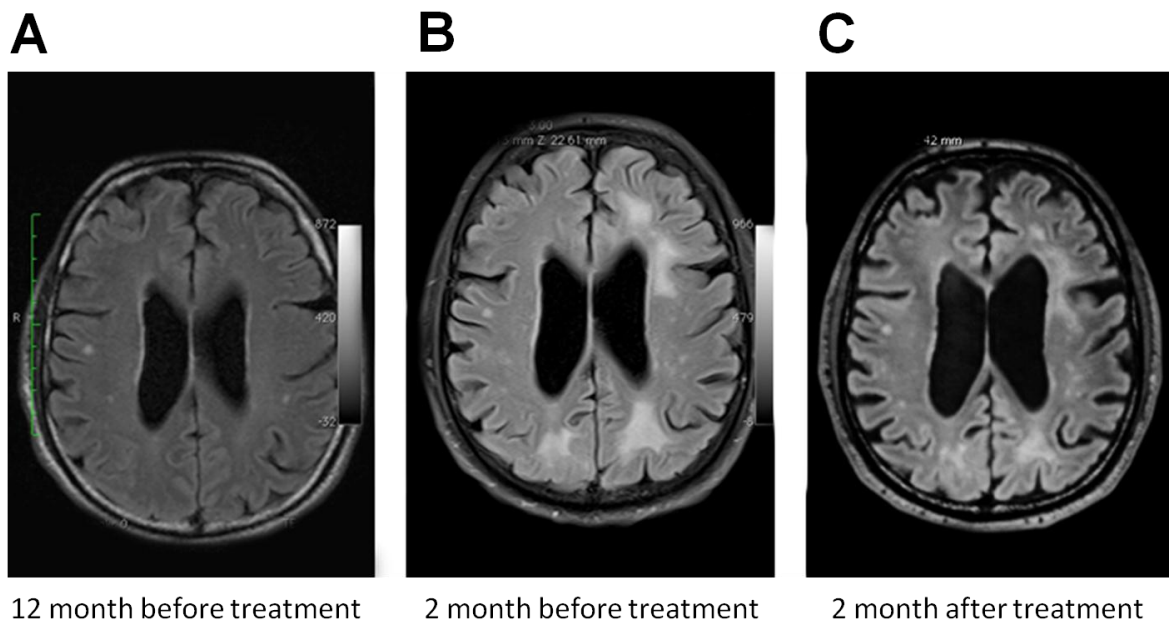


Figure 20 MRI FLAIR scans of PML brain before and after VP1 vaccination. White areas (hypointense lesions) indicate areas of demyelination. Neuroradiology, UKE, Hamburg.

3.2.3 The treatment induces VP1-specific CD4+ memory T cells

To identify the VP1-specific T cell population that was induced by the combined administration of VP1 and IL-7, a CFSE proliferation assay was conducted. CFSE incorporation allows tracking of cells by flow cytometry due to its fluorescence. Additionally, cell proliferation can be measured because the amount of CFSE is progressively declining upon cell division. Six weeks after treatment initiation PBMCs of the patient were preincubated with VP1, tetanus toxoid or without antigen, after 6 days restimulated and treated with CFSE. Five days later the cells were analyzed for their CFSE

fluorescence intensity (Figure 21A). The analysis revealed that a much higher proportion of CD4+ T cells (27% CFSE low) proliferated than CD8+ T cells (2.6% CFSE low) after VP1 stimulation.

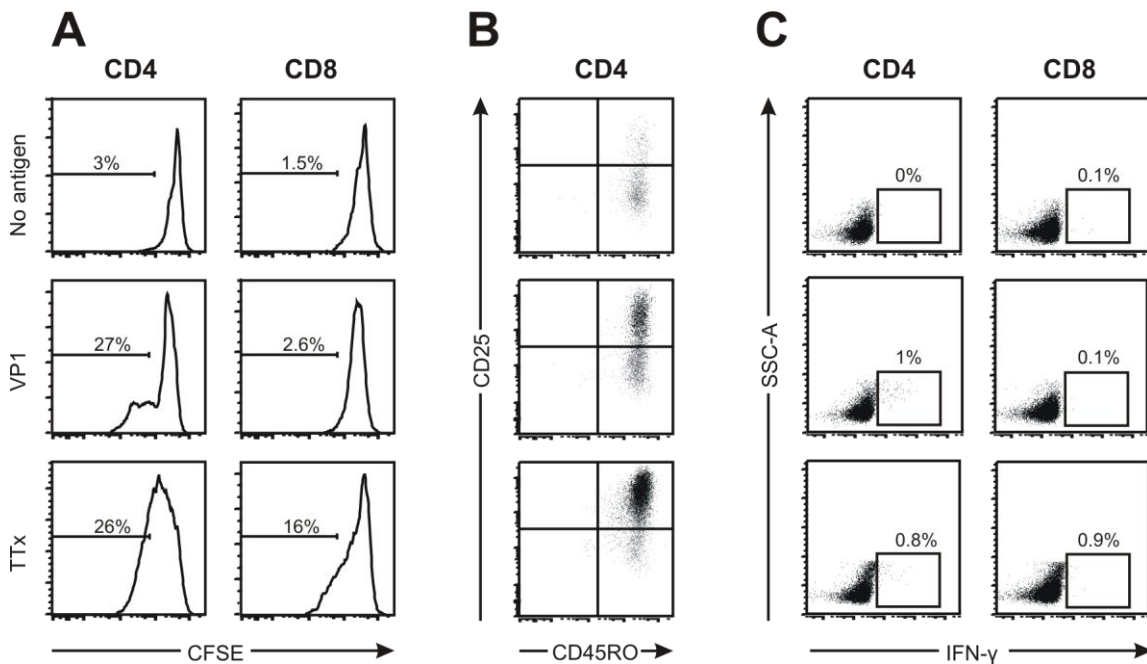


Figure 21 Analysis of VP1-specific T cells 6 weeks after treatment. A) CFSE-dilution assay of T cells stimulated with VP1 (middle), tetanus toxoid (TTx, bottom) or unstimulated (top), after 6 days restimulated and after 5 days analyzed by FACS. Cells were gated on CD4+ (left) and CD8+ (right) T cells. Percentages indicate the amount of CFSE-low cells. **B)** CD4+ T cells analysed for CD25 and CD45RO expression. CFSE-low CD4+ T cells are represented in black and CFSE-high cells are represented in grey. **C)** Intracellular IFN- γ staining after 1 wk of antigen stimulation and antigen restimulation 15h prior FACS analysis. CD4+ cells were defined as LIVE/Dead⁻ CD3⁺ CD4⁺, CD8+ cells were defined as LIVE/Dead⁻ CD3⁺ CD8⁺. Cells were stimulated without antigen (top), with VP1 (middle), or TTx (bottom). Percentages indicate IFN- γ positive cells.

Conversely, the positive control tetanus toxoid was able to stimulate both cell types (CD4+ T cells 26%, CD8+ T cells 16%), whereas the unstimulated control showed a very low frequency of background proliferation (CD4+ 3%, CD8+ 1.5%). Staining with the activation marker CD25 and the memory T cell marker CD45RO revealed that the proliferating CD4+ T cell population either stimulated with VP1 or the recall antigen tetanus toxoid had a memory phenotype (CD25+ CD45RO+).

To assess the cytokine production of VP1-specific T cells, PBMCs were preactivated with VP1 for one week and then restimulated 15h prior to FACS analysis. The preactivation process is necessary to enhance the signal to get detectable cytokine production. The analysis revealed that CD4+ T cells produced IFN- γ after VP1-encounter whereas TTx stimulation resulted in detectable levels of IFN- γ in CD4+ and CD8+ T cells (Figure 21C).

4 Discussion

4.1 *Characterization of the CD4+ T cell-mediated immune response against JC virus during PML-IRIS*

2.5 million patients worldwide suffer from multiple sclerosis, and almost 100.000 are currently treated with natalizumab. The estimated risk of developing PML after two years of natalizumab treatment is 1/400, and since approximately 20% of affected individuals so far died from the complication PML and others recovered with disabilities, the further use of this otherwise highly effective and well tolerated treatment is jeopardized. The increasing understanding of the immunological mechanisms controlling JC virus is expected to identify, who might be at higher risk to develop PML and/or lead to the development of strategies to prevent or treat already established PML. Several studies have focused on the humoral and cytotoxic immune response against JC virus (3, 113, 119, 120, 122), but less attention was paid for the role of CD4+ T cells. In particular the immunological processes that take place during PML-IRIS are poorly understood. Since PML-IRIS is the physiological state that leads to elimination of JCV from the infected brain during PML, it is reasonable to assume that important insight on immune mechanisms that normally control JCV infection can be gained from its investigation. The brain tissue that we obtained from a RRMS patient who developed PML under natalizumab treatment and subsequently PML-IRIS, allowed us to investigate the disease relevant tissue-infiltrating T cells. To our knowledge this was the first time that the immune response directed against JC virus could be analyzed with cells directly isolated from the site of inflammation. The limited accessibility of central nervous system tissue is one main reason for the lack of data in the literature and the limitation of the number of patients available for this study. However, the data provide novel insights into the inflammatory processes during PML-IRIS directly from the site of inflammation.

4.1.1 **Bi-functional Th1-2 T cells play a major role during PML IRIS**

After the patient developed first symptoms of PML, natalizumab treatment was stopped and residual antibody was washed out by plasmapheresis. Subsequently, the natalizumab-mediated block of leukocyte migration into the CNS was reversed, and consequently it came to infiltration of JC virus-specific immune cells into the brain, which caused a massive inflammatory reaction - the PML IRIS. The analysis of T cells directly isolated from the brain, revealed that the majority consisted of CD4+ T cells (70%) versus 24% CD8+ T cells (Figure 5F) which underscored the importance of CD4+ cells driving the elimination of JC virus. The two dominating T helper subsets were Th1 (IFN- γ) and Th1-2 (IFN- γ +IL-4) cells (Figure 7B). Th1-2 cells were hardly detectable in the peripheral blood but could be

found in large amounts in the intrathecal compartments CSF and brain (Figure 7B) where the strongest VP1-specific immune responses were detectable (168). Together with the finding that a significantly higher proportion of PML patients had detectable levels of Th1-2 cells in CSF or brain in comparison to CSF of non-PML patients, these data indicate that Th1-2 cells might be a critical element orchestrating the immune response against JC virus in the brain. The dual secretion of IFN- γ and IL-4 by Th1-2 cells combines the features of both Th1 and Th2 cells. IFN- γ has direct anti-viral properties (169) and it is a very potent inducer of HLA-class II (170). Its massive production explains the widespread expression of HLA-class II molecules that were found on the brain-resident cells of the patient Figure 5D (168), which are normally absent in the CNS (171). Large amounts of IL-4 activate and promote the expansion of memory B cells and plasma cells that were found among the infiltrating immune cells in the brain (Figure 5G+H). The B cells produce high titers of VP1-specific IgG antibodies that were detectable in the CSF of the patient (168). Both Th1 and Th1-2 cells expressed the chemokine receptor CXCR3 (Figure 8E) that is typically expressed by cells that can migrate across endothelial layers in the human brain (172). There is evidence that CCR4 which was expressed by the majority of Th1-2 cells (Figure 8F), plays a role in inflammatory processes in the CNS (173) pointing towards an involvement of Th1-2 to the pathogenesis of PML-IRIS.

CD4⁺ T cells simultaneously producing IFN- γ and IL-4 were previously known as Th0 cells and considered as an intermediate stage before a naïve T cell develops into a Th1 or Th2 cell. The fact that almost all brain-derived CD4⁺ T cells had a memory phenotype (Figure 5F) and that the Th1-2 T cell clones remained stable over several stimulation rounds independent of which expansion stimulus was used (Figure 9), indicates that the IFN- γ /IL-4 double producing CD4⁺ T cells are a terminally differentiated subset. This observation was confirmed by intracellular cytokine staining, cytokine secretion, chemokine receptor expression, and transcription factor analyses (Figure 8). Therefore, we propose the name Th1-2 cells. The assumption that Th1 and Th2 cells are mutually exclusive fates has already been put into question by the findings of IFN- γ /IL-4 double producing CD4⁺ T cells in measles virus infection (174), hepatitis C infection (175) and among disease-exacerbating autoreactive T cells during altered peptide ligand-based therapy of multiple sclerosis (126) and various other reports (176-179).

Whether naïve CD4⁺ T cells directly give rise to bifunctional Th1-2 cells or whether these cells differentiate from Th2 or Th1 cells due to reprogramming under inflammatory conditions in the brain, remain to be studied. However, Hegazy et al. showed in a murine virus infection model (LCMV) that non-protective GATA-3 and IL-4-producing Th2 cells were reprogrammed upon TCR trigger with LCMV peptide together with IL-12, IFN I and II to express additionally T-bet and IFN- γ (180). The co-expression of Th1 and Th2 cytokines was shown to be essential for the development of an efficient anti-viral immune response (180, 181). In addition Miner and Croft demonstrated that naïve CD4⁺ T

cells could stably differentiate into IL-4/IFN- γ producing cells after antigen exposure and moderate doses of IL-4 (182).

Our results of the transcription factor analysis in brain-derived Th1-2 CD4⁺ T cell clones (Figure 8E) that GATA-3 and T-bet can be stably expressed in the same cell, are in line with the observation from Hegazy and colleagues. This is challenging the prior hypothesis that both transcription factors strictly counter-regulate each other. A recent publication analyzing gene expression microarray data from human T cells and in silico knockouts with mathematical algorithms failed to show a counter regulatory role of both transcription factors (183). Figure 22 depicts the model of Th1 and Th2 cells extended by the finding of stable Th1-2 cells.

Our data provide evidence that Th1-2 cells play an important role in eliminating JC virus from the brain during PML-IRIS and hence probably also generally in controlling JCV infection. Whether these cells mainly orchestrate JCV-specific effector mechanisms that are mediated by antibodies or CD8⁺ T cells or participate themselves in e.g. lysis of JCV-infected astrocytes or oligodendrocytes remains to be studied.

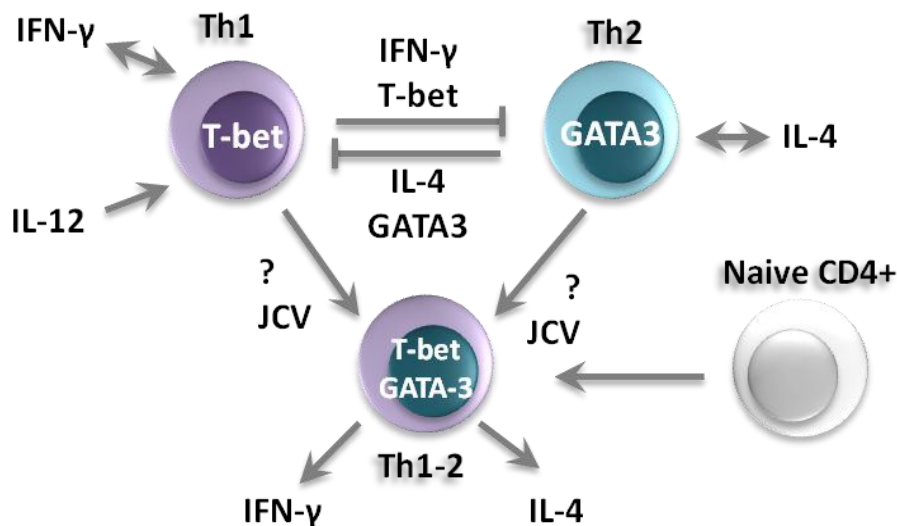


Figure 22 Theoretical model of Th1-2 development. The strict dogma that Th1 and Th2 cells counterregulate each other has to be extended. Th1-2 cells stably express T-bet and GATA-3 and excrete the cytokines IFN- γ and IL-4. Whether Th1-2 cells directly originate from a naive CD4⁺ T cell or if either Th1 or Th2 cells give rise to a Th1-2 cell due to reprogramming is not clear. Most likely JCV antigen stimulation together with a certain cytokine milieu fosters the development of Th1-2 cells.

4.1.2 Several CD4⁺ immunodominant epitopes are located within VP1

The knowledge of immunodominant epitopes is important e.g. for the design of vaccines. Epitope mapping of JC virus has so far focused on the identification of immunodominant CD8⁺ T cell epitopes. The finding that the majority of infiltrating T cells in the brain of the PML-IRIS patient were CD4⁺ T cells, together with the lack of information on the role of these cells in JC virus defense, set the focus on the fine specificity of CD4⁺ cells. By choosing 15mer peptides for the epitope mappings

of JCV CD4+ cells were preferentially addressed. Several immunodominant epitopes could be identified, which all originate from structural domains of the virus (168). However, the majority of immunodominant epitopes were located within the major capsid forming protein VP1 (Figure 10C)(168). The fact that all JCV-specific T cell clones were able to respond to single peptides and whole VP1 protein, implies that the identified peptides contain the immunogenic areas of the naturally processed and presented peptides by the APCs. Several T cell clones showed slight cross recognition of more than one peptide (Figure 10A). Some clones recognizing the immunodominant epitope VP1₃₄ are able to cross-react to the appropriate BK virus peptide (Figure 17C). BK virus is similarly widespread in the human population as JC virus. The data provide evidence that at least a part of the T cell repertoire specific for either one the virus is protective against both JCV and BKV.

Interestingly, the CD4+ immunodominant DQB1*06:02-restricted epitope VP1₃₄₋₄₈ contains an immunodominant CD8+ epitope VP1₃₆. This recently discovered HLA-A*02:01-restricted CD8+ epitope VP1₃₆ and additionally VP1₁₀₀ (119) were recognized by CD8+ T cells of the brain from the PML-IRIS patient (Figure 11). The clinical severity of PML-IRIS in the patient who was examined here, might be in part explainable by his HLA type. Besides HLA-A*02:01 he carried the HLA-class-II alleles that confers the highest risk of developing MS: HLA-DRB1*15:01 (in tight linkage disequilibrium with DRB5*01:01/DQB1*06:02) (Ebers et al, 1996; Oksenberg et al, 1996). Thus, the same peptide presented by class I and class II molecules leads to activation of CD8+ and CD4+ T cells which can lead to a particularly pronounced immune response leading to the severe symptoms of PML-IRIS.

Besides identifying VP1 as the major epitope of the CD4+ and CD8+ T cell response, we also found high anti-VP1 IgG antibody titers within the CSF of the patient. This makes particular sense since VP1 as the major capsid forming protein is accessible to antibodies that preferentially recognize conformational determinants on the surface of pathogens. This is further emphasizing the role of VP1 as major epitope in the anti-viral immune response orchestrated by CD4+, CD8+ T- and B- cells. These results provide evidence that VP1 is a promising candidate for the development of therapeutical vaccines.

4.1.3 JCV-specific T cells accumulate in the brain and not CSF

The brain is surrounded by cerebrospinal fluid that provides mechanical and immunological protection. One way to enter the brain leads immune cells across the blood-CSF barrier through the choroid plexus (184). Therefore, the CSF is often considered as a surrogate for the immune cell composition in the CNS, since brain tissue samples are hardly available. Interestingly, the comparison of the T cells composition in the different compartments, the peripheral blood, CSF, and brain revealed substantial differences (Figure 12). Due to the limited diversity of T cells in the intrathecal compartments the CDR3 spectratypes showed highly skewed profiles with few dominant peaks

representing clonally expanded T cells in the CSF and brain. Tracking of single peaks comprising CD4+ T cell clones that recognize immunodominant JCV epitopes revealed that these were absent in the CSF in many cases. These results were also reflected by the strength of the proliferative immune response towards VP1 in the different compartments with a mean SI of >600 in the brain, ~8 in the CSF, and ~2,5 in the peripheral blood after expansion (168). This is in line with the observations of Flügel and colleagues that myelin-specific T cells in an animal model of MS, the experimental autoimmune encephalomyelitis (EAE), massively migrate into the CNS and are thereby depleted in the peripheral organs (185). The weak T cell response towards VP1 and the lack of peaks from VP1-specific TCC in the CSF implies that migrating disease-relevant T cells directly accumulate in the affected tissue without being enriched in the adjacent CSF. Nevertheless, the CSF is useful for the examination of the humoral anti-JCV response, since high anti-VP1 IgG antibody titers were found in the CSF of the PML-IRIS patient.

4.1.4 A high proportion of brain-infiltrating CD4+ T cells are restricted by multiple HLA-class II elements

The brain is an immunoprivileged organ, and the limited expression of HLA-class II molecules is considered one important aspect of this immunoprivilege (171). During CNS inflammation, the release of IFN- γ leads to induction of HLA-class II molecules on CNS-resident cells such as astrocytes, microglia or glial cells, yet differentially affecting the proportion of expressed HLA-DR, -DP, and -DQ molecules on these cell types (186). The HLA-class II restriction of the VP1-specific T cell clones was assessed to analyze the predominating restriction elements in the brain during PML-IRIS. For this purpose APCs sharing single DR- and DQ molecules were used, i.e. B cell lines expressing single alleles of the MS-associated risk haplotype DRB1*15:01/DRB5*01:01/DQB1*06:02, that are inherited in tight linkage disequilibrium, and DRB1*11:03.

The surprising finding was that the majority of T cell clones were able to recognize peptides in the context of up to four different MHC-class II molecules including HLA-DR and -DQ (Figure 14A). This implies two different phenomena: first a high tendency of certain VP1 peptides to bind to different HLA molecules and second the accumulation of T cells bearing TCRs that are able to respond to different HLA molecules.

Promiscuously HLA-binding peptides have been reported to bind with higher affinity to the corresponding HLA molecules than peptides that bind to single alleles (175, 187). This can probably be explained by the high affinity range of promiscuous peptides that enables them to also bind to HLA molecules with non-optimal binding groove, whereas interaction of a peptide with general low binding affinity will not lead to detectable binding to a non-optimal binding groove of an HLA molecule. If the promiscuous VP1 peptides have indeed higher binding affinities than monogamous

VP1 peptides to their restriction elements, remains to be studied. Interestingly, four TCC (4, 6, 12, and 13) showed peptide recognition in the context of HLA-DR and -DQ. DR molecules among each other are structurally closer related than -DR and -DQ molecules. The presentation of promiscuous peptide ligands by a variety of different DR molecules has been reported in several experiment setups (71, 188-190). In fact, a promiscuous binding of antigenic peptides to different HLA-class II molecules has been suggested as a general feature of CD4+ T cell epitopes (191). The observed cross-restriction of several T cell clones isolated from the brain biopsy of the PML-IRIS patient indicate that several immunodominant peptide epitopes out of the sequence of the VP1 protein can bind to a wide variety of different restrictions elements including HLA-DR and -DQ molecules (Figure 14A).

Several cross-restricted T cell clones with the ability to recognize peptides in the context of more than two HLA molecules, could be identified among the VP1-specific, brain-derived T cells from the patient. Especially, in an immunoprivileged organ such as the brain it is conceivable that the ability to respond to the cognate antigen in context of more than one restriction element can be of great advantage. The efficient elimination of JCV would then be guaranteed by cross-restricted CD4+ T cells when the CNS-resident cells may only express certain alleles, e.g. DR or DQ, but not all alleles of the respective haplotype.

Astrocytes from MS patients showed increased HLA-DR expression after IFN- γ exposure whereas -DQ expression was limited (186). Cross-restricted TCC with a Th1-2 phenotype could contribute to the efficient lysis of infected astrocytes (42, 192) that are known host cells for JC virus during PML (193). The fact that a subset of clones (Figure 14A and Table 17) is preferentially or only restricted by HLA-DQ could indicate that the VP1₃₄₋₄₈ peptide preferentially binds to the DQW6 allele and/or that certain JCV-infected CNS cells express primarily this HLA-class II molecule during PML-IRIS. The cross-restricted clones that used multiple restriction elements were significantly more sensitive with respect to antigen avidity than TCC that were restricted by two or only one restriction element (Figure 14C). A possible explanation is the increased avidity of T cells that use more than one HLA class-II molecule for recognition is the resulting in a higher density of possible HLA interaction partners on the surface of the APC. However, one cannot infer from these data that mono-restricted T cell clones using DQB1*06:02 as restriction element are less important in antigen clearance than their more sensitive cross-restricted counterparts. Their relatively high abundance (Figure 6A and Table 17) argues that other factors are also involved.

Due to the paucity of material it was not possible to determine the HLA-DQ expression in the brain biopsy sample, but the above mentioned findings suggest that HLA-DQ expression might be elevated during the inflammatory condition of PML IRIS.

4.1.5 TCR-pMHC interaction of TRBV20/TRAV13 TCC

Analysis of clonal phenotypes, frequencies and specificities in the expanded T cell populations revealed two distinct strategies or patterns of viral epitope recognition by brain-infiltrating JCV-specific CD4⁺ T cells. Figure 10B shows that immunodominant epitope VP1₃₄ is recognized by five different clones (TCC 1-5) whereas immunodominant epitope VP1₇₄ is recognized by one clone (TCC 7), which probably underwent strong clonal expansion in the tissue, since five of the 15 characterized T cell clones were the identical clone TCC 7. If one takes these clones as representatives of the whole T cell population in the brain it seems that one recognition strategy involves a heterogeneous T cell population, whereas the other pattern implies that epitope recognition is more stringent and provided by a single T cell population that was expanded during the inflammatory process. If we take a closer look at the T cell population recognizing VP1₃₄ we find some noticeable similarities. All clones of this group have a TCR consisting of a TRBV20-1 and a TRAV13-1 chain (Table 17 and Table 18), they all are DQB1*06:02-restricted (Figure 14A), but have mixed phenotypes (Th1 and Th1-2, Table 17). This group of clones and clone 7 make up the largest CD4⁺ T cell populations in the brain assessed by their TCR Vbeta chain usage (TRBV20-1 TCC 1-5 and TRBV5-1 TCC 7, Figure 6A) and CDR3 spectratyping (Figure 13). Therefore, it appears that both types of recognition patterns are equally important for the efficient elimination of JC virus. An overview is depicted in Figure 23.

The determinants for the peptide-MHC specificity lie within the variable chains of the T cell receptor. Most likely the TRBV20-1 chain mediates the strict DQ restriction since all mono-restricted clones bear this beta chain (TCC 1, 2, 3, 5, and 10). Interestingly, TCC 4 is less stringent in its MHC interaction, since it can also recognize peptide in the context of DRB1*11:03 albeit to a lesser extent (Figure 14A). The extremely variable CDR3 loops are located over the center of the peptide-MHC complex and mediate contact to the antigenic peptide as well as with the α -helices of the MHC molecule. The less variable CDR1 and CDR2 loops contact the central parts of the MHC molecule but can also contribute to peptide binding (194, 195). The only differences between TCC 4 and the other TRBV20-1/TRAV13-1 clones are located within the CDR3 region (Figure 15). Hence, these changes are most likely responsible for the less stringent MHC recognition in TCC 4.

Based on these data it is conceivable that the CDR1 and CDR2 loops contribute to a considerable extent to peptide/MHC binding while the CDR3 region has a more modulatory function. This would mean that the random pairing of a TRBV20-1 with a TRAV13-1 chain leads to a functional TCR with a high intrinsic specificity to VP1₃₄ presented by DQB1*06:02 HLA molecules. These considerations are in line with observations of high resolution crystal structures of an immunodominant and public TCR with a conserved alpha-beta chain combination that recognizes an influenza matrix peptide in context of HLA-A*02:01 (196). Ishizuka and colleagues showed that the majority of “binding hotspots” were located within the germline encoded invariable CDR1 and CDR2 loops of the TCR beta

chain and that single common residues within CDR3 contributed by optimizing the peptide/MHC binding. To establish clarity how the different hyper variable loops of the TRBV20-1/TRAV13-1 VP1₃₄-specific clones contribute to peptide/MHC recognition crystallization studies are necessary.

The persistent infection with JC virus chronically exposes the immune system to virus-infected cells and probably leads to selection of distinct memory T cells that recognize these well. Unlike somatic hypermutation of the rearranged B cell receptor genes, it is widely assumed that the TCR is fixed as soon as the T cell enters the periphery after thymic selection. However, shaping of the T cell response also occurs after repeated infections and persistent viral infections due to preferential expansion of high avidity T cells (197). Especially under conditions of latent viral infections with very low amounts of viral antigen presented by APCs the virus-specific T cells compete against each other for their specific “substrate” (198), resulting in the expansion of T cells with increased avidity for their antigen. Lawson and colleagues showed that an immunodominant and public TCR specific for an influenza matrix peptide was not shaped by thymic selection but was accumulated due to repeated infection with influenza virus (199). The occurrence of such a high number of clones bearing a TCR with a TRBV20-1/TRAV13-1 combination specific for the epitope VP1₃₄, but with varying CDR3 sequences could be an example for the evolutionary process of T cell response optimization during persistent viral infection.

Besides the peripheral selection process for high avidity TCRs there is another hypothesis for the accumulation of clones with the same specificity, TCR $\alpha\beta$ chain combination, and different CDR3 sequences. RAG enzymes that are responsible for V(D)J gene recombination are normally silenced after thymic development. However, Serra and colleagues demonstrated that encounter with specific antigen of pancreatic islet-specific T cells led to reexpression of RAG enzymes providing the T cells with the ability to rearrange their TCRs, which then could lead to fine tuning of antigen recognition (200). The reactivation of RAG enzymes resulting in TCR editing was also reported by others (201, 202). Whether reactivation of RAG enzymes is responsible for the accumulation of TRBV20/TRAV13 clones with different CDR3 regions remains to be studied.

The results of the peptide alanine-scans indicate that glutamic acid (E41) within the core region of the peptide is critical for either TCR or MHC contact since its substitution with alanine leads to complete abrogation of the proliferation response of all clones (Figure 17A). This glutamic acid could interact with the basic amino acid lysine (K) that occurs at position 115 (IMGT numbering) within the CDR3 α region of all clones but TCC 2. There one finds a lysine residue at position 120 within the J region directly adjacent to the CDR3 loop. Alternatively, the glutamic acid could be a possible MHC anchor such that its substitution would prevent binding to the MHC molecule. Interestingly, no other amino acid substitution leads to complete abrogation of the response of TCC 1 and 5. Several substitutions are able to strongly diminish the response of both clones although not completely.

Another critical residue is phenylalanine (F43), the substitution of which abrogates the proliferative response completely in TCC 2 and 4. To differentiate exactly between MHC and TCR relevant residues in the peptide sequence, peptide-MHC binding assays have to be performed. Overall, the recognition patterns in all clones are very similar, however the observed differential effects of amino acid exchanges on T cell recognition are probably attributable to the different amino acid sequences in the CDR3 region of the TCR. The recognition patterns of TCC 1 and 5, which show the highest similarity, share an identical CDR3 α loop but less homology in the CDR3 β loop (Figure 17A, Figure 16). This might indicate a stronger involvement of the CDR3 α sequence to peptide binding. The CDR3 sequences of the beta chains from all five clones were in general more heterogeneous in terms of amino acid composition than the CDR3 sequences of the alpha chain (Figure 15) which might indicate a critical role of putative conserved residues within CDR3 α important for peptide contact.

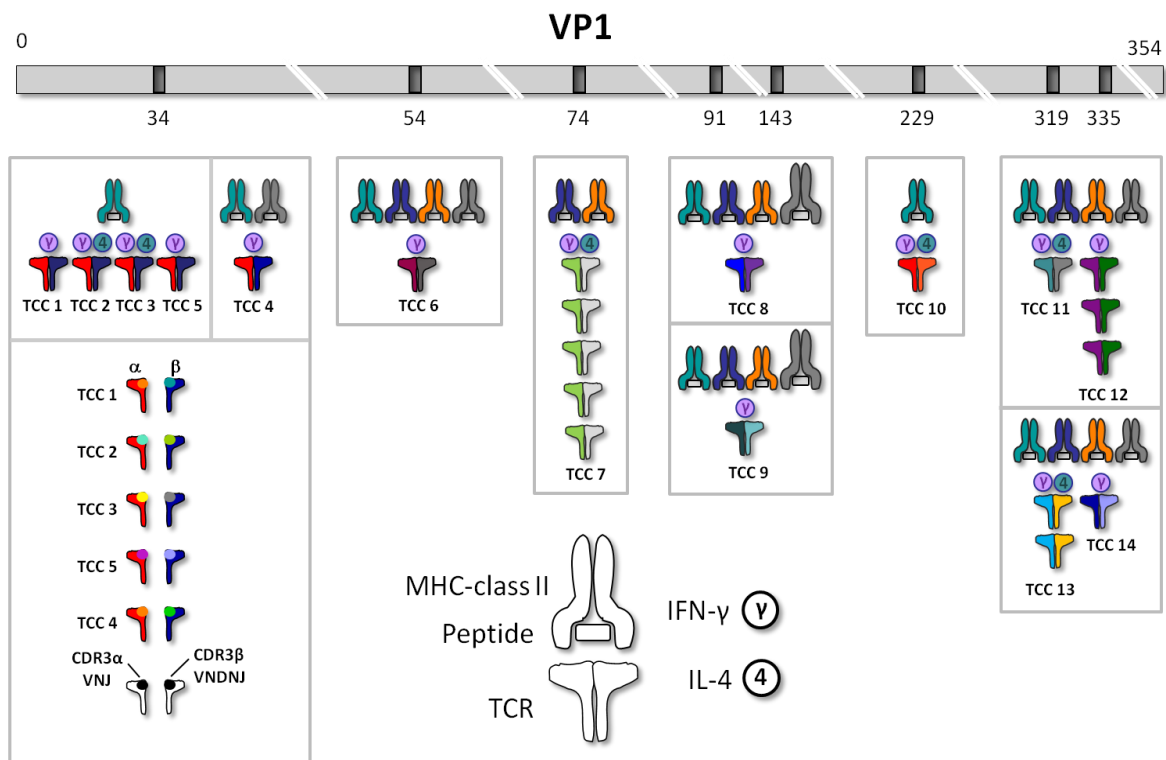


Figure 23 Multiple solutions of JCV epitope recognition by CD4+ T cells during PML IRIS.

The VP1 sequence is depicted as grey bar and immunodominant epitopes are delineated in dark grey. MHC molecules belonging to the same haplotype have the same color (cyan=DQB1*06:02, grey= DRB1*11:03, blue=DRB5*01:01, orange=DRB1*15:01). The pre-dominant use of one MHC molecule by a T cell clones is indicated by a larger MHC symbol. The TCR α and TCR β chains of different clones have various colors.

4.2 Treatment of PML and idiopathic CD4+ lymphocytopenia

The restoration of the immune system is currently the only effective approach to combat JC virus during PML. All therapeutic strategies directly targeting JC virus have so far failed to show efficacy in large cohorts (139-142). The immune system of the CD4+ lymphocytopenia patient, who had no other underlying diseases and an unremarkable clinical history, was not able to sustain a sufficient immune response against JCV, which subsequently led to PML. Here I report on the safety and efficacy of our developed treatment strategy of the combined vaccination with the major capsid-forming protein VP1 together with an adjuvant and the administration of IL-7. The patient showed no signs of adverse events and developed a stable immune response against JC virus which led to a stop of PML progression.

4.2.1 VP1 vaccination elicits CD4+ cellular and humoral immunity

The combined treatment regimen successfully induced a stable CD4+ T cell and humoral response against VP1. This was accompanied by a decline of the JCV viral load below the detection limit (Figure 19A) and at the same time an increase of leukocyte counts in the CSF was detectable (Figure 19B). These data provide evidence that the therapy was able to induce an immune response sufficient to control JCV. This notion is underscored by the clinical stabilization of the patient. Before treatment he was rapidly deteriorating and MRI scans 10 month apart before vaccination show the development of an extensive CNS lesion (Figure 20A+B). This rapid progression was stopped, Figure 20C shows an MRI scan two month after treatment (4 month after MRI scan B), and it is apparent that no new lesions appeared. His condition remained stable until today and he showed only very subtle signs of PML-IRIS on a MRI that was performed three months after vaccination.

By dissecting the immune response induced by the vaccination we could identify two cell types driving the anti-JCV reaction. Together with B cells producing JCV-specific IgG antibodies (Figure 19C) the CD4+ T cells probably were involved in eliminating JC virus (Figure 21A). Remarkably, the VP1-specific CD4+ T cells had a Th1 memory phenotype (Figure 21B+C). The induction of memory cells due to vaccination is a prerequisite for long-lasting immunity. However, conversely to the use of attenuated live vaccines that can induce immunity that lasts for decades even after a single immunization, the vaccination with pathogen subunits, normally is less persistent and require repeated vaccinations to maintain protection (203). The observation that the anti-VP1 response was boosted by repeated vaccinations (Figure 19A) implies that further injections of VP1/IL-7 could be meaningful. Recently, it was shown that the use of imiquimod containing a single TLR agonist (TLR7) induced less pronounced immune responses in melanoma patients than other adjuvants such as the saponin based iscomatrix or montanide ISA-51 together with a TLR9 agonist under similar vaccination

conditions (204). But since imiquimod was well tolerated by the treated PML patient and the elicited immune response was sufficient to stop disease progression, it remains open if combination with another agonist would be superior. It has been shown that signaling through several TLRs leads to synergistic activation of DCs resulting in enhanced and sustained Th1-polarizing capacity (205). Therefore, the combination with the closely related TLR8 agonist could be promising.

Neither the ratio of CD4/CD8 T cells did change during the treatment nor did the total lymphocyte count increase. However, we cannot exclude that the use of recombinant IL-7 (CYT107) has a general beneficial effect on the stable development of an anti-JCV immune response. Recently, it was reported that the use of CYT107 together with an experimental oral form of cidofovir (CMX001) in a patient with PML and idiopathic CD4 lymphocytopenia led to an increase of CD4+ counts and the decline of JCV viral load (206). We therefore still recommend the use of IL-7 in the treatment of PML. The direct linkage of the appearance of VP1-specific CD4+ T cells to the decline of the viral load and halt of disease progression underscores the importance of CD4+ T cells for immune protection against JC virus and are in line with the data obtained from the PML-IRIS patient. The treatment strategy was able to stop the rapid disease progression and so far has prevented the patient from developing further disability or even death caused by PML. The introduced therapeutic strategy represents a very promising and easily applicable attempt to treat or prevent PML. Possible candidates are immunocompromised or immunodeficient individuals like AIDS patients or patients with congenital immune defects. Further, patients that have to undergo immunosuppressive treatment are eligible candidates e.g. before organ transplant or treatment with monoclonal antibodies due to an underlying autoimmune disease. The next step has to assess the safety and efficacy in a larger cohort of patients.

5 Summary

In this work CD4+ T cells are characterized that are involved in the immune defence against JC virus which is the causal agent of progressive multifocal leukoencephalopathy. In particular the role of CD4+ T cells during PML immune reconstitution inflammatory syndrome was addressed. The study provided evidence that CD4+ T cells are an essential part of the defence mechanisms against JCV. The examination of tissue-infiltrating leukocytes isolated from a brain biopsy of a PML patient with IRIS revealed that the majority of T cells had a CD4+ phenotype, although, CD8+ T cells are commonly thought to be the major cell type driving the immune response against JC virus. The isolated CD4+ T cells mainly consisted of IFN- γ -secreting Th1 cells and a cell type that was able to produce simultaneously IFN- γ and IL-4. Based on these findings these cells were subsequently termed bi-functional Th1-2 cells. Besides the secretion of IFN- γ and IL-4 these cells were able to upregulate the Th1- and Th2-specific transcription factors T-bet and GATA-3. Furthermore, Th1-2 cells were characterized by the expression of the chemokine receptors CXCR3, CCR5, and CCR4. Fine specificity analyses were conducted and revealed that the majority of CD4+ immunodominant epitopes were located within the major capsid-forming protein VP1. Another interesting aspect was the finding that the T cell composition in the brain highly differed from the composition in the CSF or peripheral blood. VP1-specific clones were hardly detectable in the CSF which is frequently taken as surrogate for the T cell composition of the hard accessible brain. T cell clones specific for VP1 were isolated in order to assess their specificity, HLA restriction, antigen avidity and TCR in more detail. Most T cell clones were able to interact with different MHC-class II molecules which can be of advantage in the central nervous system where MHC expression is limited. Due to the higher avidity these cross-restricted T cell clones were significantly more sensitive. However, DQB1*06:02 mono-restricted clones are not less efficient in JCV elimination implied by their strong expansion in the brain and their recognition of immunodominant epitopes. Based on this finding it is conceivable that HLA-DQ expression is elevated in the brain during PML-IRIS. Another observation was the accumulation of different T cell clones specific for an immunodominant epitope presented by DQB1*06:02 and a certain TCR V α and V β chain combination. A functional T cell receptor consisting of this random combination of both chains might have an intrinsic affinity for this certain peptide-MHC complex, mediated by the invariant regions CDR1 and CDR2 of both chains which do not differ between the clones of this group. Conversely, the hypervariable CDR3 region seems to be important for the fine tuning of antigen recognition. In summary, multiple strategies for JCV-antigen recognition during PML-IRIS were identified that ensure efficient elimination of JC virus but as well might be involved in the excessive immune response in the brain causing the severe symptoms of the immune reconstitution inflammatory syndrome.

The second part of the work focused on the characterization of the JC virus-specific immune response during an experimental vaccination attempt of a PML patient with underlying CD4 lymphocytopenia. To boost the patients insufficient immune response against the virus he was vaccinated with VP1 protein, an adjuvant containing a TLR7 agonist, and recombinant IL-7. The viral load in the serum declined to a non-detectable level after repeated vaccination. Furthermore, an increase of VP1-specific IgG antibodies was observed as well as the induction of VP1-specific CD4+ T cells with a Th1 memory phenotype. The disease progression could be stopped. Based on these findings vaccination with VP1 is a promising and easy applicable approach for the treatment of PML patients.

6 Zusammenfassung

Diese Arbeit beschäftigte sich mit der Charakterisierung von CD4+ T-Zellen, die involviert sind bei der Immunabwehr gegen das JC-Virus (JCV), dem Verursacher von progressiver multifokaler Leukoencephalopathie (PML). Insbesondere wurde die Rolle der CD4+ T-Zellen während des inflammatorischen PML-Immunrekonstitutionssyndroms (PML-IRIS) näher beleuchtet. Es konnte belegt werden, dass CD4+ T-Zellen eine zentrale Rolle bei der Bekämpfung dieses Virus einnehmen. Bei der Untersuchung gewebeinfiltrierender Leukozyten, isoliert aus der Hirnbiopsie eines PML Patienten mit IRIS, stellte sich heraus, dass es sich bei dem Großteil der T-Zellen um CD4+ Zellen handelte und nicht um CD8+ Zellen, die gemeinhin als Hauptagitatoren gegen das JC-Virus gelten. Diese CD4+ T-Zellen setzten sich hauptsächlich zusammen aus IFN- γ -sezernierenden Th1-Zellen und einem Zelltyp, der gleichzeitig IFN- γ und IL-4 produziert und daraufhin bifunktionaler Th1-2 Typ benannt wurde. Diese bifunktionalen Th1-2 Zellen sind, neben der gleichzeitigen Produktion von IFN- γ und IL-4, in der Lage die Th1- und Th2-spezifischen Transkriptionsfaktoren T-bet und GATA-3 exprimieren. Des Weiteren konnten diese Zellen über die Chemokinrezeptoren CXCR3, CCR5 und CCR4 charakterisiert werden. Neben dem Phänotyp wurde auch die Feinspezifität der hirngewebeinfiltrierenden CD4+ T-Zellen untersucht. Dabei wurde gezeigt, dass der Großteil der immundominanten Epitope innerhalb des VP1 Proteins lokalisiert sind, welches das Haupthüllprotein des Virus bildet. Ein weiterer interessanter Fund war die Tatsache, dass die T-Zellpopulationen im Gehirn sich stark unterschieden von denen im CSF oder peripheren Blut. VP1-spezifische Klone ließen sich kaum im CSF nachweisen, das häufig als Repräsentator für die T-Zellzusammensetzung für das schwerer zugängliche Hirngewebe angesehen wird. Durch die Generierung von VP1-spezifischen CD4+ T-Zellklonen konnte deren Feinspezifität, HLA-Restriktion, Antigensensitivität und T-Zellrezeptor genauer untersucht werden. Es stellte sich heraus, dass der Hauptteil der CD4+ T-Zellklone in der Lage war mit unterschiedlichen MHC-II Molekülen zu interagieren, was vor allem im Bereich des Zentralnervensystems mit seiner Limitierung der MHC-Expression einen Vorteil darstellen könnte. Durch die höhere Avidität zeigten diese kreuzrestringierten T-Zellklone eine signifikant höhere Antigensensitivität. Nichtsdestotrotz stellen die weniger sensitiven mono-restringierten T-Zellklone eine ebenso erfolgreiche T-Zellpopulation dar, die zu der am stärksten expandierten Population im Gehirn des PML-IRIS Patienten gehörte und immundominante Epitope aus der Peptidsequenz des JC-Virus erkannte. Dadurch, dass alle isolierten mono-restringierten Klone ihr spezifisches Peptid über das HLA Molekül DQB1*06:02 erkannten liegt die Vermutung nahe, dass die DQ-Expression relativ zur DR-Expression im Gehirn während PML-IRIS erhöht ist. Ein weitere interessante Beobachtung war die Anhäufung von verschiedenen T-Zellklonen mit Spezifität für ein immundominantes Epitop präsentiert durch DQB1*06:02 und einer bestimmten TCR V α - und V β -

Kettenkombination. Ein funktionierender T-Zellrezeptor, der aus der zufälligen Kombination dieser beiden Ketten entsteht, weist womöglich eine intrinsische Affinität zu dem bestimmten MHC-Peptidkomplex auf, die durch die invarianten CDR1- und CDR2-Regionen beider Ketten vermittelt wird und sich in allen Klonen dieser Gruppe nicht unterscheidet. Die hypervariable CDR3-Region hingegen hat in dieser Kombination eher modulatorischen Charakter. Zusammenfassend lässt sich sagen, dass multiple Strategien zur JCV-Antigenerkennung im Gehirn während der PML-IRIS existieren, die eine effiziente Eliminierung des Virus gewährleisten und gleichzeitig zu der überschießenden Immunantwort im Gehirn beitragen, die zu den schweren Symptomen des Immunrekonstitutionssyndroms beitragen.

Der zweite Teil der Arbeit beschäftigte sich mit der Charakterisierung der Entwicklung einer JC-viruspezifischen Immunantwort nach einem individuellen Heilversuch an einem Patienten mit PML und idiopathischer CD4-Lymphozytopenie. Um die unzureichende Immunantwort des Patienten gegen das JC-Virus zu stärken erhielt er eine Vakzine bestehend aus VP1-Protein, einem TLR-7-haltigen Adjuvans und rekombinantem IL-7. Nach mehrmaliger Impfung sank die JC-Viruslast im Serum auf ein nicht-detektierbares Level und es war ein Anstieg der VP1-spezifischen IgG-Antikörper feststellbar, sowie eine Induktion von VP1-spezifischen CD4+ T-Zellen mit einem Th1 Memory Phänotyp. Die Krankheitsprogression konnte gestoppt werden. Die VP1-Vakzinierung stellt somit einen vielversprechenden Heilansatz bei der Therapie von PML dar.

7 Literature

1. K.-E. Astrom, E. L. Mancall, E. P. Richardson, Progressive Multifocal Leuko-Encephalopathy, *Brain* **81**, 93-111 (1958).
2. B. L. Padgett, D. L. Walker, G. M. Zurhein, R. J. Eckroade, B. H. Dessel, Cultivation of papova-like virus from human brain with progressive multifocal leucoencephalopathy., *Lancet* **1**, 1257-60 (1971).
3. A. Egli et al., Prevalence of polyomavirus BK and JC infection and replication in 400 healthy blood donors., *The Journal of infectious diseases* **199**, 837-46 (2009).
4. C. S. Tan, I. J. Koralnik, Progressive multifocal leucoencephalopathy and other disorders caused by JC virus: clinical features and pathogenesis., *Lancet neurology* **9**, 425-37 (2010).
5. R. Medzhitov, C. a Janeway, Innate immunity: the virtues of a nonclonal system of recognition., *Cell* **91**, 295-8 (1997).
6. a Isaacs, J. Lindenmann, Virus Interference. I. The Interferon, *Proceedings of the Royal Society* **147**, 258-267 (1957).
7. S. Akira, K. Takeda, T. Kaisho, Toll-like receptors: critical proteins linking innate and acquired immunity., *Nature immunology* **2**, 675-80 (2001).
8. P. C. Doherty, R. M. Zinkernagel, Capacity of Sensitized Thymus-Derived Lymphocytes to Induce Fatal Lymphocytic Choriomeningitis Is Restricted by the H-2 Gene Complex, *Journal of immunology* **114**, 30-33 (1975).
9. D. J. Shedlock, H. Shen, Requirement for CD4 T cell help in generating functional CD8 T cell memory., *Science* **300**, 337-9 (2003).
10. E. M. Janssen et al., CD4+ T cells are required for secondary expansion and memory in CD8+ T lymphocytes., *Nature* **421**, 852-6 (2003).
11. S. E. Hamilton, M. C. Wolkers, S. P. Schoenberger, S. C. Jameson, The generation of protective memory-like CD8+ T cells during homeostatic proliferation requires CD4+ T cells., *Nature immunology* **7**, 475-81 (2006).
12. M. Matloubian, R. J. Concepcion, R. Ahmed, CD4+ T cells are required to sustain CD8+ cytotoxic T-cell responses during chronic viral infection., *Journal of virology* **68**, 8056-63 (1994).
13. R. D. Cardin, J. W. Brooks, S. Sarawar, P. C. Doherty, Progressive loss of CD8+ T cell-mediated control of a gamma-herpesvirus in the absence of CD4+ T cells, *Journal of e* **184**, 863-871 (1996).
14. M. Altfeld, E. S. Rosenberg, The role of CD4(+) T helper cells in the cytotoxic T lymphocyte response to HIV-1., *Current opinion in immunology* **12**, 375-80 (2000).
15. M. E. Pipkin et al., Interleukin-2 and Inflammation Induce Distinct Transcriptional Programs that Promote the Differentiation of Effector Cytolytic T Cells, *Immunity* **32**, 79-90 (2010).

16. B. Perussia et al., Immune interferon and leukocyte-conditioned medium induce normal and leukemic myeloid cells to differentiate along the monocytic pathway., *The Journal of experimental medicine* **158**, 2058 (1983).
17. U. Boehm, T. Klamp, M. Groot, J. C. Howard, Cellular responses to interferon-gamma., *Annual review of immunology* **15**, 749-95 (1997).
18. M. S. Diamond, B. Shrestha, A. Marri, D. Mahan, M. Engle, B Cells and Antibody Play Critical Roles in the Immediate Defense of Disseminated Infection by West Nile Encephalitis Virus, *Journal of virology* **77**, 2578-2586 (2003).
19. C. Lavarini et al., IgM antibody against hepatitis B core antigen (IgM anti-HBc): diagnostic and prognostic significance in acute HBsAg positive hepatitis., *British medical journal* **287**, 1254-6 (1983).
20. A. Ahmad, J. Menezes, Antibody-dependent cellular cytotoxicity in HIV infections, *The FASEB journal* **10**, 258-266 (1996).
21. T. R. Mosmann, H. Cherwinski, M. W. Bond, M. a Giedlin, R. L. Coffman, Two types of murine helper T cell clone. I. Definition according to profiles of lymphokine activities and secreted proteins. 1986., *Journal of immunology* **175**, 5-14 (1986).
22. R. a Seder, R. Gazzinelli, a Sher, W. E. Paul, Interleukin 12 acts directly on CD4+ T cells to enhance priming for interferon gamma production and diminishes interleukin 4 inhibition of such priming., *Proceedings of the National Academy of Sciences of the United States of America* **90**, 10188-92 (1993).
23. S. J. Szabo et al., A novel transcription factor, T-bet, directs Th1 lineage commitment., *Cell* **100**, 655-69 (2000).
24. N. G. Jacobson et al., Interleukin 12 signaling in T helper type 1 (Th1) cells involves tyrosine phosphorylation of signal transducer and activator of transcription (Stat)3 and Stat4, *The Journal of experimental medicine* **181**, 1755-1762 (1995).
25. D. Ando, J. Clayton, D. Kono, J. Urban, E. Sercarz, Encephalitogenic T cells in the B10.PL model of experimental allergic encephalomyelitis (EAE) are of the Th-1 lymphokine subtype, *Cell Immunol.* **124**, 132-43 (1989).
26. D. Robinson et al., Predominant TH2-like Bronchoalveolar T-Lymphocyte Population in Atopic Asthma, *The New England Journal of Medicine* **326**, 298-304 (1992).
27. S. L. Swain, a D. Weinberg, M. English, G. Huston, IL-4 directs the development of Th2-like helper effectors., *Journal of immunology* **145**, 3796-806 (1990).
28. M. H. Kaplan, U. Schindler, S. T. Smiley, M. J. Grusby, Stat6 is required for mediating responses to IL-4 and for development of Th2 cells., *Immunity* **4**, 313-9 (1996).
29. W. Zheng, R. a Flavell, The transcription factor GATA-3 is necessary and sufficient for Th2 cytokine gene expression in CD4 T cells., *Cell* **89**, 587-96 (1997).
30. T. Gajewski, F. Fitch, Anti-proliferative effect of IFN-gamma in immune regulation. I. IFN-gamma inhibits the proliferation of Th2 but not Th1 murine helper T lymphocyte clones., *The Journal of Immunology* **140**, 4245-4252 (1988).

31. R. Fernandez-Botran, V. Sanders, T. Mosmann, E. Vitetta, Lymphokine-mediated regulation of the proliferative response of clones of T helper 1 and T helper 2 cells, *Journal of Experimental Medicine* **168** (1988).
32. R. Z. li et al., A CD4 + T-cell subset inhibits responses and prevents colitis, *Nature* **389**, 737-742 (1997).
33. S. Sakaguchi, N. Sakaguchi, M. Asano, M. Itoh, M. Toda, Immunologic self-tolerance maintained by activated T cells expressing IL-2 receptor alpha-chains (CD25)., *The Journal of Immunology* **155**, 1151-64 (1995).
34. S. Hori, T. Nomura, S. Sakaguchi, Control of regulatory T cell development by the transcription factor Foxp3., *Science* **299**, 1057-61 (2003).
35. S. Sakaguchi, T. Yamaguchi, T. Nomura, M. Ono, Regulatory T cells and immune tolerance., *Cell* **133**, 775-87 (2008).
36. S. Z. Josefowicz, A. Rudensky, Control of regulatory T cell lineage commitment and maintenance., *Immunity* **30**, 616-25 (2009).
37. I. I. Ivanov et al., The orphan nuclear receptor RORgammat directs the differentiation program of proinflammatory IL-17+ T helper cells., *Cell* **126**, 1121-33 (2006).
38. C. a Murphy et al., Divergent pro- and antiinflammatory roles for IL-23 and IL-12 in joint autoimmune inflammation., *The Journal of experimental medicine* **198**, 1951-7 (2003).
39. N. Fazilleau, L. Mark, L. J. McHeyzer-Williams, M. G. McHeyzer-Williams, Follicular helper T cells: lineage and location., *Immunity* **30**, 324-35 (2009).
40. R. I. Nurieva et al., Bcl6 mediates the development of T follicular helper cells., *Science* **325**, 1001-5 (2009).
41. A. Kelso, Th1 and Th2 subsets: paradigms lost?, *Immunology today* **16**, 374-9 (1995).
42. B. Hemmer et al., Human T-cell response to myelin basic protein peptide (83-99): extensive heterogeneity in antigen recognition, function, and phenotype., *Neurology* **49**, 1116-26 (1997).
43. M. Messi et al., Memory and flexibility of cytokine gene expression as separable properties of human T(H)1 and T(H)2 lymphocytes., *Nature immunology* **4**, 78-86 (2003).
44. M. Ahmadzadeh, D. L. Farber, Functional plasticity of an antigen-specific memory CD4 T cell population., *Proceedings of the National Academy of Sciences of the United States of America* **99**, 11802-7 (2002).
45. J. J. O'Shea, W. E. Paul, Mechanisms underlying lineage commitment and plasticity of helper CD4+ T cells., *Science* **327**, 1098-102 (2010).
46. K. M. Murphy, B. Stockinger, Effector T cell plasticity: flexibility in the face of changing circumstances., *Nature immunology* **11**, 674-80 (2010).
47. T. Mak, M. Saunders, in *The Immune Response Basic and Clinical Principles*, (2006), pp. 311-340.

48. E. Padovan et al., Expression of two T cell receptor alpha chains: dual receptor T cells., *Science* **262**, 422-4 (1993).
49. E. Padovan et al., Normal T lymphocytes can express two different T cell receptor beta chains: implications for the mechanism of allelic exclusion., *The Journal of experimental medicine* **181**, 1587-91 (1995).
50. F. Davodeau et al., Dual T cell receptor beta chain expression on human T lymphocytes., *The Journal of experimental medicine* **181**, 1391-8 (1995).
51. S. R. Carding, P. J. Egan, Gammadelta T cells: functional plasticity and heterogeneity., *Nature reviews. Immunology* **2**, 336-45 (2002).
52. Y. Tanaka et al., Nonpeptide ligands for human gamma delta T cells., *Proceedings of the National Academy of Sciences of the United States of America* **91**, 8175-9 (1994).
53. D. G. Schatz, P. C. Swanson, V(D)J Recombination: Mechanisms of Initiation., *Annual review of genetics* **12**, 167-202 (2011).
54. C. A. Janeway Jr, The T cell receptor as a multicomponent signalling machine: CD4/CD8 coreceptors and CD45 in T cell activation, *Annual review of immunology* **10**, 645–674 (1992).
55. R. N. Germain, MHC-dependent antigen processing and peptide presentation: providing ligands for T lymphocyte activation., *Cell* **76**, 287-99 (1994).
56. O. Olerup, J. Hillert, HLA class II-associated genetic susceptibility in multiple sclerosis: a critical evaluation, *Tissue Antigens* **38**, 1-15 (1991).
57. K. C. Garcia et al., An $\alpha\beta$ T Cell Receptor Structure at 2.5 Å and Its Orientation in the TCR-MHC Complex, *Science* **274**, 209-219 (1996).
58. D. H. Fremont, W. a Rees, H. Kozono, Biophysical studies of T-cell receptors and their ligands., *Current opinion in immunology* **8**, 93-100 (1996).
59. J. L. Jorgensen, U. Esser, B. Fazekas de St Groth, P. A. Reay, M. M. Davis, Mapping T-cell receptor-peptide contacts by variant peptide immunization of single-chain transgenics., *Nature* **355**, 224-30 (1992).
60. Y. Nakagawa, H. Kikuchi, H. Takahashi, Molecular analysis of TCR and peptide/MHC interaction using P18-I10-derived peptides with a single D-amino acid substitution., *Biophysical journal* **92**, 2570-82 (2007).
61. M. J. Nicholson, M. Hahn, K. W. Wucherpfennig, Unusual features of self-peptide/MHC binding by autoimmune T cell receptors., *Immunity* **23**, 351-60 (2005).
62. D. K. Sethi et al., A highly tilted binding mode by a self-reactive T cell receptor results in altered engagement of peptide and MHC., *The Journal of experimental medicine* **208**, 91-102 (2011).
63. D. Mason, A very high level of crossreactivity is an essential feature of the T-cell receptor., *Immunology today* **19**, 395-404 (1998).

64. M. Sospedra et al., Combining positional scanning peptide libraries, HLA-DR transfectants and bioinformatics to dissect the epitope spectrum of HLA class II cross-restricted CD4+ T cell clones., *Journal of immunological methods* **353**, 93-101 (2010).
65. G. J. Kersh, P. M. Allen, Structural basis for T cell recognition of altered peptide ligands: a single T cell receptor can productively recognize a large continuum of related ligands., *The Journal of experimental medicine* **184**, 1259-68 (1996).
66. M. D. Tallquist, a J. Weaver, L. R. Pease, Degenerate recognition of alloantigenic peptides on a positive-selecting class I molecule., *Journal of immunology* **160**, 802-9 (1998).
67. M. Vergelli et al., Differential activation of human autoreactive T cell clones by altered peptide ligands derived from myelin basic protein peptide (87-99)., *European journal of immunology* **26**, 2624-34 (1996).
68. B. B. B. Hemmer et al., Identification of High Potency Microbial and Self Ligands for a Human Autoreactive Class II – restricted T Cell Clone, *Journal of experimental medicine* **185**, 1651 (1997).
69. B. Hemmer, M. Vergelli, C. Pinilla, R. Houghten, R. Martin, Probing degeneracy in T-cell recognition using peptide combinatorial libraries, *Immunology today* **19**, 163–168 (1998).
70. B. Hemmer, M. Vergelli, B. Gran, N. Ling, Predictable TCR antigen recognition based on peptide scans leads to the identification of agonist ligands with no sequence homology., *Journal of immunological methods* **160**, 3631-3636 (1998).
71. M. Sospedra et al., Redundancy in antigen-presenting function of the HLA-DR and -DQ molecules in the multiple sclerosis-associated HLA-DR2 haplotype., *Journal of immunology* **176**, 1951-61 (2006).
72. J. Hennecke, D. C. Wiley, Structure of a complex of the human alpha/beta T cell receptor (TCR) HA1.7, influenza hemagglutinin peptide, and major histocompatibility complex class II molecule, HLA-DR4 (DRA*0101 and DRB1*0401): insight into TCR cross-restriction and alloreactivity., *The Journal of experimental medicine* **195**, 571-81 (2002).
73. S. Hawke et al., Cross-restriction of a T cell clone to HLA-DR alleles associated with rheumatoid arthritis: clues to arthritogenic peptide motifs., *Arthritis and rheumatism* **42**, 1040-50 (1999).
74. D. G. Doherty et al., Structural basis of specificity and degeneracy of T cell recognition: pluriallelic restriction of T cell responses to a peptide antigen involves both specific and promiscuous interactions between the T cell receptor, peptide, and HLA-DR., *Journal of immunology* **161**, 3527-35 (1998).
75. X. Zhang et al., Degenerate TCR recognition and dual DR2 restriction of autoreactive T cells: implications for the initiation of the autoimmune response in multiple sclerosis., *European journal of immunology* **38**, 1297-309 (2008).
76. B. L. Padgett, G. M. Zurhein, D. L. Walker, R. J. Eckroade, B. H. Dessel, Cultivation of Papova-like Virus from Human Brain with Progressive Multifocal Leukoencephalopathy, *The Lancet* **297**, 1257-1260 (1971).
77. S. Bofill-Mas, R. Girones, Excretion and transmission of JCV in human populations., *Journal of neurovirology* **7**, 345-9 (2001).

78. L. Ricciardiello et al., JC virus DNA sequences are frequently present in the human upper and lower gastrointestinal tract, *Gastroenterology* **119**, 1228-35 (2000).
79. M. C. Monaco, P. N. Jensen, J. Hou, L. C. Durham, E. O. Major, Detection of JC virus DNA in human tonsil tissue: evidence for site of initial viral infection., *Journal of virology* **72**, 9918-23 (1998).
80. M. C. Monaco, W. J. Atwood, M. Gravel, C. S. Tornatore, E. O. Major, JC virus infection of hematopoietic progenitor cells, primary B lymphocytes, and tonsillar stromal cells: implications for viral latency., *Journal of virology* **70**, 7004-12 (1996).
81. P. Chesters, J. Heritage, D. McCance, Persistence of DNA sequences of BK virus and JC virus in normal human tissues and in diseased tissues, *J Infect Dis* **147**, 676-84 (1983).
82. H. H. Hirsch et al., Prospective study of polyomavirus type BK replication and nephropathy in renal-transplant recipients, *New England Journal of Medicine* **347**, 488-96 (2002).
83. C. K. Liu, G. Wei, W. J. Atwood, Infection of glial cells by the human polyomavirus JC is mediated by an N-linked glycoprotein containing terminal alpha(2-6)-linked sialic acids., *Journal of virology* **72**, 4643-9 (1998).
84. G. F. Elphick et al., The human polyomavirus, JCV, uses serotonin receptors to infect cells., *Science (New York, N.Y.)* **306**, 1380-3 (2004).
85. S. Eash et al., Differential Distribution of the JC Virus Receptor- Type Sialic Acid in Normal Human Tissues, *American Journal of Pathology* **164**, 419-428 (2004).
86. J. a Gray et al., Cell-type specific effects of endocytosis inhibitors on 5-hydroxytryptamine(2A) receptor desensitization and resensitization reveal an arrestin-, GRK2-, and GRK5-independent mode of regulation in human embryonic kidney 293 cells., *Molecular pharmacology* **60**, 1020-30 (2001).
87. M. I. Fonseca, Y. G. Ni, D. D. Dunning, R. Miledi, Distribution of serotonin 2A, 2C and 3 receptor mRNA in spinal cord and medulla oblongata., *Molecular brain research* **89**, 11-9 (2001).
88. Z. Cohen et al., Multiple microvascular and astroglial 5-hydroxytryptamine receptor subtypes in human brain: molecular and pharmacologic characterization., *Journal of cerebral blood flow and metabolism* **19**, 908-17 (1999).
89. S. D. Gardner, A. M. Field, D. V. Coleman, B. Hulme, New human papovavirus (B.K.) isolated from urine after renal transplantation., *Lancet* **1**, 1253-7 (1971).
90. T. Allander et al., Identification of a third human polyomavirus., *Journal of virology* **81**, 4130-6 (2007).
91. A. M. Gaynor et al., Identification of a novel polyomavirus from patients with acute respiratory tract infections., *PLoS pathogens* **3**, e64 (2007).
92. H. Feng, M. Shuda, Y. Chang, P. S. Moore, Clonal integration of a polyomavirus in human Merkel cell carcinoma., *Science* **319**, 1096-100 (2008).
93. R. M. Schowalter, D. V. Pastrana, K. A. Pumphrey, A. L. Moyer, C. B. Buck, Merkel cell polyomavirus and two previously unknown polyomaviruses are chronically shed from human skin., *Cell host & microbe* **7**, 509-15 (2010).

94. E. van der Meijden et al., Discovery of a new human polyomavirus associated with trichodysplasia spinulosa in an immunocompromized patient., *PLoS pathogens* **6** (2010)
95. N. Scuda et al., A novel human polyomavirus closely related to the african green monkey-derived lymphotropic polyomavirus., *Journal of virology* **85**, 4586-90 (2011).
96. J. Li et al., T-cell responses to peptide fragments of the BK virus T antigen: implications for cross-reactivity of immune response to JC virus., *The Journal of general virology* **87**, 2951-60 (2006).
97. P. N. Jensen, E. O. Major, A classification scheme for human polyomavirus JCV variants based on the nucleotide sequence of the noncoding regulatory region, *Journal of neurovirology* **7**, 280-287 (2001).
98. L. J. Marshall, E. O. Major, Molecular regulation of JC virus tropism: insights into potential therapeutic targets for progressive multifocal leukoencephalopathy., *Journal of neuroimmune pharmacology* **5**, 404-17 (2010).
99. Y. Yogo et al., Isolation of a possible archetypal JC virus DNA sequence from nonimmunocompromised individuals., *Journal of virology* **64**, 3139-43 (1990).
100. T. Flaegstad et al., Amplification and sequencing of the control regions of BK and JC virus from human urine by polymerase chain reaction, *Virology* **180**, 553-60 (1991).
101. L. Gorelik et al., Progressive multifocal leukoencephalopathy (PML) development is associated with mutations in JC virus capsid protein VP1 that change its receptor specificity., *The Journal of infectious diseases* **204**, 103-14 (2011).
102. A. M. Daniel, R. J. Frisque, Transcription initiation sites of prototype and variant JC virus early and late messenger RNAs, *Virology* **194**, 97-109 (1992).
103. E. Major, K. Amemiya, G. Elder, S. Houff, Glial cells of the human developing brain and B cells of the immune system share a common DNA binding factor for recognition of the regulatory sequences of the human polyomavirus, JCV, *J Neurosci Res* **27**, 461-71 (1990).
104. A. Egli et al., Prevalence of Polyomavirus BK and JC Infection and Replication in 400 Healthy Blood Donors., *The Journal of infectious diseases* **199**, 837-846 (2009).
105. P. M. Eng et al., Characteristics and antecedents of progressive multifocal leukoencephalopathy in an insured population., *Neurology* **67**, 884-6 (2006).
106. G. L. Stoner, C. F. Ryschkewitsch, D. L. Walker, H. D. Webster, JC papovavirus large tumor (T)-antigen expression in brain tissue of acquired immune deficiency syndrome (AIDS) and non-AIDS patients with progressive multifocal leukoencephalopathy., *Proceedings of the National Academy of Sciences of the United States of America* **83**, 2271-5 (1986).
107. R. C. Holman, R. S. Janssen, J. W. Buehler, M. T. Zelasky, W. C. Hooper, Epidemiology of progressive multifocal leukoencephalopathy in the United States: analysis of national mortality and AIDS surveillance data., *Neurology* **41**, 1733-6 (1991).
108. A. Antinori et al., Clinical epidemiology and survival of progressive multifocal leukoencephalopathy in the era of highly active antiretroviral therapy: data from the Italian Registry Investigative Neuro AIDS (IRINA)., *Journal of neurovirology* **9 Suppl 1**, 47-53 (2003).

109. N. Khanna et al., Incidence and outcome of progressive multifocal leukoencephalopathy over 20 years of the Swiss HIV Cohort Study., *Clinical infectious diseases: an official publication of the Infectious Diseases Society of America* **48**, 1459-66 (2009).
110. F. N. Engsig et al., Incidence, clinical presentation, and outcome of progressive multifocal leukoencephalopathy in HIV-infected patients during the highly active antiretroviral therapy era: a nationwide cohort study., *The Journal of infectious diseases* **199**, 77-83 (2009).
111. I. J. Koralnik, Progressive multifocal leukoencephalopathy revisited: Has the disease outgrown its name?, *Annals of neurology* **60**, 162-73 (2006).
112. E. O. Major, Progressive multifocal leukoencephalopathy in patients on immunomodulatory therapies., *Annual review of medicine* **61**, 35-47 (2010).
113. T. Weber et al., Analysis of the systemic and intrathecal humoral immune response in progressive multifocal leukoencephalopathy., *The Journal of infectious diseases* **176**, 250-4 (1997).
114. B. L. Padgett, D. L. Walker, Prevalence of antibodies in human sera against JC virus, an isolate from a case of progressive multifocal leukoencephalopathy., *The Journal of infectious diseases* **127**, 467-70 (1973).
115. E. A. Engels et al., Antibodies to JC and BK viruses among persons with non-Hodgkin lymphoma., *International journal of cancer* **117**, 1013-9 (2005).
116. A. Stolt, K. Sasnauskas, P. Koskela, M. Lehtinen, J. Dillner, Seroepidemiology of the human polyomaviruses., *The Journal of general virology* **84**, 1499-504 (2003).
117. T. Weber, F. Weber, H. Petry, W. Lüke, Immune response in progressive multifocal leukoencephalopathy: an overview., *Journal of neurovirology* **7**, 311-7 (2001).
118. N. Khanna et al., JC virus-specific immune responses in human immunodeficiency virus type 1 patients with progressive multifocal leukoencephalopathy., *Journal of virology* **83**, 4404-11 (2009).
119. R. A. Du Pasquier et al., Low frequency of cytotoxic T lymphocytes against the novel HLA-A*0201-restricted JC virus epitope VP1(p36) in patients with proven or possible progressive multifocal leukoencephalopathy., *Journal of virology* **77**, 11918-26 (2003).
120. Y. Chen et al., BKV and JCV large T antigen-specific CD8+ T cell response in HLA A*0201+ kidney transplant recipients with polyomavirus nephropathy and patients with progressive multifocal leukoencephalopathy, *Journal of Clinical Virology* **42**, 198-202 (2008).
121. R. A. Du Pasquier et al., JCV-specific cellular immune response correlates with a favorable clinical outcome in HIV-infected individuals with progressive multifocal leukoencephalopathy., *Journal of neurovirology* **7**, 318-22 (2001).
122. R. a Du Pasquier et al., A prospective study demonstrates an association between JC virus-specific cytotoxic T lymphocytes and the early control of progressive multifocal leukoencephalopathy., *Brain* **127**, 1970-8 (2004).
123. J. Gasnault et al., Critical role of JC virus-specific CD4 T-cell responses in preventing progressive multifocal leukoencephalopathy., *AIDS* **17**, 1443-9 (2003).

124. S. Gheuens et al., Role of CD4+ and CD8+ T-Cell Responses against JC Virus in the Outcome of Patients with Progressive Multifocal Leukoencephalopathy (PML) and PML with Immune Reconstitution Inflammatory Syndrome., *Journal of virology* **85**, 7256-63 (2011).
125. M. Sospedra, R. Martin, Immunology of multiple sclerosis., *Annual review of immunology* **23**, 683-747 (2005).
126. B. Bielekova et al., Encephalitogenic potential of the myelin basic protein peptide (amino acids 83-99) in multiple sclerosis: results of a phase II clinical trial with an altered peptide ligand., *Nature medicine* **6**, 1167-75 (2000).
127. C. B. Pettinelli, D. E. McFarlin, Adoptive transfer of experimental allergic encephalomyelitis in SJL/J mice after in vitro activation of lymph node cells by myelin basic protein: requirement for Lyt 1+ 2- T lymphocytes., *Journal of immunology* **127**, 1420-3 (1981).
128. B. Bielekova et al., Expansion and functional relevance of high-avidity myelin-specific CD4+ T cells in multiple sclerosis., *Journal of immunology* **172**, 3893-904 (2004).
129. A. Chang, W. W. Tourtellotte, R. Rudick, B. D. Trapp, Premyelinating oligodendrocytes in chronic lesions of multiple sclerosis., *The New England journal of medicine* **346**, 165-73 (2002).
130. C. H. Polman et al., A randomized, placebo-controlled trial of natalizumab for relapsing multiple sclerosis., *The New England journal of medicine* **354**, 899-910 (2006).
131. L. Steinman, Blocking adhesion molecules as therapy for multiple sclerosis: natalizumab., *Nature reviews. Drug discovery* **4**, 510-8 (2005).
132. J. R. Kanwar et al., Beta7 integrins contribute to demyelinating disease of the central nervous system., *Journal of neuroimmunology* **103**, 146-52 (2000).
133. M. del Pilar Martin et al., Decrease in the numbers of dendritic cells and CD4+ T cells in cerebral perivascular spaces due to natalizumab., *Archives of neurology* **65**, 1596-603 (2008).
134. C. S. Tan et al., Detection of JC virus DNA and proteins in the bone marrow of HIV-positive and HIV-negative patients: implications for viral latency and neurotropic transformation., *The Journal of infectious diseases* **199**, 881-8 (2009).
135. S. A. Houff et al., Involvement of JC virus-infected mononuclear cells from the bone marrow and spleen in the pathogenesis of progressive multifocal leukoencephalopathy., *The New England journal of medicine* **318**, 301-5 (1988).
136. C. Warnke et al., [Risk stratification of progressive multifocal leukoencephalopathy under natalizumab : Recommendations for JC virus serology.], *Der Nervenarzt* **82** (2011),
137. R. Weissert, Progressive multifocal leukoencephalopathy, *Journal of Neuroimmunology* **231**, 73-77 (2011).
138. I. L. Tan, J. C. McArthur, D. B. Clifford, E. O. Major, A. Nath, Immune reconstitution inflammatory syndrome in natalizumab-associated PML., *Neurology* (2011).

139. A. De Luca et al., Cidofovir in addition to antiretroviral treatment is not effective for AIDS-associated progressive multifocal leukoencephalopathy: a multicohort analysis., *AIDS (London, England)* **22**, 1759-67 (2008).
140. C. D. Hall et al., Failure of Cytarabine in Progressive Multifocal Leukoencephalopathy Associated with Human Immunodeficiency Virus Infection, *New England Journal of Medicine* **338**, 1345-1351 (1998).
141. D. Cettomai, J. C. McArthur, Mirtazapine use in human immunodeficiency virus-infected patients with progressive multifocal leukoencephalopathy., *Archives of neurology* **66**, 255-8 (2009).
142. M. Brickelmaier et al., Identification and characterization of mefloquine efficacy against JC virus in vitro., *Antimicrobial agents and chemotherapy* **53**, 1840-9 (2009).
143. M. P. Busch et al., Screening of blood donors for idiopathic CD4+ T-lymphocytopenia., *Transfusion* **34**, 192-7 (1994).
144. CDC, Unexplained CD4+ T-lymphocyte depletion in persons without evident HIV infection--United States., *MMWR. Morbidity and mortality weekly report* **41**, 541-5 (1992).
145. V. Puri et al., Progressive multifocal leukoencephalopathy in a patient with idiopathic CD4+T lymphocytopenia., *Neurology India* **58**, 118-21.
146. S. Takeda et al., Progressive multifocal leukoencephalopathy showing extensive spinal cord involvement in a patient with lymphocytopenia., *Neuropathology: official journal of the Japanese Society of Neuropathology* **29**, 485-93 (2009).
147. S. Haider et al., Progressive multifocal leukoencephalopathy and idiopathic CD4+lymphocytopenia: a case report and review of reported cases., *Clinical infectious diseases: an official publication of the Infectious Diseases Society of America* **31**, E20-2 (2000).
148. A. Iwasaki, R. Medzhitov, Regulation of adaptive immunity by the innate immune system., *Science* **327**, 291-5 (2010).
149. T. Ito et al., Interferon-alpha and interleukin-12 are induced differentially by Toll-like receptor 7 ligands in human blood dendritic cell subsets., *The Journal of experimental medicine* **195**, 1507-12 (2002).
150. M. Moniuszko et al., Recombinant interleukin-7 induces proliferation of naive macaque CD4+ and CD8+ T cells in vivo., *Journal of virology* **78**, 9740-9 (2004).
151. G. Miller, M. Lipman, Release of infectious Epstein-Barr virus by transformed marmoset leukocytes., *Proceedings of the National Academy of Sciences of the United States of America* **70**, 190-4 (1973).
152. S. Kovats et al., Coordinate defects in human histocompatibility leukocyte antigen class II expression and antigen presentation in bare lymphocyte syndrome., *The Journal of experimental medicine* **179**, 2017-22 (1994).
153. P. a Muraro et al., Rapid identification of local T cell expansion in inflammatory organ diseases by flow cytometric T cell receptor Vbeta analysis., *Journal of immunological methods* **246**, 131-43 (2000).

154. R. Geiger, T. Duhon, A. Lanzavecchia, F. Sallusto, Human naive and memory CD4+ T cell repertoires specific for naturally processed antigens analyzed using libraries of amplified T cells., *The Journal of experimental medicine* **206**, 1525-34 (2009).
155. H. Lindå et al., Progressive multifocal leukoencephalopathy after natalizumab monotherapy., *The New England journal of medicine* **361**, 1081-7 (2009).
156. C. Ryschkewitsch et al., Comparison of PCR-southern hybridization and quantitative real-time PCR for the detection of JC and BK viral nucleotide sequences in urine and cerebrospinal fluid., *Journal of virological methods* **121**, 217-21 (2004).
157. A. Dumoulin, H. H. Hirsch, Reevaluating and optimizing polyomavirus BK and JC real-time PCR assays to detect rare sequence polymorphisms., *Journal of clinical microbiology* **49**, 1382-8 (2011).
158. S. Bofill-Mas et al., Quantification and stability of human adenoviruses and polyomavirus JCPyV in wastewater matrices., *Applied and environmental microbiology* **72**, 7894-6 (2006).
159. G. S. Ogg et al., Quantitation of HIV-1-Specific Cytotoxic T Lymphocytes and Plasma Load of Viral RNA, *Science* **279**, 2103-2106 (1998).
160. M. Han et al., Invariant or highly conserved TCR alpha are expressed on double-negative (CD3+CD4-CD8-) and CD8+ T cells., *Journal of immunology* **163**, 301-11 (1999).
161. J. Currier, H. Deulofeut, K. Barren, P. Kehn, Mitogens, superantigens, and nominal antigens elicit distinctive patterns of TCRB CDR3 diversity, *Human immunology* **48**, 39-51 (1996).
162. P. Loetscher et al., CCR5 is characteristic of Th1 lymphocytes., *Nature* **391**, 344-5 (1998).
163. S. Qin et al., The chemokine receptors CXCR3 and CCR5 mark subsets of T cells associated with certain inflammatory reactions., *The Journal of clinical investigation* **101**, 746-54 (1998).
164. R. Bonecchi et al., Differential expression of chemokine receptors and chemotactic responsiveness of type 1 T helper cells (Th1s) and Th2s., *The Journal of experimental medicine* **187**, 129-34 (1998).
165. L. Colantonio, H. Recalde, F. Sinigaglia, D. D'Ambrosio, Modulation of chemokine receptor expression and chemotactic responsiveness during differentiation of human naive T cells into Th1 or Th2 cells., *European journal of immunology* **32**, 1264-73 (2002).
166. F. Sallusto, D. Lenig, C. R. Mackay, A. Lanzavecchia, Flexible programs of chemokine receptor expression on human polarized T helper 1 and 2 lymphocytes., *The Journal of experimental medicine* **187**, 875-83 (1998).
167. I. J. Koralnik et al., Association of prolonged survival in HLA-A2+ progressive multifocal leukoencephalopathy patients with a CTL response specific for a commonly recognized JC virus epitope., *Journal of immunology* **168**, 499-504 (2002).
168. L. Aly et al., Central role of JC virus-specific CD4+ lymphocytes in progressive multi-focal leukoencephalopathy-immune reconstitution inflammatory syndrome., *Brain* **134**, 2687-702 (2011).
169. E. F. Wheelock, Interferon-like virus-inhibitor induced in human leukocytes by phytohemagglutinin., *Science* **149**, 310-1 (1965).

170. F. M. Rosa, M. M. Cochet, M. Fellous, Interferon and major histocompatibility complex genes: a model to analyse eukaryotic gene regulation?, *Interferon* **7**, 47-87 (1986).
171. A. S. Daar, S. V. Fuggle, J. W. Fabre, A. Ting, P. J. Morris, The detailed distribution of MHC Class II antigens in normal human organs., *Transplantation* **38**, 293-8 (1984).
172. A. Rappert et al., CXCR3-dependent microglial recruitment is essential for dendrite loss after brain lesion., *The Journal of neuroscience* **24**, 8500-9 (2004).
173. E. A. Forde, R.-N. E. Dogan, W. J. Karpus, CCR4 contributes to the pathogenesis of experimental autoimmune encephalomyelitis by regulating inflammatory macrophage function., *Journal of neuroimmunology* **236**, 17-26 (2011).
174. R. C. Howe, I. G. Ovsyannikova, N. a Pinsky, G. a Poland, Identification of Th0 cells responding to measles virus., *Human immunology* **66**, 104-15 (2005).
175. H. M. Diepolder et al., Immunodominant CD4+ T-cell epitope within nonstructural protein 3 in acute hepatitis C virus infection., *Journal of virology* **71**, 6011-9 (1997).
176. X. Paliard et al., Simultaneous production of IL-2, IL-4, and IFN-gamma by activated human CD4+ and CD8+ T cell clones., *Journal of immunology* **141**, 849-55 (1988).
177. G. S. Firestein et al., A new murine CD4+ T cell subset with an unrestricted cytokine profile., *Journal of immunology* **143**, 518-25 (1989).
178. U. Andersson et al., Simultaneous production of interleukin 2, interleukin 4 and interferon-gamma by activated human blood lymphocytes., *European journal of immunology* **20**, 1591-6 (1990).
179. L. H. Elson, T. B. Nutman, D. D. Metcalfe, C. Prussin, Flow cytometric analysis for cytokine production identifies T helper 1, T helper 2, and T helper 0 cells within the human CD4+CD27- lymphocyte subpopulation., *Journal of immunology* **154**, 4294-301 (1995).
180. A. N. Hegazy et al., Interferons direct Th2 cell reprogramming to generate a stable GATA-3(+)T-bet(+) cell subset with combined Th2 and Th1 cell functions., *Immunity* **32**, 116-28 (2010).
181. M. Löhning et al., Long-lived virus-reactive memory T cells generated from purified cytokine-secreting T helper type 1 and type 2 effectors., *The Journal of experimental medicine* **205**, 53-61 (2008).
182. K. T. Miner, M. Croft, Generation, persistence, and modulation of Th0 effector cells: role of autocrine IL-4 and IFN-gamma., *Journal of immunology* **160**, 5280-7 (1998).
183. M. Pedicini et al., Combining network modeling and gene expression microarray analysis to explore the dynamics of Th1 and Th2 cell regulation., *PLoS computational biology* **6**, e1001032 (2010).
184. R. M. Ransohoff, P. Kivisäkk, G. Kidd, Three or more routes for leukocyte migration into the central nervous system., *Nature reviews. Immunology* **3**, 569-81 (2003).
185. A. Flügel et al., Migratory activity and functional changes of green fluorescent effector cells before and during experimental autoimmune encephalomyelitis., *Immunity* **14**, 547-60 (2001).

186. E. Ulvestad et al., HLA class II molecules (HLA-DR, -DP, -DQ) on cells in the human CNS studied in situ and in vitro., *Immunology* **82**, 535-41 (1994).
187. D. O'Sullivan et al., On the interaction of promiscuous antigenic peptides with different DR alleles. Identification of common structural motifs., *Journal of immunology* **147**, 2663-9 (1991).
188. R. Martin et al., A myelin basic protein peptide is recognized by cytotoxic T cells in the context of four HLA-DR types associated with multiple sclerosis., *The Journal of experimental medicine* **173**, 19-24 (1991).
189. Y. Li, H. Li, R. Martin, R. A. Mariuzza, Structural basis for the binding of an immunodominant peptide from myelin basic protein in different registers by two HLA-DR2 proteins., *Journal of molecular biology* **304**, 177-88 (2000).
190. D. O'Sullivan, J. Sidney, M. F. Del Guercio, S. M. Colón, A. Sette, Truncation analysis of several DR binding epitopes., *Journal of immunology* **146**, 1240-6 (1991).
191. O. Lund et al., Definition of supertypes for HLA molecules using clustering of specificity matrices., *Immunogenetics* **55**, 797-810 (2004).
192. W. Zhou et al., Functional characterization of BK virus-specific CD4+ T cells with cytotoxic potential in seropositive adults., *Viral immunology* **20**, 379-88 (2007).
193. W. J. Atwood, K. Amemiya, R. Traub, J. Harms, E. O. Major, Interaction of the human polyomavirus, JCV, with human B-lymphocytes., *Virology* **190**, 716-23 (1992).
194. J. Hennecke, D. C. Wiley, T cell receptor-MHC interactions up close., *Cell* **104**, 1-4 (2001).
195. K. C. Garcia, L. Teyton, I. A. Wilson, Structural basis of T cell recognition., *Annual review of immunology* **17**, 369-97 (1999).
196. J. Ishizuka et al., The structural dynamics and energetics of an immunodominant T cell receptor are programmed by its Vbeta domain., *Immunity* **28**, 171-82 (2008).
197. B. Han et al., Developmental control of CD8 T cell-avidity maturation in autoimmune diabetes., *The Journal of clinical investigation* **115**, 1879-87 (2005).
198. D. a Price et al., Avidity for antigen shapes clonal dominance in CD8+ T cell populations specific for persistent DNA viruses., *The Journal of experimental medicine* **202**, 1349-61 (2005).
199. T. M. Lawson et al., Influenza A antigen exposure selects dominant Vbeta17+ TCR in human CD8+ cytotoxic T cell responses., *International immunology* **13**, 1373-81 (2001).
200. P. Serra et al., RAG-dependent peripheral T cell receptor diversification in CD8+ T lymphocytes., *Proceedings of the National Academy of Sciences of the United States of America* **99**, 15566-71 (2002).
201. J. S. Hale, M. Wubeshet, P. J. Fink, TCR revision generates functional CD4+ T cells., *Journal of immunology* **185**, 6528-34 (2010).
202. E. Lantelme et al., Cutting edge: recombinase-activating gene expression and V(D)J recombination in CD4+CD3^{low} mature T lymphocytes., *Journal of immunology* **164**, 3455-9 (2000).

203. B. Pulendran, R. Ahmed, Immunological mechanisms of vaccination., *Nature immunology* **131**, 509-17 (2011).
204. S. Adams et al., Immunization of malignant melanoma patients with full-length NY-ESO-1 protein using TLR7 agonist imiquimod as vaccine adjuvant., *Journal of immunology* **181**, 776-84 (2008).
205. G. Napolitani, A. Rinaldi, F. Bertoni, F. Sallusto, A. Lanzavecchia, Selected Toll-like receptor agonist combinations synergistically trigger a T helper type 1-polarizing program in dendritic cells., *Nature immunology* **6**, 769-76 (2005).
206. A. Patel, J. Patel, J. Ikwuagwu, A case of progressive multifocal leukoencephalopathy and idiopathic CD4+ lymphocytopenia., *The Journal of antimicrobial chemotherapy* **65**, 2697-8 (2010).

8 Appendix

Abbreviations

ADCC	Antibody dependent cellular cytotoxicity
AIDS	Acquired immune deficiency syndrome
ANOVA	Analysis of variance
APC	Antigen presenting cell
AUC	Area under the curve
BBB	Blood brain barrier
BLS	Bare lymphocyte syndrome
BSA	Bovine serum albumin
C	Constant region
CD	Cluster of differentiation
CFSE	Carboxyfluorescein succinimidyl ester
CNS	Central nervous system
CPM	Counts per minute
CSF	Cerebrospinal fluid
CTL	Cytotoxic T lymphocyte
D	Diversity segment
DC	Dendritic cell
DMSO	Dimethylsulfoxid
EAE	Experimental autoimmune encephalomyelitis
EBV	Ebstein-Barr-virus
EDTA	Ethylenediaminetetraacetic acid
FITC	Fluorescein isothiocyanate
FOXP	Forkhead box protein
HAART	Highly active anti-retroviral therapy
HIES	Hyper Immunoglobulin E syndrome
HLA	Human leukocyte antigen
i.v.	Intravenously
ICC	Intracellular cytokine staining
ICL	Idiopathic CD4 lymphocytopenia
IFN	Interferon
Ig	Immunoglobulin
IL	Interleukin
IMGT	Im Muno Gene Tics
IRIS	Immune reconstitution inflammatory syndrome
iTreg	Inducible regulatory T cells
J	Joining segment
JCV	John Cunningham Virus
LCMV	Lymphocytic choriomeningitis virus
MHC	Major histocompatibility complex
MRI	Magnet resonance imaging
mRNA	Messenger RNA
MS	Multiple sclerosis
NaCl	Sodium chloride
NaOH	Sodium hydroxide
NK	Natural killer cell

NKT	Natural killer T cell
nTreg	Naturally occurring regulatory T cells
PBMC	Peripheral blood monocytes
PBS	Phosphate buffered saline
PE	Phycoerythrin
PMA	Phorbol myristate acetate
PML	Progressive multifocal leukoencephalopathy
PPMS	Primary progressive multiple sclerosis
PRR	Pattern-recognition receptors
RRMS	Relapsing-remitting multiple sclerosis
RT	Room temperature
SI	Stimulation index
SPMS	Secondary progressive multiple sclerosis
STAT	Signal Transducers and Activators of Transcription protein
TCC	T cell clone
TCR	T cell receptor
TGF-β	Tumour growth factor- β
Th	T helper
TLR	Toll-like receptor
TNF	Tumour necrosis factor
TRAV	T cell receptor alpha variable chain
TRBV	T cell receptor beta variable chain
Treg	Regulatory T cells
Tris	Tris(hydroxymethyl) aminomethane
TTx	Tetanus toxoid
V	Variable chain
VCAM	Vascular cell adhesion protein
VLA	Very Late Antigen

List of publications

Aly L*, Yousef S*, Schippling S, Jelcic I, Breiden P, Matschke J, Schulz R, Bofill-Mas S, Jones L, Demina V, Linnebank M, Ogg G, Girones R, Weber T, Sospedra M, Martin R. Central role of JC virus-specific CD4+ lymphocytes in progressive multi-focal leukoencephalopathy-immune reconstitution inflammatory syndrome. *Brain*. 2011 Sep;134(Pt 9):2687-702.

* These authors contributed equally to this work.